

On optimal tests for rotational symmetry against new classes of hyperspherical distributions

Eduardo García-Portugués^{1,2,4}, Davy Paindaveine^{3,4}, and Thomas Verdebout^{3,4}

Abstract

Motivated by the central role played by rotationally symmetric distributions in directional statistics, we consider the problem of testing rotational symmetry on the hypersphere. We adopt a semiparametric approach and tackle problems where the location of the symmetry axis is either specified or unspecified. For each problem, we define two tests and study their asymptotic properties under very mild conditions. We introduce two new classes of directional distributions that extend the rotationally symmetric class and are of independent interest. We prove that each test is locally asymptotically maximin, in the Le Cam sense, for one kind of the alternatives given by the new classes of distributions, both for specified and unspecified symmetry axis. The tests, aimed to detect location-like and scatter-like alternatives, are combined into convenient hybrid tests that are consistent against both alternatives. We perform Monte Carlo experiments that illustrate the finite-sample performances of the proposed tests and their agreement with the asymptotic results. Finally, the practical relevance of our tests is illustrated on a real data application from astronomy. The R package `rotasym` implements the proposed tests and allows practitioners to reproduce the data application.

Keywords: Directional data; Local asymptotic normality; Locally asymptotically maximin tests; Rotational symmetry.

1 Introduction

1.1 Motivation

Directional statistics deals with data belonging to the unit hypersphere $\mathcal{S}^{p-1} := \{\mathbf{x} \in \mathbb{R}^p : \|\mathbf{x}\|^2 = \mathbf{x}^T \mathbf{x} = 1\}$ of \mathbb{R}^p . The most popular parametric model in directional statistics, which can be traced back to the beginning of the 20th century, is the von Mises–Fisher (vMF) model characterized by the density $\mathbf{x} \mapsto c_{p,\kappa}^M \exp(\kappa \mathbf{x}^T \boldsymbol{\theta})$ (densities on \mathcal{S}^{p-1} throughout are with respect to the surface area measure σ_{p-1} on \mathcal{S}^{p-1}), where $\boldsymbol{\theta} \in \mathcal{S}^{p-1}$ is a location parameter (it is the modal location on the sphere), $\kappa > 0$ is a concentration parameter (the larger the value of κ , the more the probability mass is concentrated about $\boldsymbol{\theta}$), and $c_{p,\kappa}^M$ is a normalizing constant. The vMF model belongs to a much broader model characterized by *rotationally symmetric* densities of the form $\mathbf{x} \mapsto c_{p,g} g(\mathbf{x}^T \boldsymbol{\theta})$, where g is a function from $[-1, 1]$ to $[0, \infty)$ and where $c_{p,g}$ is a normalizing constant. The rotationally symmetric model is indexed by the finite-dimensional parameter $\boldsymbol{\theta}$ and the infinite-dimensional parameter g , hence is of a semiparametric nature. Clearly, the (parametric) vMF submodel is obtained with $g(t) = \exp(\kappa t)$, $\kappa > 0$. Note that for axial distributions ($g(-t) = g(t)$ for any t), only the pair $\{\pm \boldsymbol{\theta}\}$ is identified, whereas non-axial distributions allow identifying $\boldsymbol{\theta}$ under mild conditions (identifiability of $\boldsymbol{\theta}$ is discussed below).

¹Department of Statistics, Carlos III University of Madrid (Spain).

²UC3M-BS Institute of Financial Big Data, Carlos III University of Madrid (Spain).

³Département de Mathématique, Université Libre de Bruxelles (Belgium).

⁴ECARES, Université Libre de Bruxelles (Belgium).

⁵Corresponding author. e-mail: edgarcia@est-econ.uc3m.es.

Rotationally symmetric distributions are often regarded as the most natural non-uniform distributions on the sphere and tend to have more tractable normalizing constants than non-rotationally symmetric models. As the following examples show, rotational symmetry plays a central role in applied directional statistics. Rotational symmetry is a common assumption in the analysis of fibre textures, as the distribution of crystallographic orientations typically has a favored direction that may be taken as the mode of a rotationally symmetric distribution, see, e.g., Chapter 5 of Bunge (2015). Guan and Smith (2017) used a rotationally symmetric distribution as a noise in their probabilistic camera model. Mixtures of vMF distributions are used in Lashkari et al. (2010) in their analysis of Functional Magnetic Resonance Imaging (fMRI) data. They used mixtures of vMF to model their concept of *selectivity profiles*, each component of the mixture corresponding to a functional system concentrated about a favored direction on the sphere. Both rotationally and non-rotationally symmetric models are used in Xiao and Johnson (2015) in the study of neuronal population volumes. The objective was to fit the distribution of neuronal spike activity around one or more active electrodes. Finally, the real data application provided in Section 6 indicates that rotational symmetry may also be relevant in astronomy.

Rotational symmetry has also been extensively adopted in the literature as a core assumption for performing inference with directional data. A (far from exhaustive) list of references illustrating this follows: Rivest (1989), Ko and Chang (1993), and Chang and Rivest (2001) considered regression and M-estimation under rotationally symmetric assumptions; Lo and Cabrera (1987) considered Bayes procedures for rotationally symmetric models; Larsen et al. (2002) considered von Mises–Fisher likelihood ratios; Tsai and Sen (2007), Ley et al. (2013), and Paindaveine and Verdebout (2015) proposed rank tests and estimators for the mode of a rotationally symmetric distribution; Ley et al. (2014) proposed a concept of quantiles for rotationally symmetric distributions; Paindaveine and Verdebout (2017) considered inference for the direction of weak rotationally symmetric signals, whereas Paindaveine and Verdebout (2019) tackled high-dimensional hypothesis testing in the same framework.

Rotationally symmetric distributions, however, impose a rather stringent symmetry on the hyper-sphere, which makes it crucial to test for rotational symmetry prior to basing data analysis or inference on rotational symmetry assumptions. The problem of testing rotational symmetry has mainly been considered in the circular case ($p = 2$), where rotational symmetry is referred to as *reflective symmetry*. Tests of reflective symmetry about a specified location $\boldsymbol{\theta}$ have been considered in Schach (1969), using a linear rank test, and in Mardia and Jupp (2000), using sign-based statistics, whereas Pewsey (2002) introduced a test based on second-order trigonometric moments for unspecified $\boldsymbol{\theta}$. Ley and Verdebout (2014) and Meintanis and Verdebout (2019) developed specified- $\boldsymbol{\theta}$ tests that are locally and asymptotically optimal against specific alternatives. For $p \geq 3$, however, the problem is much more difficult, which explains that the corresponding literature is much sparser: to the best of our knowledge, for $p \geq 3$, only Jupp and Spurr (1983) and Ley and Verdebout (2017) addressed the problem of testing rotational symmetry in a *semiparametric* way (that is, without specifying the function g). The former considered a test for symmetry in dimension $p \geq 2$ using the Sobolev tests machinery from Giné (1975), whereas the latter established the efficiency of the Watson (1983) test against a new type of non-rotationally symmetric alternatives. Both papers restricted to the specified- $\boldsymbol{\theta}$ problem, so that no tests for rotational symmetry about an unspecified location $\boldsymbol{\theta}$ are available in dimension $p \geq 3$. Goodness-of-fit tests within the directional framework (i.e., tests for checking that the distribution on \mathcal{S}^{p-1} belongs to a given parametric class of distributions) have received comparatively more attention in the literature. For instance, Boulerice and Ducharme (1997) proposed goodness-of-fit tests based on spherical harmonics for a specific class of rotationally symmetric distributions. More recently, Figueiredo (2012) considered goodness-of-fit tests for vMF distributions, while Boente et al. (2014) introduced goodness-of-fit tests based on kernel density estimation for any (possibly non-rotationally symmetric) distribution.

1.2 Summary of the main contributions

In this paper, we consider the problem of testing rotational symmetry on the unit hypersphere \mathcal{S}^{p-1} in any dimension $p \geq 3$. The methodological contributions are threefold. Firstly, we tackle the specified- $\boldsymbol{\theta}$ problem and propose two tests that aim to detect *scatter*-like and *location*-like departures from the null hypothesis. Secondly, we introduce two new classes \mathcal{C}_1 and \mathcal{C}_2 of distributions on \mathcal{S}^{p-1} that are of independent interest and that may serve as natural alternatives to rotational symmetry. In particular, the class \mathcal{C}_1 is an “elliptical” extension of the class of rotationally symmetric distributions based on the angular Gaussian distributions from Tyler (1987). We prove that, for the specified- $\boldsymbol{\theta}$ problem, the proposed scatter and location tests are locally asymptotically maximin against alternatives in \mathcal{C}_1 and \mathcal{C}_2 , respectively. Thirdly, we tackle the more challenging unspecified- $\boldsymbol{\theta}$ problem. We establish that the scatter test is unaffected asymptotically by the estimation of $\boldsymbol{\theta}$ under the null (and therefore also under contiguous alternatives) but that the location test shows a much more involved asymptotic behavior affected by the estimation of $\boldsymbol{\theta}$. We therefore propose corrected versions of the location test that keep strong optimality properties against alternatives in \mathcal{C}_2 . Finally, using the asymptotic independence (under the null) between the location and scatter test statistics, we introduce, both for the specified and unspecified- $\boldsymbol{\theta}$ problems, hybrid tests that can asymptotically show power both against alternatives in \mathcal{C}_1 and alternatives in \mathcal{C}_2 .

The outline of the paper is as follows. In Section 2, we consider the problem of testing for rotational symmetry about a specified location $\boldsymbol{\theta}$. The asymptotic distributions of two tests proposed for that aim are given in Section 2.1. Section 2.2 introduces two non-rotationally symmetric extensions of the class of rotationally symmetric distributions, which are used in Sections 2.3–2.4 to investigate the non-null asymptotic behavior of the proposed tests. In Section 3, our tests are extended to the unspecified- $\boldsymbol{\theta}$ problem. Hybrid tests are introduced in Section 4. Monte Carlo experiments that illustrate the finite-sample performances of the proposed tests and their agreement with the asymptotic results are given in Section 5. We present a real data application in Section 6 and discuss perspectives for future research in Section 7. Supplementary materials collect the proofs of the main results and detail the delicate construction of optimal location tests in the unspecified- $\boldsymbol{\theta}$ problem. The R package `rotasym` allows practitioners to perform the proposed tests and reproduce the data application.

2 Testing rotational symmetry about a specified $\boldsymbol{\theta}$

A random vector \mathbf{X} with values in \mathcal{S}^{p-1} is said to be *rotationally symmetric* about $\boldsymbol{\theta} \in \mathcal{S}^{p-1}$ if and only if $\mathbf{O}\mathbf{X} \stackrel{\mathcal{D}}{=} \mathbf{X}$ for any $p \times p$ orthogonal matrix \mathbf{O} satisfying $\mathbf{O}\boldsymbol{\theta} = \boldsymbol{\theta}$ (throughout, $\stackrel{\mathcal{D}}{=}$ denotes equality in distribution). For any $\mathbf{x} \in \mathcal{S}^{p-1}$, write

$$v_{\boldsymbol{\theta}}(\mathbf{x}) := \mathbf{x}^T \boldsymbol{\theta} \quad \text{and} \quad \mathbf{u}_{\boldsymbol{\theta}}(\mathbf{x}) := \frac{\boldsymbol{\Gamma}_{\boldsymbol{\theta}}^T \mathbf{x}}{\|\boldsymbol{\Gamma}_{\boldsymbol{\theta}}^T \mathbf{x}\|} = \frac{\boldsymbol{\Gamma}_{\boldsymbol{\theta}}^T \mathbf{x}}{(1 - v_{\boldsymbol{\theta}}^2(\mathbf{x}))^{1/2}}, \quad (1)$$

where $\boldsymbol{\Gamma}_{\boldsymbol{\theta}}$ denotes an arbitrary $p \times (p-1)$ matrix whose columns form an orthonormal basis of the orthogonal complement to $\boldsymbol{\theta}$ (so that $\boldsymbol{\Gamma}_{\boldsymbol{\theta}}^T \boldsymbol{\Gamma}_{\boldsymbol{\theta}} = \mathbf{I}_{p-1}$ and $\boldsymbol{\Gamma}_{\boldsymbol{\theta}} \boldsymbol{\Gamma}_{\boldsymbol{\theta}}^T = \mathbf{I}_p - \boldsymbol{\theta} \boldsymbol{\theta}^T$). This allows considering the *tangent-normal* decomposition

$$\mathbf{x} = v_{\boldsymbol{\theta}}(\mathbf{x})\boldsymbol{\theta} + (\mathbf{I}_p - \boldsymbol{\theta} \boldsymbol{\theta}^T)\mathbf{x} = v_{\boldsymbol{\theta}}(\mathbf{x})\boldsymbol{\theta} + (1 - v_{\boldsymbol{\theta}}^2(\mathbf{x}))^{1/2} \boldsymbol{\Gamma}_{\boldsymbol{\theta}} \mathbf{u}_{\boldsymbol{\theta}}(\mathbf{x}). \quad (2)$$

If \mathbf{X} is rotationally symmetric about $\boldsymbol{\theta}$, then the distribution of the random $(p-1)$ -vector $\boldsymbol{\Gamma}_{\boldsymbol{\theta}}^T \mathbf{X}$ is spherically symmetric about the origin of \mathbb{R}^{p-1} , so that the *multivariate sign* $\mathbf{u}_{\boldsymbol{\theta}}(\mathbf{X})$ is uniformly distributed over \mathcal{S}^{p-2} , hence it satisfies the moment conditions

$$\mathbb{E}[\mathbf{u}_{\boldsymbol{\theta}}(\mathbf{X})] = \mathbf{0} \quad \text{and} \quad \mathbb{E}[\mathbf{u}_{\boldsymbol{\theta}}(\mathbf{X}) \mathbf{u}_{\boldsymbol{\theta}}^T(\mathbf{X})] = \frac{1}{p-1} \mathbf{I}_{p-1}. \quad (3)$$

Note also that $\mathbf{u}_{\boldsymbol{\theta}}(\mathbf{X})$ and the cosine $v_{\boldsymbol{\theta}}(\mathbf{X})$ are then mutually independent. This multivariate sign is therefore a quantity that is more appealing than the ‘‘projection’’ $\boldsymbol{\Gamma}_{\boldsymbol{\theta}}^T \mathbf{X}$, that is neither distribution-free nor independent of $v_{\boldsymbol{\theta}}(\mathbf{X})$. If \mathbf{X} admits a density, then this density is of the form

$$\mathbf{x} \mapsto f_{\boldsymbol{\theta},g}(\mathbf{x}) = c_{p,g} g(\mathbf{x}^T \boldsymbol{\theta}), \quad (4)$$

where $c_{p,g} (> 0)$ is a normalizing constant and $g : [-1, 1] \rightarrow [0, \infty)$ is henceforth referred to as an *angular function*. Then, $v_{\boldsymbol{\theta}}(\mathbf{X})$ is absolutely continuous with respect to the Lebesgue measure on $[-1, 1]$ and the corresponding density is

$$v \mapsto \tilde{g}_p(v) := \omega_{p-1} c_{p,g} (1 - v^2)^{(p-3)/2} g(v), \quad (5)$$

where $\omega_{p-1} := 2\pi^{\frac{p-1}{2}}/\Gamma(\frac{p-1}{2})$ is the surface area of \mathcal{S}^{p-2} . Application of (5) to the vMF with location $\boldsymbol{\theta}$ and concentration κ (notation: $\mathcal{M}_p(\boldsymbol{\theta}, \kappa)$), that is, to $g(t) = \exp(\kappa t)$, gives $c_{p,g} = c_{p,\kappa}^{\mathcal{M}} = \kappa^{\frac{p-2}{2}} / ((2\pi)^{\frac{p}{2}} I_{\frac{p-2}{2}}(\kappa))$, where I_{ν} is the order- ν modified Bessel function of the first kind.

2.1 The proposed tests

In view of the above considerations, it is natural to test the null of rotational symmetry about $\boldsymbol{\theta}$ by testing that $\mathbf{u}_{\boldsymbol{\theta}}(\mathbf{X})$ is uniformly distributed over \mathcal{S}^{p-2} . Since there are extremely diverse alternatives to uniformity on \mathcal{S}^{p-2} , one may first want to consider *location* alternatives and *scatter* alternatives, the ones associated with violations of the expectation and the covariance conditions in (3), respectively. The tests we propose in this paper are designed to detect such alternatives.

Let $\mathbf{X}_1, \dots, \mathbf{X}_n$ be a random sample from a distribution on \mathcal{S}^{p-1} and consider the problem of testing the null $\mathcal{H}_{0,\boldsymbol{\theta}}$: ‘‘ \mathbf{X}_1 is rotationally symmetric about $\boldsymbol{\theta}$ ’’. Writing $\mathbf{U}_{i,\boldsymbol{\theta}} := \mathbf{u}_{\boldsymbol{\theta}}(\mathbf{X}_i)$, $i = 1, \dots, n$, the first test we propose rejects the null for large values of

$$Q_{\boldsymbol{\theta}}^{\text{loc}} := \frac{p-1}{n} \sum_{i,j=1}^n \mathbf{U}_{i,\boldsymbol{\theta}}^T \mathbf{U}_{j,\boldsymbol{\theta}} = n(p-1) \|\bar{\mathbf{U}}_{\boldsymbol{\theta}}\|^2,$$

with $\bar{\mathbf{U}}_{\boldsymbol{\theta}} := \frac{1}{n} \sum_{i=1}^n \mathbf{U}_{i,\boldsymbol{\theta}}$. This test statistic coincides with the celebrated Rayleigh (1919) test statistic computed from the $\mathbf{U}_{i,\boldsymbol{\theta}}$ ’s. Alternatively, if it is assumed that the \mathbf{X}_i ’s are sampled from a rotationally symmetric distribution (about an unspecified location), then the test also coincides with the Paindaveine and Verdebout (2015) *sign* test for the null that the unknown location is equal to $\boldsymbol{\theta}$. Since, under the null $\mathcal{H}_{0,\boldsymbol{\theta}}$, the $\mathbf{U}_{i,\boldsymbol{\theta}}$ ’s form a random sample from the uniform distribution over \mathcal{S}^{p-2} , the Central Limit Theorem (CLT) readily entails that $\sqrt{n} \bar{\mathbf{U}}_{\boldsymbol{\theta}} \xrightarrow{\mathcal{D}} \mathcal{N}(\mathbf{0}, \frac{1}{p-1} \mathbf{I}_{p-1})$, and hence that $Q_{\boldsymbol{\theta}}^{\text{loc}} \xrightarrow{\mathcal{D}} \chi_{p-1}^2$ under $\mathcal{H}_{0,\boldsymbol{\theta}}$, where $\xrightarrow{\mathcal{D}}$ denotes convergence in distribution. The resulting test, $\phi_{\boldsymbol{\theta}}^{\text{loc}}$ say, then rejects the null $\mathcal{H}_{0,\boldsymbol{\theta}}$ at asymptotic level α whenever $Q_{\boldsymbol{\theta}}^{\text{loc}} > \chi_{p-1,1-\alpha}^2$, where $\chi_{\ell,1-\alpha}^2$ denotes the α -upper quantile of the chi-square distribution with ℓ degrees of freedom. As we will show, this test typically detects the location alternatives violating the expectation condition in (3).

In contrast, the second test we propose is designed to show power against the scatter alternatives that violate the isotropic covariance condition in (3). This second test rejects $\mathcal{H}_{0,\boldsymbol{\theta}}$ for large values of

$$Q_{\boldsymbol{\theta}}^{\text{sc}} := \frac{p^2 - 1}{2n} \sum_{i,j=1}^n \left((\mathbf{U}_{i,\boldsymbol{\theta}}^T \mathbf{U}_{j,\boldsymbol{\theta}})^2 - \frac{1}{p-1} \right) = \frac{n(p^2 - 1)}{2} \left(\text{tr}[\mathbf{S}_{\boldsymbol{\theta}}^2] - \frac{1}{p-1} \right),$$

where we let $\mathbf{S}_{\boldsymbol{\theta}} := \frac{1}{n} \sum_{i=1}^n \mathbf{U}_{i,\boldsymbol{\theta}} \mathbf{U}_{i,\boldsymbol{\theta}}^T$. Using again the fact that, under $\mathcal{H}_{0,\boldsymbol{\theta}}$, the $\mathbf{U}_{i,\boldsymbol{\theta}}$ ’s form a random sample from the uniform distribution over \mathcal{S}^{p-2} , it readily follows from Hallin and Paindaveine (2006b) that $Q_{\boldsymbol{\theta}}^{\text{sc}} \xrightarrow{\mathcal{D}} \chi_{(p-2)(p+1)/2}^2$ under $\mathcal{H}_{0,\boldsymbol{\theta}}$. The resulting test, $\phi_{\boldsymbol{\theta}}^{\text{sc}}$ say, then rejects the null $\mathcal{H}_{0,\boldsymbol{\theta}}$

at asymptotic level α whenever $Q_{\boldsymbol{\theta}}^{\text{sc}} > \chi^2_{(p-2)(p+1)/2, 1-\alpha}$.

For each test, thus, the asymptotic distribution of the test statistic, under the null of rotational symmetry about a *specified* location $\boldsymbol{\theta}$, follows from results available in the literature. Note that these are results under the usual fixed- p large- n asymptotic framework. In a high-dimensional asymptotic framework where $p = p_n$ goes to infinity with n (at an arbitrary rate), it can be showed that, under the null,

$$\frac{Q_{\boldsymbol{\theta}}^{\text{loc}} - (p_n - 1)}{\sqrt{2(p_n - 1)}} \xrightarrow{\mathcal{D}} \mathcal{N}(0, 1) \quad \text{and} \quad \frac{Q_{\boldsymbol{\theta}}^{\text{sc}} - \frac{(p_n - 2)(p_n + 1)}{2}}{\sqrt{(p_n - 2)(p_n + 1)}} \xrightarrow{\mathcal{D}} \mathcal{N}(0, 1), \quad (6)$$

which allows also to apply the tests in high dimensions. The proofs of these high-dimensional limiting results are actually based on Paindaveine and Verdebout (2016). For instance, the asymptotic normality result for $Q_{\boldsymbol{\theta}}^{\text{loc}}$ in (6) is Theorem 2.2 from that paper, whereas the one for $Q_{\boldsymbol{\theta}}^{\text{sc}}$ follows rather directly from Theorem 2.5 *ibid.*

Yet, two important questions remain open at this stage: (i) do $\phi_{\boldsymbol{\theta}}^{\text{loc}}$ and $\phi_{\boldsymbol{\theta}}^{\text{sc}}$ behave well under non-null distributions? In particular, are there alternatives to $\mathcal{H}_{0,\boldsymbol{\theta}}$ against which these tests would enjoy some power optimality? (ii) To test rotational symmetry about an unspecified location $\boldsymbol{\theta}$, can one use the tests $\phi_{\boldsymbol{\theta}}^{\text{loc}}$ and $\phi_{\boldsymbol{\theta}}^{\text{sc}}$ obtained by replacing $\boldsymbol{\theta}$ with an appropriate estimator $\hat{\boldsymbol{\theta}}$ in $\phi_{\boldsymbol{\theta}}^{\text{loc}}$ and $\phi_{\boldsymbol{\theta}}^{\text{sc}}$? We address (i) in Sections 2.3 and 2.4 (for appropriate scatter and location alternatives, respectively), and (ii) in Section 3.

2.2 Non-rotationally symmetric tangent distributions

As explained in the previous section, if \mathbf{X} is rotationally symmetric about $\boldsymbol{\theta}$, then the sign $\mathbf{U} := \mathbf{u}_{\boldsymbol{\theta}}(\mathbf{X})$ (see (1)) is uniformly distributed over \mathcal{S}^{p-2} and is independent of the cosine $V := v_{\boldsymbol{\theta}}(\mathbf{X})$. Vice versa, it directly follows from the tangent-normal decomposition in (2) that any rotational distribution on \mathcal{S}^{p-1} can be obtained as the distribution of

$$V\boldsymbol{\theta} + \sqrt{1 - V^2} \boldsymbol{\Gamma}_{\boldsymbol{\theta}} \mathbf{U}, \quad (7)$$

where \mathbf{U} is a random vector that is uniformly distributed over \mathcal{S}^{p-2} and where the random variable V with values in $[-1, 1]$ is independent of \mathbf{U} . In this section, we introduce natural alternatives to rotational symmetry by relaxing some of the distributional constraints on \mathbf{U} in (7). Rather than assuming that \mathbf{U} is uniformly distributed over \mathcal{S}^{p-2} , we construct two families of non-rotationally symmetric distributions for which \mathbf{U} follows an *angular central Gaussian distribution* (Tyler, 1987) and a vMF distribution.

For the first family, recall that the random $(p - 1)$ -vector \mathbf{U} has an angular central Gaussian distribution on \mathcal{S}^{p-2} with shape parameter $\boldsymbol{\Lambda}$ (notation: $\mathbf{U} \sim \mathcal{A}_{p-1}(\boldsymbol{\Lambda})$) if it admits the density $\mathbf{u} \mapsto c_{p-1,\boldsymbol{\Lambda}}^{\mathcal{A}} (\mathbf{u}^T \boldsymbol{\Lambda}^{-1} \mathbf{u})^{-(p-1)/2}$ with respect to the surface area measure σ_{p-2} on \mathcal{S}^{p-2} , where $c_{p-1,\boldsymbol{\Lambda}}^{\mathcal{A}} := (\omega_{p-1} (\det \boldsymbol{\Lambda})^{1/2})^{-1}$ is a normalizing constant. Here, the scatter parameter $\boldsymbol{\Lambda}$ is a $(p-1) \times (p-1)$ symmetric and positive-definite matrix that is normalized into a shape matrix in the sense that $\text{tr}[\boldsymbol{\Lambda}] = p - 1$ (without this normalization, $\boldsymbol{\Lambda}$ would be identified up to a positive scalar factor only). Letting \mathcal{G} be the set of all cumulative distribution functions G over $[-1, 1]$, and \mathcal{L}_{p-1} be the collection of shape matrices $\boldsymbol{\Lambda}$, we then introduce the family of *tangent elliptical distributions*.

Definition 1. Let $\boldsymbol{\theta} \in \mathcal{S}^{p-1}$, $G \in \mathcal{G}$, and $\boldsymbol{\Lambda} \in \mathcal{L}_{p-1}$. Then the random vector \mathbf{X} has a tangent elliptical distribution on \mathcal{S}^{p-1} with location $\boldsymbol{\theta}$, angular distribution function G , and shape $\boldsymbol{\Lambda}$ if and only if $\mathbf{X} \stackrel{\mathcal{D}}{=} V\boldsymbol{\theta} + \sqrt{1 - V^2} \boldsymbol{\Gamma}_{\boldsymbol{\theta}} \mathbf{U}$, where $V \sim G$ and $\mathbf{U} \sim \mathcal{A}_{p-1}(\boldsymbol{\Lambda})$ are mutually independent. If V admits the density (5) involving the angular function g , then we will write $\mathbf{X} \sim \mathcal{TE}_p(\boldsymbol{\theta}, g, \boldsymbol{\Lambda})$.

Clearly, rotationally symmetric distributions are obtained for $\mathbf{\Lambda} = \mathbf{I}_{p-1}$. Since the distribution $\mathcal{A}_{p-1}(\mathbf{\Lambda})$ can be obtained by projecting radially on \mathcal{S}^{p-2} a $(p-1)$ -dimensional elliptical distribution with location $\mathbf{0}$ and scatter $\mathbf{\Lambda}$, the distributions in Definition 1 form an *elliptical extension* of the class of the (by nature, spherical) rotationally symmetric distributions, which justifies the terminology. In the absolutely continuous case, the following result provides the density of a tangent elliptical distribution.

Theorem 1. *If $\mathbf{X} \sim \mathcal{TE}_p(\boldsymbol{\theta}, g, \mathbf{\Lambda})$, then \mathbf{X} is absolutely continuous and the corresponding density is $\mathbf{x} \mapsto f_{\boldsymbol{\theta}, g, \mathbf{\Lambda}}^{\mathcal{TE}}(\mathbf{x}) = \omega_{p-1} c_{p, g} c_{p-1, \mathbf{\Lambda}}^{\mathcal{A}} g(v_{\boldsymbol{\theta}}(\mathbf{x})) (\mathbf{u}_{\boldsymbol{\theta}}^T(\mathbf{x}) \mathbf{\Lambda}^{-1} \mathbf{u}_{\boldsymbol{\theta}}(\mathbf{x}))^{-(p-1)/2}$.*

As mentioned above, tangent elliptical distributions provide an elliptical extension of the class of rotationally symmetric distributions, hence in particular of vMF distributions. Another elliptical extension of vMF distributions is the Kent (1982) class of Fisher–Bingham distributions. The tangent elliptical distributions show several advantages with respect to the latter: (i) they form a semiparametric class of distributions that contains *all* rotationally symmetric distributions; (ii) the densities of tangent elliptical distributions involve normalizing constants that are simple to compute (see, e.g., Kume and Wood (2005) for the delicate problem of approximating normalizing constants in the Fisher–Bingham model); (iii) simulation is straightforward.

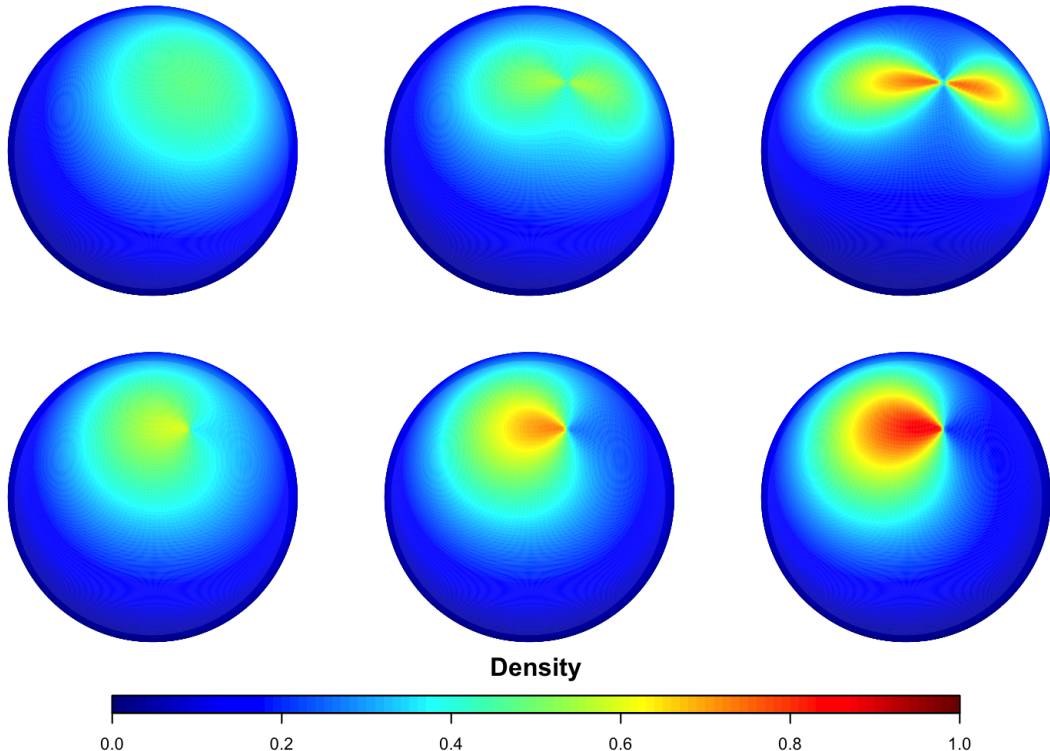


Figure 1: Contour plots of tangent elliptical and tangent vMF densities, both with $g(z) = \exp(3z)$. Top row: from left to right, tangent elliptical with shape matrices $\mathbf{\Lambda} = \begin{pmatrix} 1+a & 0 \\ 0 & 1-a \end{pmatrix}$, $a = 0$ (rotationally symmetric), $a = 0.15$, and $a = 0.45$. Bottom row: from left to right, tangent vMF densities with skewness intensities $\kappa = 0.25, 0.50$, and 0.75 .

The second class of distributions we introduce, namely the class of *tangent vMF distributions*, is obtained by assuming that $\mathbf{U} \sim \mathcal{M}_{p-1}(\boldsymbol{\mu}, \kappa)$. Unlike the tangent elliptical distributions, under which \mathbf{U} assumes an axial distribution on \mathcal{S}^{p-2} , the unimodality of $\mathcal{M}_{p-1}(\boldsymbol{\mu}, \kappa)$ in the tangent space provides a skewed distribution for \mathbf{X} about $\boldsymbol{\theta}$ (see the bottom row of Figure 1). Theorem 2 provides the density of the tangent vMF distributions in the absolutely continuous case. Its proof is along the same lines as the proof of Theorem 1, hence is omitted.

Definition 2. Let $\boldsymbol{\theta} \in \mathcal{S}^{p-1}$, $G \in \mathcal{G}$, $\boldsymbol{\mu} \in \mathcal{S}^{p-2}$, and $\kappa \geq 0$. Then the random vector \mathbf{X} has a tangent vMF distribution on \mathcal{S}^{p-1} with location $\boldsymbol{\theta}$, angular distribution function G , skewness direction $\boldsymbol{\mu}$, and skewness intensity κ if and only if $\mathbf{X} \stackrel{\mathcal{D}}{=} V\boldsymbol{\theta} + \sqrt{1-V^2} \boldsymbol{\Gamma}_{\boldsymbol{\theta}} \mathbf{U}$, where $V \sim G$ and $\mathbf{U} \sim \mathcal{M}_{p-1}(\boldsymbol{\mu}, \kappa)$ are mutually independent. If V admits the density (5) involving the angular function g , then we will write $\mathbf{X} \sim \mathcal{T}\mathcal{M}_p(\boldsymbol{\theta}, g, \boldsymbol{\mu}, \kappa)$.

Theorem 2. If $\mathbf{X} \sim \mathcal{T}\mathcal{M}_p(\boldsymbol{\theta}, g, \boldsymbol{\mu}, \kappa)$, then \mathbf{X} is absolutely continuous and the corresponding density is $\mathbf{x} \mapsto f_{\boldsymbol{\theta}, g, \boldsymbol{\mu}, \kappa}^{\mathcal{T}\mathcal{M}}(\mathbf{x}) = \omega_{p-1} c_{p, g} c_{p-1, \kappa}^{\mathcal{M}} g(v_{\boldsymbol{\theta}}(\mathbf{x})) \exp(\kappa \boldsymbol{\mu}^T \mathbf{u}_{\boldsymbol{\theta}}(\mathbf{x}))$.

Note that, albeit our framework is $p \geq 3$, the distributions of Definitions 1 and 2 are also properly defined for $p = 2$. In that case, the sign \mathbf{U} takes values in $\mathcal{S}^0 = \{-1, 1\}$, $\omega_1 = 2$, and the angular central Gaussian and the vMF densities become probability mass functions over \mathcal{S}^0 . The former, since it is an axial distribution, puts equal mass in ± 1 . Since $I_{-\frac{1}{2}}(\kappa) = \sqrt{2/(\pi\kappa)} \cosh(\kappa)$, the vMF associated with $\mu \in \mathcal{S}^0$ assigns probabilities $\exp(\pm\mu\kappa)/(\exp(-\mu\kappa) + \exp(\mu\kappa))$ to ± 1 , respectively. Therefore, only the tangent vMF distributions provide alternatives to rotational symmetry when $p = 2$. This is coherent with the fact that $Q_{\boldsymbol{\theta}}^{\text{sc}}$ is a non-random test statistic when $p = 2$ and therefore does not provide any reasonable test. In order to deal with non-degenerate tests, we restrict to $p \geq 3$ in the sequel.

2.3 Non-null results for tangent elliptical alternatives

In this section, we investigate the performances of the tests $\phi_{\boldsymbol{\theta}}^{\text{loc}}$ and $\phi_{\boldsymbol{\theta}}^{\text{sc}}$ under the tangent elliptical alternatives to rotational symmetry introduced above. To do so, we need the following notation: $\text{vech}(\mathbf{A})$ for the $(p(p+1)/2)$ -dimensional vector stacking the upper-triangular entries of a $p \times p$ symmetric matrix $\mathbf{A} = (A_{ij})$; $\mathring{\text{vech}}(\mathbf{A})$ for $\text{vech}(\mathbf{A})$ with the first entry (A_{11}) excluded; \mathbf{M}_p for the matrix satisfying $\mathbf{M}_p^T \mathring{\text{vech}}(\mathbf{A}) = \text{vec}(\mathbf{A})$ for any $p \times p$ symmetric matrix \mathbf{A} with $\text{tr}[\mathbf{A}] = 0$; $\mathbf{J}_p := \sum_{i,j=1}^p (\mathbf{e}_{p,i} \mathbf{e}_{p,j}^T) \otimes (\mathbf{e}_{p,i} \mathbf{e}_{p,j}^T) = (\text{vec} \mathbf{I}_p) (\text{vec} \mathbf{I}_p)^T$; $\mathbf{K}_p := \sum_{i,j=1}^p (\mathbf{e}_{p,i} \mathbf{e}_{p,j}^T) \otimes (\mathbf{e}_{p,j} \mathbf{e}_{p,i}^T)$ for the *commutation matrix*, where $\mathbf{e}_{p,\ell}$ denotes the ℓ -th vector of the canonical basis of \mathbb{R}^p . Since the shape matrix $\boldsymbol{\Lambda}$ of a tangent elliptical distribution is symmetric and satisfies $\text{tr}[\boldsymbol{\Lambda}] = p-1$, it is completely characterized by $\mathring{\text{vech}}(\boldsymbol{\Lambda})$. Throughout, we let $V_{i,\boldsymbol{\theta}} := v_{\boldsymbol{\theta}}(\mathbf{X}_i) = \mathbf{X}_i^T \boldsymbol{\theta}$ and we denote as $\chi_{\nu}^2(\lambda)$ the chi-square distribution with ν degrees of freedom and non-centrality parameter λ (so that $\chi_{\nu}^2(0) \stackrel{\mathcal{D}}{=} \chi_{\nu}^2$).

In order to examine log-likelihood ratios involving the angular functions g , we need to assume some regularity conditions on g . More precisely, we will restrict to the collection \mathcal{G}_a of non-constant angular functions $g : [-1, 1] \rightarrow (0, \infty)$ that are absolutely continuous and for which $\mathcal{J}_p(g) := \int_{-1}^1 \varphi_g^2(t)(1-t^2)\tilde{g}_p(t) dt$ is finite, where $\varphi_g := \dot{g}/g$ involves the almost everywhere derivative \dot{g} of g .

Consider then the semiparametric model $\{P_{\boldsymbol{\theta}, g, \boldsymbol{\Lambda}}^{\mathcal{T}\mathcal{E}(n)} : \boldsymbol{\theta} \in \mathcal{S}^{p-1}, g \in \mathcal{G}_a, \boldsymbol{\Lambda} \in \mathcal{L}^{p-1}\}$, where $P_{\boldsymbol{\theta}, g, \boldsymbol{\Lambda}}^{\mathcal{T}\mathcal{E}(n)}$ denotes the probability measure associated with observations $\mathbf{X}_1, \dots, \mathbf{X}_n$ that are randomly sampled from the tangent elliptical distribution $\mathcal{T}\mathcal{E}_p(\boldsymbol{\theta}, g, \boldsymbol{\Lambda})$. In the rotationally symmetric case, that is, for $\boldsymbol{\Lambda} = \mathbf{I}_{p-1}$, we will simply write $P_{\boldsymbol{\theta}, g}^{(n)}$ instead of $P_{\boldsymbol{\theta}, g, \mathbf{I}_{p-1}}^{\mathcal{T}\mathcal{E}(n)}$. Investigating the optimality of tests of rotational symmetry against tangent elliptical alternatives requires studying the asymptotic behavior of tangent elliptical log-likelihood ratios associated with local deviations from $\boldsymbol{\Lambda} = \mathbf{I}_{p-1}$. This leads to the following *Local Asymptotic Normality* (LAN) result.

Theorem 3. Fix $\boldsymbol{\theta} \in \mathcal{S}^{p-1}$ and $g \in \mathcal{G}_a$. Let $\boldsymbol{\tau}_n := (\mathbf{t}_n^T, \mathring{\text{vech}}(\mathbf{L}_n)^T)^T$, where (\mathbf{t}_n) is a bounded sequence in \mathbb{R}^p such that $\boldsymbol{\theta}_n := \boldsymbol{\theta} + n^{-1/2} \mathbf{t}_n \in \mathcal{S}^{p-1}$ for any n , and where (\mathbf{L}_n) is a bounded sequence of $(p-1) \times (p-1)$ matrices such that $\boldsymbol{\Lambda}_n := \mathbf{I}_{p-1} + n^{-1/2} \mathbf{L}_n \in \mathcal{L}_{p-1}$ for any n . Then, the tangent elliptical log-likelihood ratio associated with local deviations $\boldsymbol{\Lambda}_n$ from $\boldsymbol{\Lambda} = \mathbf{I}_{p-1}$ satisfies

$$\log \frac{dP_{\boldsymbol{\theta}_n, g, \boldsymbol{\Lambda}_n}^{\mathcal{T}\mathcal{E}(n)}}{dP_{\boldsymbol{\theta}, g}^{(n)}} = \boldsymbol{\tau}_n^T \boldsymbol{\Delta}_{\boldsymbol{\theta}, g}^{\mathcal{T}\mathcal{E}(n)} - \frac{1}{2} \boldsymbol{\tau}_n^T \boldsymbol{\Gamma}_{\boldsymbol{\theta}, g}^{\mathcal{T}\mathcal{E}} \boldsymbol{\tau}_n + o_P(1) \quad (8)$$

as $n \rightarrow \infty$ under $P_{\theta,g}^{(n)}$, where the central sequence

$$\Delta_{\theta,g}^{\mathcal{T}\mathcal{E}(n)} := \begin{pmatrix} \Delta_{\theta,g;1}^{(n)} \\ \Delta_{\theta;2}^{\mathcal{T}\mathcal{E}(n)} \end{pmatrix} := \begin{pmatrix} \frac{1}{\sqrt{n}} \sum_{i=1}^n \varphi_g(V_{i,\theta})(1 - V_{i,\theta}^2)^{1/2} \mathbf{\Gamma}_{\theta} \mathbf{U}_{i,\theta} \\ \frac{p-1}{2\sqrt{n}} \mathbf{M}_p \sum_{i=1}^n \text{vec}(\mathbf{U}_{i,\theta} \mathbf{U}_{i,\theta}^T - \frac{1}{p-1} \mathbf{I}_{p-1}) \end{pmatrix}$$

is, still under $P_{\theta,g}^{(n)}$, asymptotically normal with mean zero and covariance matrix

$$\mathbf{\Gamma}_{\theta,g}^{\mathcal{T}\mathcal{E}} := \begin{pmatrix} \mathbf{\Gamma}_{\theta,g;11} & \mathbf{0} \\ \mathbf{0} & \mathbf{\Gamma}_{\theta;22}^{\mathcal{T}\mathcal{E}} \end{pmatrix} := \begin{pmatrix} \frac{\mathcal{J}_p(g)}{p-1} (\mathbf{I}_p - \theta\theta^T) & \mathbf{0} \\ \mathbf{0} & \frac{p-1}{4(p+1)} \mathbf{M}_p (\mathbf{I}_{(p-1)^2} + \mathbf{K}_{p-1}) \mathbf{M}_p^T \end{pmatrix}.$$

The restriction that $g \in \mathcal{G}_a$ guarantees that the g -parametric submodel of the tangent elliptical model has a finite Fisher information for θ in the vicinity of rotational symmetry. Any LAN result requires a finite Fisher information condition of this sort (along with a smoothness condition that allows defining Fisher information). The LAN result in Theorem 3 easily provides the following corollary.

Corollary 1. Fix $\theta \in \mathcal{S}^{p-1}$ and $g \in \mathcal{G}_a$. Let $(\mathbf{\Lambda}_n)$ and (\mathbf{L}_n) be as in Theorem 3, now with $\mathbf{L}_n \rightarrow \mathbf{L} \neq \mathbf{0}$. Then, under $P_{\theta,g,\mathbf{\Lambda}_n}^{\mathcal{T}\mathcal{E}(n)}$: (i) $Q_{\theta}^{\text{loc}} \xrightarrow{\mathcal{D}} \chi_{p-1}^2$; (ii) $Q_{\theta}^{\text{sc}} \xrightarrow{\mathcal{D}} \chi_{(p-2)(p+1)/2}^2(\lambda)$, with $\lambda = (p-1)\text{tr}[\mathbf{L}^2]/(2(p+1))$.

First note that (i) implies that, for the local alternatives considered, the null and non-null asymptotic distributions of Q_{θ}^{loc} do coincide, so that the test $\phi_{\theta}^{\text{loc}}$ has asymptotic power α against such alternatives. On the contrary, (ii) shows that the test $\phi_{\theta}^{\text{sc}}$ exhibits non-trivial asymptotic powers against any alternatives associated with $\mathbf{\Lambda}_n = \mathbf{I}_{p-1} + n^{-1/2} \mathbf{L}_n$, $\mathbf{L}_n \rightarrow \mathbf{L} \neq \mathbf{0}$ (note indeed that $\text{tr}[\mathbf{L}^2]$ is the squared Frobenius norm of \mathbf{L}). Note also that, since \mathbf{L} has trace zero by construction, the non-centrality parameter $(p-1)\text{tr}[\mathbf{L}^2]/(2(p+1))$ above is proportional to the variance of the eigenvalues of \mathbf{L} , which is in line with the fact that $\phi_{\theta}^{\text{sc}}$ has the nature of a sphericity test.

While Corollary 1 shows that the test $\phi_{\theta}^{\text{sc}}$ can detect local alternatives of a tangent elliptical nature, it does not provide information on the possible optimality of this test. General results on the Le Cam's asymptotic theory of statistical experiments (see, e.g., Chapter 5 of Ley and Verdebou, 2017a) together with Theorem 3 directly entail that, when testing $\{P_{\theta,g}^{(n)}\}$ against $\bigcup_{\mathbf{\Lambda} \in \mathcal{L}_{p-1} \setminus \{\mathbf{I}_p\}} \{P_{\theta,g,\mathbf{\Lambda}}^{\mathcal{T}\mathcal{E}(n)}\}$, a locally asymptotically maximin test at asymptotic level α rejects the null whenever

$$Q_{\theta}^{\text{sc}} = (\Delta_{\theta;2}^{\mathcal{T}\mathcal{E}(n)})^T (\mathbf{\Gamma}_{\theta;22}^{\mathcal{T}\mathcal{E}})^{-1} \Delta_{\theta;2}^{\mathcal{T}\mathcal{E}(n)} > \chi_{(p-2)(p+1)/2, 1-\alpha}^2. \quad (9)$$

Now, using the closed form for the inverse of $\mathbf{\Gamma}_{\theta;22}^{\mathcal{T}\mathcal{E}}$ in Lemma 5.2 from Hallin and Paindaveine (2006a), it is easy to show that the test statistic in (9) coincides with Q_{θ}^{sc} . Since this holds at any angular function g in \mathcal{G}_a , we proved the following result.

Corollary 2. When testing $\bigcup_{g \in \mathcal{G}_a} \{P_{\theta,g}^{(n)}\}$ against $\bigcup_{g \in \mathcal{G}_a} \bigcup_{\mathbf{\Lambda} \in \mathcal{L}_{p-1} \setminus \{\mathbf{I}_p\}} \{P_{\theta,g,\mathbf{\Lambda}}^{\mathcal{T}\mathcal{E}(n)}\}$, the test $\phi_{\theta}^{\text{sc}}$ is locally asymptotically maximin at asymptotic level α .

We conclude that, when testing rotational symmetry about a specified location θ against tangent elliptical alternatives, the location test Q_{θ}^{loc} does not show any power, while the scatter test Q_{θ}^{sc} is optimal in the Le Cam sense, at any angular function $g \in \mathcal{G}_a$.

2.4 Non-null results under tangent vMF alternatives

To investigate the non-null behavior of the proposed tests under tangent vMF alternatives, we consider the semiparametric model $\{P_{\theta,g,\mu,\kappa}^{\mathcal{T}\mathcal{M}(n)} : \theta \in \mathcal{S}^{p-1}, g \in \mathcal{G}_a, \mu \in \mathcal{S}^{p-2}, \kappa \geq 0\}$, where $P_{\theta,g,\mu,\kappa}^{\mathcal{T}\mathcal{M}(n)}$ denotes the probability measure associated with observations $\mathbf{X}_1, \dots, \mathbf{X}_n$ that are randomly sampled

from the tangent vMF distribution $\mathcal{T}\mathcal{M}_p(\boldsymbol{\theta}, g, \boldsymbol{\mu}, \kappa)$; for $\kappa = 0$, $P_{\boldsymbol{\theta}, g, \boldsymbol{\mu}, \kappa}^{\mathcal{T}\mathcal{M}(n)}$ is defined as the rotationally symmetric hypothesis $P_{\boldsymbol{\theta}, g}^{(n)}$ (see the notation introduced in Section 2.3). To investigate the optimality properties of tests of rotational symmetry against such alternatives, it is convenient to parametrize this model with $\boldsymbol{\theta}$, g , and $\boldsymbol{\delta}$, where we let $\boldsymbol{\delta} := \kappa \boldsymbol{\mu}$; obviously, we will then use the notation $P_{\boldsymbol{\theta}, g, \boldsymbol{\delta}}^{\mathcal{T}\mathcal{M}(n)}$. In this new parametrization, the null hypothesis of rotational symmetry about $\boldsymbol{\theta}$ coincides with $\mathcal{H}_{0, \boldsymbol{\theta}} : \boldsymbol{\delta} = \mathbf{0}$. The main advantage of the parametrization in $\boldsymbol{\delta} \in \mathbb{R}^{p-1}$ over the original one in $(\kappa, \boldsymbol{\mu}) \in [0, \infty) \times \mathcal{S}^{p-2}$ is that the $\boldsymbol{\delta}$ -parameter space is standard (it is the Euclidean space \mathbb{R}^{p-1}), while the $(\kappa, \boldsymbol{\mu})$ -one is curved.

As for tangent elliptical distributions, our investigation of optimality issues is based on a LAN result.

Theorem 4. *Fix $\boldsymbol{\theta} \in \mathcal{S}^{p-1}$ and $g \in \mathcal{G}_a$. Let $\boldsymbol{\tau}_n := (\mathbf{t}_n^T, \mathbf{d}_n^T)^T$, where (\mathbf{t}_n) is a bounded sequence in \mathbb{R}^p such that $\boldsymbol{\theta}_n := \boldsymbol{\theta} + n^{-1/2} \mathbf{t}_n \in \mathcal{S}^{p-1}$ for any n , and $\boldsymbol{\delta}_n := n^{-1/2} \mathbf{d}_n$ with (\mathbf{d}_n) a bounded sequence in \mathbb{R}^{p-1} . Then, the tangent vMF log-likelihood ratio associated with local deviations $\boldsymbol{\delta}_n$ from $\boldsymbol{\delta} = \mathbf{0}$ is*

$$\log \frac{dP_{\boldsymbol{\theta}_n, g, \boldsymbol{\delta}_n}^{\mathcal{T}\mathcal{M}(n)}}{dP_{\boldsymbol{\theta}, g}^{(n)}} = \boldsymbol{\tau}_n^T \boldsymbol{\Delta}_{\boldsymbol{\theta}, g}^{\mathcal{T}\mathcal{M}(n)} - \frac{1}{2} \boldsymbol{\tau}_n^T \boldsymbol{\Gamma}_{\boldsymbol{\theta}, g}^{\mathcal{T}\mathcal{M}} \boldsymbol{\tau}_n + o_P(1),$$

as $n \rightarrow \infty$ under $P_{\boldsymbol{\theta}, g}^{(n)}$, where the central sequence

$$\boldsymbol{\Delta}_{\boldsymbol{\theta}, g}^{\mathcal{T}\mathcal{M}(n)} := \begin{pmatrix} \boldsymbol{\Delta}_{\boldsymbol{\theta}, g; 1}^{(n)} \\ \boldsymbol{\Delta}_{\boldsymbol{\theta}; 2}^{\mathcal{T}\mathcal{M}(n)} \end{pmatrix} := \begin{pmatrix} \frac{1}{\sqrt{n}} \sum_{i=1}^n \varphi_g(V_{i, \boldsymbol{\theta}})(1 - V_{i, \boldsymbol{\theta}}^2)^{1/2} \boldsymbol{\Gamma}_{\boldsymbol{\theta}} \mathbf{U}_{i, \boldsymbol{\theta}} \\ \frac{1}{\sqrt{n}} \sum_{i=1}^n \mathbf{U}_{i, \boldsymbol{\theta}} \end{pmatrix}$$

is, still under $P_{\boldsymbol{\theta}, g}^{(n)}$, asymptotically normal with mean zero and covariance matrix

$$\boldsymbol{\Gamma}_{\boldsymbol{\theta}, g}^{\mathcal{T}\mathcal{M}} := \begin{pmatrix} \boldsymbol{\Gamma}_{\boldsymbol{\theta}, g; 11} & \boldsymbol{\Gamma}_{\boldsymbol{\theta}, g; 12}^{\mathcal{T}\mathcal{M}} \\ \boldsymbol{\Gamma}_{\boldsymbol{\theta}, g; 21}^{\mathcal{T}\mathcal{M}} & \boldsymbol{\Gamma}_{22}^{\mathcal{T}\mathcal{M}} \end{pmatrix} := \begin{pmatrix} \frac{\mathcal{J}_p(g)}{p-1} (\mathbf{I}_p - \boldsymbol{\theta} \boldsymbol{\theta}^T) & \frac{\mathcal{I}_p(g)}{p-1} \boldsymbol{\Gamma}_{\boldsymbol{\theta}} \\ \frac{\mathcal{I}_p(g)}{p-1} \boldsymbol{\Gamma}_{\boldsymbol{\theta}}^T & \frac{1}{p-1} \mathbf{I}_{p-1} \end{pmatrix},$$

with $\mathcal{I}_p(g) := \int_{-1}^1 \varphi_g(t) \sqrt{1-t^2} \tilde{g}_p(t) dt$.

Unlike for the LAN property in Theorem 3, the Fisher information matrix associated with the LAN property above, namely $\boldsymbol{\Gamma}_{\boldsymbol{\theta}, g}^{\mathcal{T}\mathcal{M}}$, is not block-diagonal. Also, Jensen's inequality ensures that $\mathcal{J}_p(g) \geq \mathcal{I}_p^2(g)$, which confirms the finiteness of $\mathcal{I}_p(g)$ and the positive semidefiniteness of $\boldsymbol{\Gamma}_{\boldsymbol{\theta}, g}^{\mathcal{T}\mathcal{M}}$. It is also easy to check that the *only* angular functions for which Jensen's inequality is actually an equality (hence, for which $\boldsymbol{\Gamma}_{\boldsymbol{\theta}, g}^{\mathcal{T}\mathcal{M}}$ is singular) are of the form $g(t) = C \exp(\kappa \arcsin(t))$ for some real constants C and κ .

Corollary 3. *Fix $\boldsymbol{\theta} \in \mathcal{S}^{p-1}$ and $g \in \mathcal{G}_a$. Let $(\boldsymbol{\mu}_n)$ be a sequence in \mathcal{S}^{p-2} that converges to $\boldsymbol{\mu}$. Let $\kappa_n := n^{-1/2} k_n$, where (k_n) is a sequence in $(0, \infty)$ that converges to $k > 0$. Then, under $P_{\boldsymbol{\theta}, g, \boldsymbol{\mu}_n, \kappa_n}^{\mathcal{T}\mathcal{M}(n)}$:*

(i) $Q_{\boldsymbol{\theta}}^{\text{loc}} \xrightarrow{\mathcal{D}} \chi_{p-1}^2(\lambda)$, with $\lambda = k^2/(p-1)$; (ii) $Q_{\boldsymbol{\theta}}^{\text{sc}} \xrightarrow{\mathcal{D}} \chi_{(p-2)(p+1)/2}^2$.

The location test $\phi_{\boldsymbol{\theta}}^{\text{loc}}$ and the scatter test $\phi_{\boldsymbol{\theta}}^{\text{sc}}$ therefore exhibit opposite non-null behaviors under tangent vMF alternatives, compared to what occurs under tangent elliptical alternatives in Section 2.3: under tangent vMF alternatives, $\phi_{\boldsymbol{\theta}}^{\text{sc}}$ has asymptotic power equal to the nominal level α , whereas $\phi_{\boldsymbol{\theta}}^{\text{loc}}$ shows non-trivial asymptotic powers. Since the latter test is the test rejecting the null hypothesis of rotational symmetry about $\boldsymbol{\theta}$ whenever

$$Q_{\boldsymbol{\theta}}^{\text{loc}} = (\boldsymbol{\Delta}_{\boldsymbol{\theta}; 2}^{\mathcal{T}\mathcal{M}(n)})^T (\boldsymbol{\Gamma}_{22}^{\mathcal{T}\mathcal{M}})^{-1} \boldsymbol{\Delta}_{\boldsymbol{\theta}; 2}^{\mathcal{T}\mathcal{M}(n)} > \chi_{p-1, 1-\alpha}^2,$$

it is actually locally asymptotically maximin at asymptotic level α when testing $\{P_{\boldsymbol{\theta}, g}^{(n)}\}$ against $\bigcup_{\boldsymbol{\mu} \in \mathcal{S}^{p-2}} \bigcup_{\kappa > 0} \{P_{\boldsymbol{\theta}, g, \boldsymbol{\mu}, \kappa}^{\mathcal{T}\mathcal{M}(n)}\}$. Moreover, since $Q_{\boldsymbol{\theta}}^{\text{loc}}$ does not depend on g , we have the following result.

Corollary 4. *When testing $\bigcup_{g \in \mathcal{G}_a} \{P_{\boldsymbol{\theta},g}^{(n)}\}$ against $\bigcup_{g \in \mathcal{G}_a} \bigcup_{\boldsymbol{\mu} \in \mathcal{S}^{p-2}} \bigcup_{\kappa > 0} \{P_{\boldsymbol{\theta},g,\boldsymbol{\mu},\kappa}^{\mathcal{T}\mathcal{M}(n)}\}$, the test $Q_{\boldsymbol{\theta}}^{\text{loc}}$ is locally asymptotically maximin at asymptotic level α .*

We conclude that the location test $\phi_{\boldsymbol{\theta}}^{\text{loc}}$ and the scatter test $\phi_{\boldsymbol{\theta}}^{\text{sc}}$ are optimal in the Le Cam sense, for any angular function in $g \in \mathcal{G}_a$, against tangent vMF alternatives and tangent elliptical alternatives, respectively.

3 Testing rotational symmetry about an unspecified $\boldsymbol{\theta}$

The tests $\phi_{\boldsymbol{\theta}}^{\text{loc}}$ and $\phi_{\boldsymbol{\theta}}^{\text{sc}}$ studied above allow testing for rotational symmetry about a given location $\boldsymbol{\theta}$. Often, however, it is desirable to rather test for rotational symmetry about an unspecified $\boldsymbol{\theta}$. Natural tests for this unspecified- $\boldsymbol{\theta}$ problem are obtained by substituting an estimator $\hat{\boldsymbol{\theta}}$ for $\boldsymbol{\theta}$ in $\phi_{\boldsymbol{\theta}}^{\text{loc}}$ and $\phi_{\boldsymbol{\theta}}^{\text{sc}}$. In the present ULAN framework (it is easy to strengthen the LAN results in Theorems 3–4 into ULAN—*Uniformly Locally Asymptotically Normal*—ones), this estimator $\hat{\boldsymbol{\theta}}$ should actually satisfy the following assumption:

$A_{\mathcal{G}'}$ The estimator $\hat{\boldsymbol{\theta}}$ (with values in \mathcal{S}^{p-1}) is part of a sequence that is: (i) *root- n consistent* under any $g \in \mathcal{G}'$, i.e., $\sqrt{n}(\hat{\boldsymbol{\theta}} - \boldsymbol{\theta}) = O_P(1)$ under $\bigcup_{g \in \mathcal{G}'} \{P_{\boldsymbol{\theta},g}^{(n)}\}$; (ii) *locally and asymptotically discrete*, i.e., for all $\boldsymbol{\theta}$ and for all $C > 0$, there exists a positive integer $M = M(C)$ such that the number of possible values of $\hat{\boldsymbol{\theta}}$ in $\{\mathbf{t} \in \mathcal{S}^{p-1} : \sqrt{n}\|\mathbf{t} - \boldsymbol{\theta}\| \leq C\}$ is bounded by M , uniformly as $n \rightarrow \infty$.

Part (i) of Assumption $A_{\mathcal{G}'}$ requires that $\hat{\boldsymbol{\theta}}$ is root- n consistent under the null hypothesis for a broad range \mathcal{G}' of angular functions g . The restriction to such a \mathcal{G}' is explained by the fact that classical estimators of $\boldsymbol{\theta}$ typically address either monotone rotationally symmetric distributions (g is monotone increasing) or axial ones ($g(-t) = g(t)$ for any t), but cannot deal with both types. Practitioners are thus expected to take \mathcal{G}' as the collection of monotone or symmetric angular functions, depending on the types of directional data (unimodal or axial data) they are facing. In the unimodal case, the classical choice is the *spherical mean* $\hat{\boldsymbol{\theta}} = \bar{\mathbf{X}}/\|\bar{\mathbf{X}}\|$, with $\bar{\mathbf{X}} := \frac{1}{n} \sum_{i=1}^n \mathbf{X}_i$, whereas, in the axial case, estimators of $\boldsymbol{\theta}$ are typically based on the eigenvectors of the covariance matrix $\mathbf{S} := \frac{1}{n} \sum_{i=1}^n (\mathbf{X}_i - \bar{\mathbf{X}})(\mathbf{X}_i - \bar{\mathbf{X}})^T$. As for part (ii), it is a purely technical requirement with little practical implications in the sense that, for fixed n , any estimate can be considered part of a locally and asymptotically discrete sequence of estimators; see, e.g., page 2467 in Ilmonen and Paindaveine (2011) for a discussion.

Now, the impact of plugging an estimator $\hat{\boldsymbol{\theta}}$ satisfying Assumption $A_{\mathcal{G}'}$ in our specified- $\boldsymbol{\theta}$ tests crucially depends on the tests considered. We first focus on scatter tests.

3.1 Scatter tests

The block-diagonality of the Fisher information matrix in Theorem 3 entails that the replacement in $Q_{\boldsymbol{\theta}}^{\text{sc}}$ of $\boldsymbol{\theta}$ with an estimator $\hat{\boldsymbol{\theta}}$ satisfying $A_{\mathcal{G}'}$ has no asymptotic impact under the null hypothesis. More precisely, we have the following result.

Proposition 1. *Let $\hat{\boldsymbol{\theta}}$ satisfy $A_{\mathcal{G}'}$. Then, for any $\boldsymbol{\theta} \in \mathcal{S}^{p-1}$ and any $g \in \mathcal{G}_a \cap \mathcal{G}'$, $Q_{\hat{\boldsymbol{\theta}}}^{\text{sc}} - Q_{\boldsymbol{\theta}}^{\text{sc}} = o_P(1)$ as $n \rightarrow \infty$ under $P_{\boldsymbol{\theta},g}^{(n)}$.*

From contiguity, the null asymptotic equivalence in this proposition extends to local alternatives of the form $P_{\boldsymbol{\theta},g,\boldsymbol{\Lambda}_n}^{\mathcal{T}\mathcal{E}(n)}$, with $\boldsymbol{\Lambda}_n = \mathbf{I}_{p-1} + n^{-1/2}\mathbf{L}_n$ as in Theorem 3. Therefore, the test, $\phi_{\dagger}^{\text{sc}}$ say, that rejects the null of rotational symmetry about an unspecified location when $Q_{\hat{\boldsymbol{\theta}}}^{\text{sc}} > \chi_{(p-2)(p+1)/2,1-\alpha}^2$ remains optimal in the Le Cam sense against the tangent elliptical alternatives introduced in Section 2.2. More precisely, this test is locally asymptotically maximin at asymptotic level α when testing $\bigcup_{\boldsymbol{\theta} \in \mathcal{S}^{p-1}} \bigcup_{g \in \mathcal{G}_a \cap \mathcal{G}'} \{P_{\boldsymbol{\theta},g}^{(n)}\}$ against $\bigcup_{\boldsymbol{\theta} \in \mathcal{S}^{p-1}} \bigcup_{g \in \mathcal{G}_a \cap \mathcal{G}'} \bigcup_{\boldsymbol{\Lambda} \in \mathcal{L}_{p-1} \setminus \{\mathbf{I}_p\}} \{P_{\boldsymbol{\theta},g,\boldsymbol{\Lambda}}^{\mathcal{T}\mathcal{E}(n)}\}$. Of course, the

same contiguity argument also implies that $\phi_{\dagger}^{\text{sc}}$ has asymptotic power α against the local tangent vMF alternatives considered in Corollary 3.

3.2 Location tests

Since, on the contrary, the Fisher information matrix is not block-diagonal in Theorem 4, the story is very different for location tests. The ULAN extension of this theorem yields that, if $\hat{\boldsymbol{\theta}}$ satisfies Assumption A $_{\mathcal{G}'}$, then

$$\Delta_{\hat{\boldsymbol{\theta}};2}^{\mathcal{T}\mathcal{M}(n)} - \Delta_{\boldsymbol{\theta};2}^{\mathcal{T}\mathcal{M}(n)} = -\boldsymbol{\Gamma}_{\boldsymbol{\theta},g;21}^{\mathcal{T}\mathcal{M}} \sqrt{n}(\hat{\boldsymbol{\theta}} - \boldsymbol{\theta}) + o_P(1) \quad (10)$$

as $n \rightarrow \infty$ under $P_{\boldsymbol{\theta},g}^{(n)}$, with $g \in \mathcal{G}_a \cap \mathcal{G}'$, so that $Q_{\hat{\boldsymbol{\theta}}}^{\text{loc}}$ is no more asymptotically chi-square distributed under the same sequence of (null) hypotheses. Unlike for $Q_{\boldsymbol{\theta}}^{\text{sc}}$, thus, the substitution of $\hat{\boldsymbol{\theta}}$ for $\boldsymbol{\theta}$ in $Q_{\boldsymbol{\theta}}^{\text{loc}}$ unfortunately has a non-negligible asymptotic impact. The non-block-diagonality of the Fisher information matrix in Theorem 4 also implies that the optimal unspecified- $\boldsymbol{\theta}$ location tests will show asymptotic powers under contiguous alternatives that are strictly smaller than those of the corresponding specified- $\boldsymbol{\theta}$ tests.

The construction of these optimal unspecified- $\boldsymbol{\theta}$ location tests relies on *efficient central sequences* and is very technical, hence is deferred to the supplementary material. Here, we only describe the vMF version of the resulting tests and state its main properties. This vMF test, $\phi_{\text{vMF}}^{\text{loc}}$ say, rejects the null hypothesis of rotational symmetry about an unspecified $\boldsymbol{\theta}$ whenever

$$Q_{\text{vMF}}^{\text{loc}} := \hat{\boldsymbol{\Delta}}^T \hat{\boldsymbol{\Gamma}}^{-1} \hat{\boldsymbol{\Delta}} > \chi_{p-1,1-\alpha}^2,$$

where

$$\hat{\boldsymbol{\Delta}} := \frac{1}{\sqrt{n}} \sum_{i=1}^n \left(1 - \hat{D}_p (1 - V_{i,\hat{\boldsymbol{\theta}}}^2)^{1/2} \right) \mathbf{U}_{i,\hat{\boldsymbol{\theta}}} \quad \text{and} \quad \hat{\boldsymbol{\Gamma}} := \frac{1}{p-1} \left(1 - 2\hat{D}_p \hat{E}_p + \hat{D}_p^2 (1 - \hat{F}_p) \right) \mathbf{I}_{p-1}$$

involve the quantities

$$\hat{D}_p := \frac{(p-2) \sum_{i=1}^n V_{i,\hat{\boldsymbol{\theta}}} (1 - V_{i,\hat{\boldsymbol{\theta}}}^2)^{-1/2}}{(p-1) \sum_{i=1}^n V_{i,\hat{\boldsymbol{\theta}}}}, \quad \hat{E}_p := \frac{1}{n} \sum_{i=1}^n (1 - V_{i,\hat{\boldsymbol{\theta}}}^2)^{1/2}, \quad \text{and} \quad \hat{F}_p := \frac{1}{n} \sum_{i=1}^n V_{i,\hat{\boldsymbol{\theta}}}^2.$$

Denoting as \mathcal{G}_b the collection of angular functions g for which $\int_{-1}^1 t(1-t^2)^{-1/2} \tilde{g}_p(t) dt < \infty$ (note that, for any $p \geq 3$, \mathcal{G}_b contains all angular functions g that are bounded in a neighborhood of ± 1), we show in the supplementary material that $\phi_{\text{vMF}}^{\text{loc}}$ is optimal in the Le Cam sense (more precisely, it is locally asymptotically maximin) at asymptotic level α when testing

$$\bigcup_{\boldsymbol{\theta} \in \mathcal{S}^{p-1}} \bigcup_{g \in \mathcal{G}_a \cap \mathcal{G}_b \cap \mathcal{G}'} \{P_{\boldsymbol{\theta},g}^{(n)}\} \quad \text{against} \quad \bigcup_{\boldsymbol{\theta} \in \mathcal{S}^{p-1}} \bigcup_{\eta > 0} \bigcup_{\boldsymbol{\mu} \in \mathcal{S}^{p-2}} \bigcup_{\kappa > 0} \{P_{\boldsymbol{\theta},g_{\eta},\boldsymbol{\mu},\kappa}^{\mathcal{T}\mathcal{M}(n)}\},$$

with $g_{\eta}(t) := \exp(\eta t)$. This vMF test therefore meets the asymptotic level constraint under all rotational symmetric densities and achieves Le Cam optimality against any tangent vMF alternatives involving a vMF angular density g . It is easy to show, however, that this test still has asymptotic power α against the local tangent elliptical alternatives considered in Corollary 1.

4 Hybrid tests

The location and scatter tests, either in the specified- $\boldsymbol{\theta}$ or unspecified- $\boldsymbol{\theta}$ situations, are based on the empirical checking of the moment conditions in (3). Both are necessary conditions for the uniformity of $\mathbf{u}_{\boldsymbol{\theta}}(\mathbf{X})$ over \mathcal{S}^{p-2} , hence for rotational symmetry. For the families of alternatives introduced in Section 2.2, the tests present rather extreme behaviors: either they are optimal (in the Le Cam sense), or they are blind to the alternatives. While this antithesis is desirable for testing against a specific kind of alternative, it is also a double-edged sword, since knowing the alternative on which rotational symmetry might be violated can be challenging in practice, specially for high-dimensional settings. As we explain below, a possible way out is to construct *hybrid* tests that show non-trivial asymptotic powers against both types of alternatives considered.

Consider first the problem of testing rotational symmetry about a specified location $\boldsymbol{\theta}$. Since $\mathbf{U}_{i,\boldsymbol{\theta}}$ and $\text{vec}(\mathbf{U}_{i,\boldsymbol{\theta}}\mathbf{U}_{i,\boldsymbol{\theta}}^T)$ are uncorrelated, $\Delta_{\boldsymbol{\theta};2}^{\mathcal{T}\mathcal{M}(n)}$ and $\Delta_{\boldsymbol{\theta};2}^{\mathcal{T}\mathcal{E}(n)}$ are uncorrelated, too. The CLT then readily entails that, under $P_{\boldsymbol{\theta},g}^{(n)}$,

$$\begin{pmatrix} \Delta_{\boldsymbol{\theta};2}^{\mathcal{T}\mathcal{M}(n)} \\ \Delta_{\boldsymbol{\theta};2}^{\mathcal{T}\mathcal{E}(n)} \end{pmatrix} \xrightarrow{\mathcal{D}} \mathcal{N}\left(\begin{pmatrix} \mathbf{0} \\ \mathbf{0} \end{pmatrix}, \begin{pmatrix} \boldsymbol{\Gamma}_{22}^{\mathcal{T}\mathcal{M}} & \mathbf{0} \\ \mathbf{0} & \boldsymbol{\Gamma}_{\boldsymbol{\theta};22}^{\mathcal{T}\mathcal{E}} \end{pmatrix}\right),$$

which implies that, under $\mathcal{H}_{0,\boldsymbol{\theta}}$,

$$\begin{aligned} Q_{\boldsymbol{\theta}}^{\text{hyb}} := Q_{\boldsymbol{\theta}}^{\text{loc}} + Q_{\boldsymbol{\theta}}^{\text{sc}} &= (\Delta_{\boldsymbol{\theta};2}^{\mathcal{T}\mathcal{M}(n)})^T (\boldsymbol{\Gamma}_{22}^{\mathcal{T}\mathcal{M}})^{-1} \Delta_{\boldsymbol{\theta};2}^{\mathcal{T}\mathcal{M}(n)} + (\Delta_{\boldsymbol{\theta};2}^{\mathcal{T}\mathcal{E}(n)})^T (\boldsymbol{\Gamma}_{\boldsymbol{\theta};22}^{\mathcal{T}\mathcal{E}})^{-1} \Delta_{\boldsymbol{\theta};2}^{\mathcal{T}\mathcal{E}(n)} \\ &\xrightarrow{\mathcal{D}} \chi_{(p-1)+(p-2)(p+1)/2}^2. \end{aligned}$$

The resulting hybrid test, $\phi_{\boldsymbol{\theta}}^{\text{hyb}}$ say, then rejects the null hypothesis at asymptotic level α whenever $Q_{\boldsymbol{\theta}}^{\text{hyb}} > \chi_{(p-1)+(p-2)(p+1)/2,1-\alpha}^2$. In a high-dimensional asymptotic framework where $p = p_n$ goes to infinity with n (still at an arbitrary rate), we have that, under the null hypothesis of rotational symmetry about $\boldsymbol{\theta}$,

$$\frac{Q_{\boldsymbol{\theta}}^{\text{hyb}} - \frac{p_n(p_n+1)-4}{2}}{\sqrt{p_n(p_n+1)-4}} \xrightarrow{\mathcal{D}} \mathcal{N}(0, 1).$$

This can be obtained by using the same CLT for martingale differences that was used in Paindaveine and Verdebout (2016); see Section 2.1 for a discussion. Coming back to the low-dimensional setup, this test, as announced, can detect both contiguous tangent elliptical and tangent vMF alternatives.

Corollary 5. Fix $\boldsymbol{\theta} \in \mathcal{S}^{p-1}$ and $g \in \mathcal{G}_a$. Let $(\boldsymbol{\Lambda}_n)$, (\mathbf{L}_n) , (κ_n) , and (k_n) be as in Corollaries 1 and 3. Then: (i) under $P_{\boldsymbol{\theta},g,\boldsymbol{\Lambda}_n}^{\mathcal{T}\mathcal{E}(n)}$, $Q_{\boldsymbol{\theta}}^{\text{hyb}} \xrightarrow{\mathcal{D}} \chi_{(p-1)+(p-2)(p+1)/2}^2(\lambda)$, with $\lambda = (p-1)\text{tr}[\mathbf{L}^2]/(2(p+1))$; (ii) under $P_{\boldsymbol{\theta},g,\boldsymbol{\mu}_n,\kappa_n}^{\mathcal{T}\mathcal{M}(n)}$, $Q_{\boldsymbol{\theta}}^{\text{hyb}} \xrightarrow{\mathcal{D}} \chi_{(p-1)+(p-2)(p+1)/2}^2(\lambda)$, with $\lambda = k^2/(p-1)$.

The same construction applies in the unspecified- $\boldsymbol{\theta}$ problem, where, under any (null) rotationally symmetric distribution $P_{\boldsymbol{\theta},g}^{(n)}$, the hybrid test statistic $Q_{\text{vMF}}^{\text{hyb}} := Q_{\text{vMF}}^{\text{loc}} + Q_{\boldsymbol{\theta}}^{\text{sc}}$ will be asymptotically $\chi_{(p-1)+(p-2)(p+1)/2}^2$. The resulting test, that rejects the null hypothesis at asymptotic level α when $Q_{\text{vMF}}^{\text{hyb}} > \chi_{(p-1)+(p-2)(p+1)/2,1-\alpha}^2$, will be denoted as $\phi_{\text{vMF}}^{\text{hyb}}$ in the sequel. It is easy to check that, like the specified- $\boldsymbol{\theta}$ test $\phi_{\boldsymbol{\theta}}^{\text{hyb}}$, the test $\phi_{\text{vMF}}^{\text{hyb}}$ can detect both types of alternatives considered.

The aggregation of the tests statistics carried out in the hybrid statistic $Q_{\boldsymbol{\theta}}^{\text{hyb}}$ can of course be performed in other ways. For instance, one could balance equally the contribution of the location

and scatter test statistics by adopting the well-known Fisher's method (Fisher, 1925) for combining independent test statistics. This approach yields, under $\mathcal{H}_{0,\theta}$,

$$\tilde{Q}_{\theta}^{\text{hyb}} := -2 \log(1 - F_{p-1}(Q_{\theta}^{\text{loc}})) - 2 \log(1 - F_{(p-2)(p+1)/2}(Q_{\theta}^{\text{sc}})) \xrightarrow{\mathcal{D}} \chi_4^2, \quad (11)$$

where F_{ν} is the cumulative distribution function of a χ_{ν}^2 . The resulting test, $\tilde{\phi}_{\theta}^{\text{hyb}}$ say, rejects $\mathcal{H}_{0,\theta}$ at asymptotic level α whenever $\tilde{Q}_{\theta}^{\text{hyb}} > \chi_{4,1-\alpha}^2$. For the unspecified- θ case, obvious modifications give $\tilde{\phi}_{\theta}^{\text{hyb}}$, the test that rejects at asymptotic level α whenever $\tilde{Q}_{\text{vMF}}^{\text{hyb}} > \chi_{4,1-\alpha}^2$, where $\tilde{Q}_{\text{vMF}}^{\text{hyb}}$ is obtained by replacing Q_{θ}^{loc} and Q_{θ}^{sc} by $Q_{\text{vMF}}^{\text{loc}}$ and Q_{θ}^{sc} , respectively, in (11). As with the original hybrid tests, these new tests can detect both types of alternatives considered, either in the specified or unspecified- θ cases. Note that, if $p = 3$, then $\tilde{Q}_{\theta}^{\text{hyb}} = Q_{\theta}^{\text{hyb}}$ and $\tilde{Q}_{\text{vMF}}^{\text{hyb}} = Q_{\text{vMF}}^{\text{hyb}}$.

5 Simulations

In this section, we investigate the finite-sample performances of the proposed tests through two Monte Carlo exercises; see the supplementary material for two additional simulation exercises. In the specified- θ problem, we will consider the tests $\phi_{\theta}^{\text{loc}}$ and $\phi_{\theta}^{\text{sc}}$ from Section 2.1, as well as the hybrid tests $\phi_{\theta}^{\text{hyb}}$ and $\tilde{\phi}_{\theta}^{\text{hyb}}$ from Section 4 (the latter only performed for \mathcal{S}^3 , as it equals $\phi_{\theta}^{\text{hyb}}$ for \mathcal{S}^2). As explained in Section 2.1, these tests look for possible departures from rotational symmetry about θ by checking whether or not the sign vector is uniformly distributed over \mathcal{S}^{p-2} . Clearly, competing tests for rotational symmetry about θ can be obtained by applying other tests of uniformity over \mathcal{S}^{p-2} , such as (for $p = 3$) the well-known Kuiper's test or (for $p > 3$) the Giné's (F_n) test; see pages 99 and 209 of Mardia and Jupp (2000), respectively. This generates a Kuiper test $\phi_{\theta}^{\text{KU}}$ of rotational symmetry on \mathcal{S}^2 and a Giné test $\phi_{\theta}^{\text{GI}}$ of rotational symmetry on \mathcal{S}^{p-1} with $p > 3$, both about a specified θ . Since they are based on omnibus tests of uniformity over \mathcal{S}^{p-2} , both $\phi_{\theta}^{\text{KU}}$ and $\phi_{\theta}^{\text{GI}}$ are expected to show some power against both tangent vMF and tangent elliptical alternatives. Still for the specified- θ problem, we will also consider the semiparametric test from Ley and Verdebout (2017), denoted as $\phi_{\theta}^{\text{LV}}$. Now, for the unspecified- θ problem, we will restrict to the proposed semiparametric tests $\phi_{\dagger}^{\text{sc}}$, $\phi_{\text{vMF}}^{\text{loc}}$, and $\phi_{\text{vMF}}^{\text{hyb}}$, from Sections 3.1, 3.2, and 4, respectively. To the best of our knowledge, indeed, these unspecified- θ tests have no competitors in the literature. In particular, it is unclear how to turn the omnibus specified- θ tests $\phi_{\theta}^{\text{KU}}$ and $\phi_{\theta}^{\text{GI}}$ into unspecified- θ ones.

5.1 The unspecified- θ problem on \mathcal{S}^2

The first simulation exercise focuses on the unspecified- θ problem and intends to show, in particular, that using specified- θ tests with a misspecified value of θ leads to severe violations of the nominal level constraint. For two sample sizes ($n = 100, 200$) and two types of alternatives to rotational symmetry ($r = 1, 2$), we generated $N = 5,000$ mutually independent random samples of the form

$$\mathbf{X}_{i;\ell}^{(r)}, \quad i = 1, \dots, n, \quad \ell = 0, \dots, 5, \quad r = 1, 2,$$

with values in \mathcal{S}^2 . The $\mathbf{X}_{i;\ell}^{(1)}$'s follow a $\mathcal{TE}_3(\theta_0, g_1, \Lambda_{\ell})$ with location $\theta_0 := (1/\sqrt{2}, -1/\sqrt{2}, 0)^T$, angular function $t \mapsto g_1(t) := \exp(2t)$, and shape $\Lambda_{\ell} := 2\text{diag}(1 + \ell/2, 1)/(2 + \ell/2)$. The $\mathbf{X}_{i;\ell}^{(2)}$'s follow a $\mathcal{TM}_3(\theta_0, g_1, \mu, \kappa_{\ell})$ with skewness direction $\mu := (1, 0)^T$ and skewness intensity $\kappa_{\ell} := \ell$. In both cases, $\ell = 0$ corresponds to the null of rotational symmetry, whereas $\ell = 1, \dots, 5$ provide increasingly severe alternatives. For each replication, we performed, at asymptotic level $\alpha = 5\%$, the specified- θ tests $\phi_{\theta}^{\text{loc}}$, $\phi_{\theta}^{\text{sc}}$, $\phi_{\theta}^{\text{hyb}}$, $\phi_{\theta}^{\text{LV}}$, and $\phi_{\theta}^{\text{KU}}$, all based on the *misspecified* location value $\theta := (1, 0, 0)^T$, and the unspecified- θ tests $\phi_{\dagger}^{\text{sc}}$, $\phi_{\text{vMF}}^{\text{loc}}$, and $\phi_{\text{vMF}}^{\text{hyb}}$, all computed with the spherical mean to estimate θ .

Due to misspecification, it is expected that only the unspecified- $\boldsymbol{\theta}$ tests will exhibit null rejection frequencies close to 5%. This is confirmed in Figure 2, that shows that all (mis)specified- $\boldsymbol{\theta}$ tests are severely liberal. For the two sample sizes and the two types of alternatives considered, Figure 3 plots the empirical powers of the three unspecified- $\boldsymbol{\theta}$ tests (a power comparison involving the specified- $\boldsymbol{\theta}$ tests would be meaningless since these tests do not meet the level constraint). Inspection of Figure 3 reveals that: (i) as expected, $\phi_{\dagger}^{\text{sc}}$ dominates $\phi_{\text{vMF}}^{\text{loc}}$ under tangent elliptical alternatives while the opposite occurs under tangent vMF alternatives; (ii) the hybrid test detects both types of alternatives and performs particularly well against tangent vMF ones.

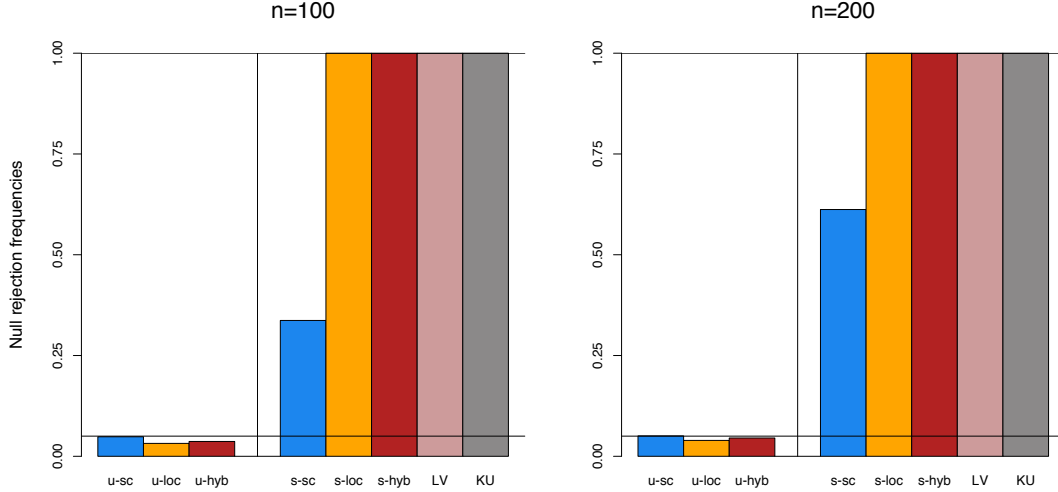


Figure 2: Null rejection frequencies, for sample sizes $n = 100$ and $n = 200$, of the unspecified- $\boldsymbol{\theta}$ tests $\phi_{\dagger}^{\text{sc}}$ (u-sc), $\phi_{\text{vMF}}^{\text{loc}}$ (u-loc), and $\phi_{\text{vMF}}^{\text{hyb}}$ (u-hyb), as well as the (mis)specified- $\boldsymbol{\theta}$ tests $\phi_{\boldsymbol{\theta}}^{\text{sc}}$ (s-sc), $\phi_{\boldsymbol{\theta}}^{\text{loc}}$ (s-loc), $\phi_{\boldsymbol{\theta}}^{\text{hyb}}$ (s-hyb), $\phi_{\boldsymbol{\theta}}^{\text{LV}}$ (LV), and $\phi_{\boldsymbol{\theta}}^{\text{KU}}$ (KU). All tests are performed at asymptotic level 5%; see Section 5.1 for details.

5.2 The specified- $\boldsymbol{\theta}$ problem on \mathcal{S}^2

The second simulation exercise focuses on the specified- $\boldsymbol{\theta}$ problem on \mathcal{S}^2 , with $\boldsymbol{\theta} := (1, 0, 0)^T$. We generated $N = 5,000$ mutually independent random samples of the form $\mathbf{X}_{i;\ell}^{(r)}$, $i = 1, \dots, n$, $\ell = 0, \dots, 5$, $r = 1, 2, 3$, with values in \mathcal{S}^2 . The $\mathbf{X}_{i;\ell}^{(1)}$'s follow a $\mathcal{TE}_3(\boldsymbol{\theta}, g_2, \boldsymbol{\Lambda}_\ell)$ with angular function $t \mapsto g_2(t) := \exp(5t)$ and with $\boldsymbol{\Lambda}_\ell$ as in Section 5.1, whereas the $\mathbf{X}_{i;\ell}^{(2)}$'s follow a $\mathcal{TM}_3(\boldsymbol{\theta}, g_2, \boldsymbol{\mu}, \kappa_\ell)$ with skewness direction $\boldsymbol{\mu} := (1, 0)^T$ and skewness intensity $\kappa_\ell := \ell/6$. The $\mathbf{X}_{i;\ell}^{(3)}$'s have a Fisher–Bingham distribution with location $\boldsymbol{\theta}$, concentration 2, and shape matrix $\mathbf{A}_\ell := \text{diag}(0, \ell/2, -\ell/2)$; we refer to Mardia and Jupp (2000) for details on Fisher–Bingham distributions, which, for the zero shape matrix, reduce to a vMF distribution. For $r = 1, 2, 3$, thus, the value $\ell = 0$ corresponds to the null of rotational symmetry about $\boldsymbol{\theta}$, whereas $\ell = 1, \dots, 5$ provide increasingly severe alternatives. For each replication, we performed, at asymptotic level $\alpha = 5\%$, the specified- $\boldsymbol{\theta}$ tests $\phi_{\boldsymbol{\theta}}^{\text{loc}}$, $\phi_{\boldsymbol{\theta}}^{\text{sc}}$, $\phi_{\boldsymbol{\theta}}^{\text{hyb}}$, $\phi_{\boldsymbol{\theta}}^{\text{LV}}$, and $\phi_{\boldsymbol{\theta}}^{\text{KU}}$ (based on the true value of $\boldsymbol{\theta}$). For the sake of comparison, we also considered the unspecified- $\boldsymbol{\theta}$ tests $\phi_{\dagger}^{\text{sc}}$, $\phi_{\text{vMF}}^{\text{loc}}$, and $\phi_{\text{vMF}}^{\text{hyb}}$, based on the spherical mean.

Figure 4 plots the resulting empirical power curves for sample sizes $n = 100$ and $n = 200$. Inspection of the figure confirms the theoretical results: (i) $\phi_{\boldsymbol{\theta}}^{\text{sc}}$ dominates the other tests under tangent elliptical alternatives, whereas $\phi_{\boldsymbol{\theta}}^{\text{loc}}$ dominates the other tests under tangent vMF alternatives (even if the latter dominance is less prominent); (ii) $\phi_{\boldsymbol{\theta}}^{\text{sc}}$ and $\phi_{\dagger}^{\text{sc}}$ exhibit extremely similar performances, as expected from Proposition 1 and the comments below that result; (iii) $\phi_{\boldsymbol{\theta}}^{\text{hyb}}$ and $\phi_{\boldsymbol{\theta}}^{\text{KU}}$ show non-trivial powers against each type of alternatives but are always dominated by some other test. Moreover, it should

be noted that $\phi_{\theta}^{\text{sc}}$ and $\phi_{\theta}^{\text{hyb}}$ perform well under Fisher–Bingham alternatives, which was expected since, parallel to tangent elliptical alternatives, Fisher–Bingham alternatives are of an elliptical nature.

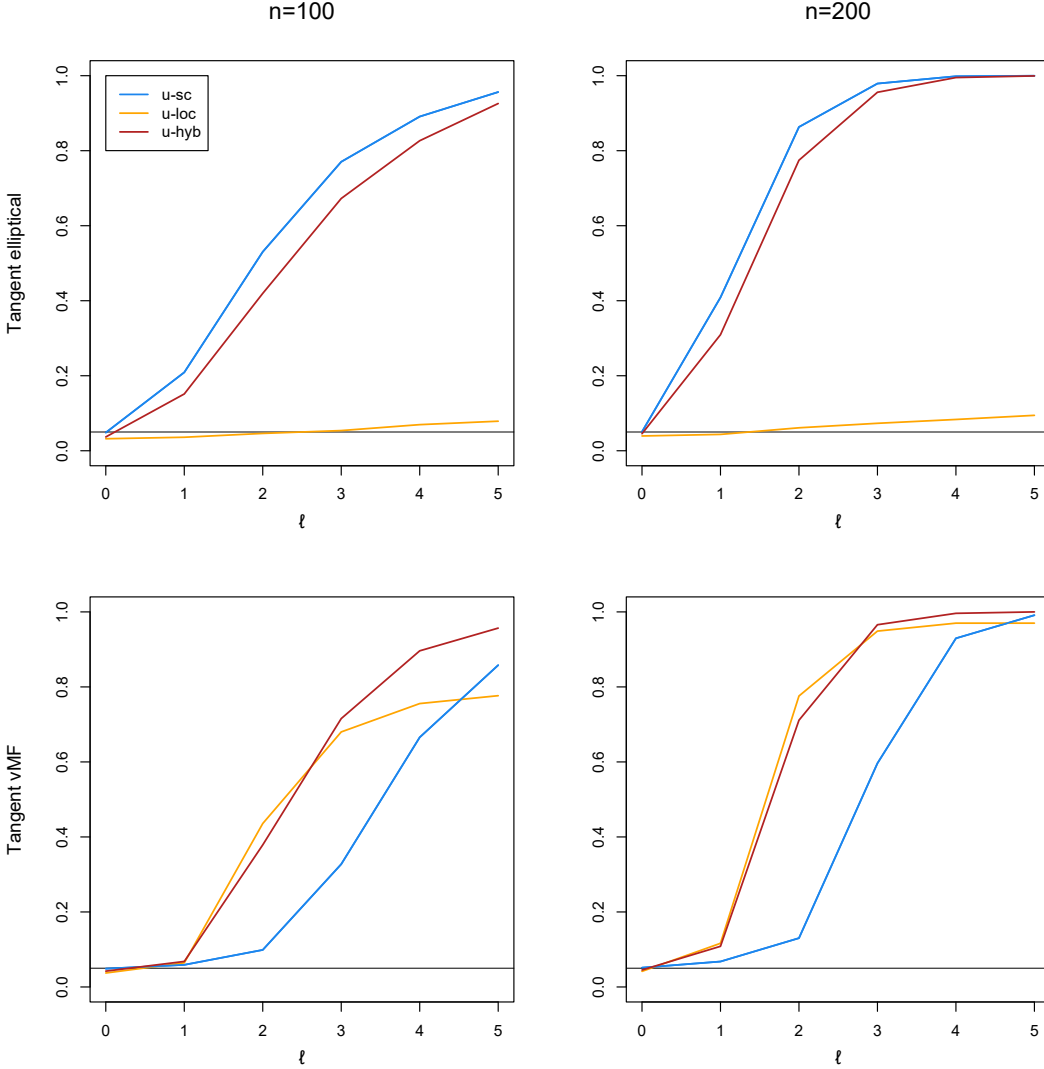


Figure 3: Rejection frequencies, under tangent elliptical alternatives (top row) and tangent vMF ones (bottom row), of the unspecified- θ tests $\phi_{\dagger}^{\text{sc}}$, $\phi_{\text{vMF}}^{\text{loc}}$, and $\phi_{\text{vMF}}^{\text{hyb}}$ for $n = 100$ (left column) and $n = 200$ (right column). Both tests are performed at asymptotic level 5%; see Section 5.1 for details.

It may be surprising at first that, under tangent vMF alternatives, the (optimal) unspecified- θ test $\phi_{\text{vMF}}^{\text{loc}}$ shows little power compared to the specified- θ test $\phi_{\theta}^{\text{loc}}$. This, however, only reflects the fact that the cost of the unspecification of θ is high for the (vMF) angular function considered. Actually, the results of the previous sections allow us to quantify this cost theoretically. Under the sequence of alternatives considered in Corollary 3, the Asymptotic Relative Efficiency (ARE) of the unspecified- θ test $\phi_{\text{vMF}}^{\text{loc}}$ with respect to the specified- θ test $\phi_{\theta}^{\text{loc}}$ is obtained as the usual ratio of the corresponding non-centrality parameters in the asymptotic non-null chi-square distributions of the corresponding statistics. It follows from (17) in the supplementary material and from Corollary 3 that, at the vMF with concentration η , $\text{ARE}(\eta) = 1 - \mathcal{I}_p^2(g_{\eta})/\mathcal{J}_p(g_{\eta}) = 1 - (2\Gamma(\frac{p}{2})^2 I_{\frac{p-1}{2}}(\eta)^2)/((p-1)\Gamma(\frac{p-1}{2})^2 I_{\frac{p-2}{2}}(\eta)I_{\frac{p}{2}}(\eta))$, still with $g_{\eta}(r) = \exp(\eta r)$. Figure 5 provides plots of this ARE as a function of η , for various values of p . For the tangent vMF alternatives considered in the present simulation exercise (for which $\eta = 5$ and $p = 3$), the ARE is 0.171, which

explains the poor performance of $\phi_{\text{vMF}}^{\text{loc}}$ compared to $\phi_{\boldsymbol{\theta}}^{\text{loc}}$. This, of course, is not incompatible with the optimality of $\phi_{\text{vMF}}^{\text{loc}}$ in the unspecified- $\boldsymbol{\theta}$ problem.

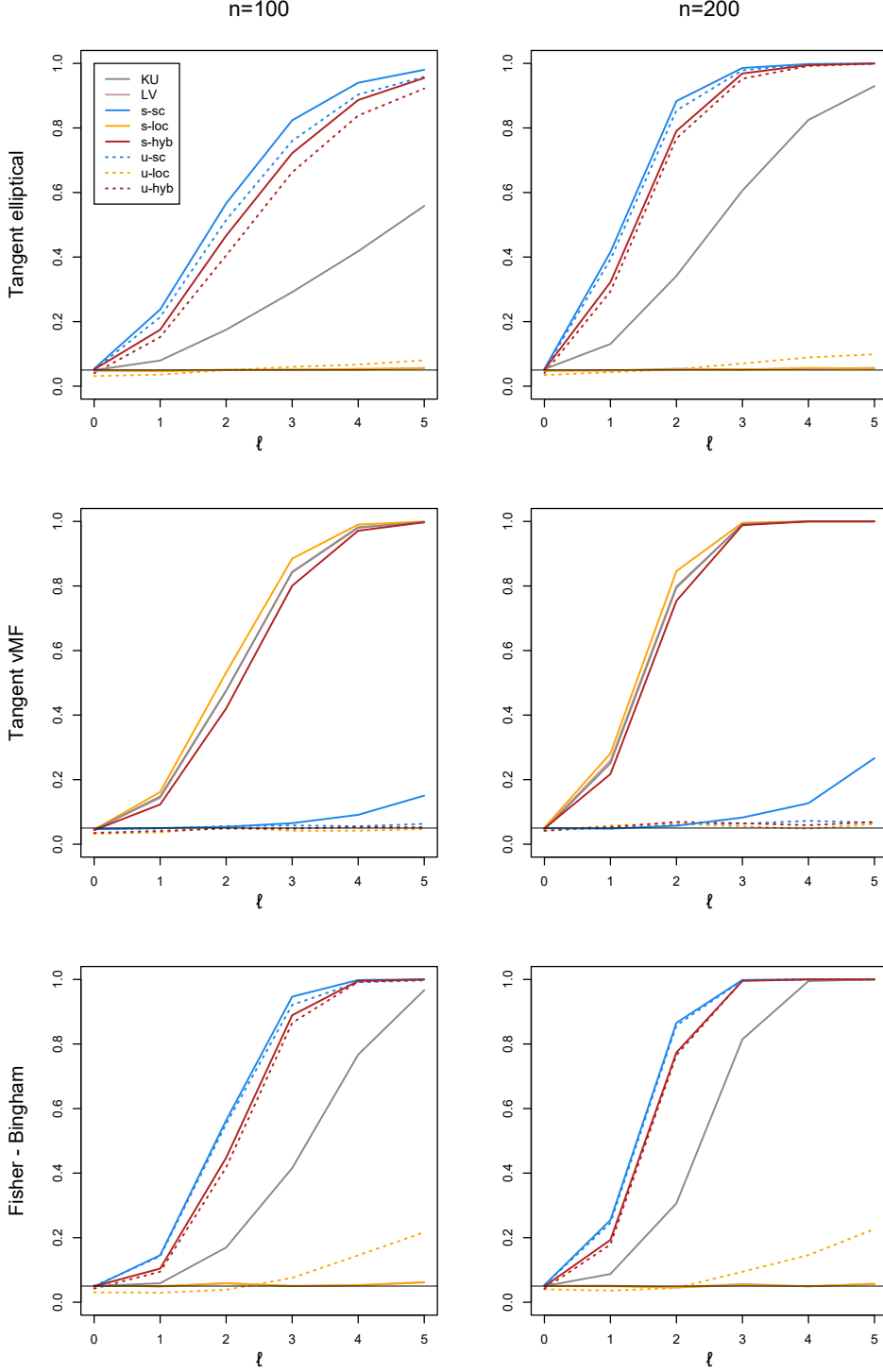


Figure 4: Rejection frequencies, under tangent elliptical alternatives (top row), tangent vMF alternatives (middle row), and Fisher–Bingham alternatives (bottom row), of the specified- $\boldsymbol{\theta}$ tests $\phi_{\boldsymbol{\theta}}^{\text{sc}}$ (s-sc), $\phi_{\boldsymbol{\theta}}^{\text{loc}}$ (s-loc), $\phi_{\boldsymbol{\theta}}^{\text{hyb}}$ (s-hyb), $\phi_{\boldsymbol{\theta}}^{\text{LV}}$ (LV), and $\phi_{\boldsymbol{\theta}}^{\text{KU}}$ (KU), as well as the unspecified- $\boldsymbol{\theta}$ tests $\phi_{\dagger}^{\text{sc}}$ (u-sc), $\phi_{\text{vMF}}^{\text{loc}}$ (u-loc), and $\phi_{\text{vMF}}^{\text{hyb}}$ (u-hyb). Sample sizes are $n = 100$ (left column) and $n = 200$ (right column). All tests are performed at asymptotic level 5%; see Section 5.2 for details.

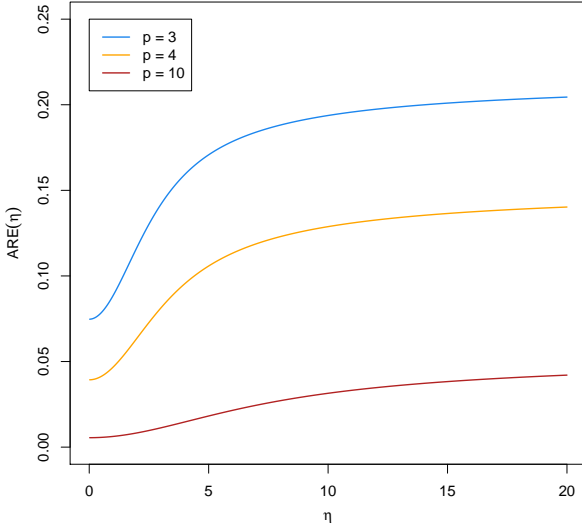


Figure 5: Plots, for several dimensions p , of the asymptotic relative efficiency, as a function of η , of the unspecified- θ test ϕ_{vMF}^{loc} with respect to the specified- θ test $\phi_{\theta}^{\text{loc}}$ under the sequence of alternatives considered in Corollary 3 at the vMF with concentration η .

6 Real data applications

We illustrate in this section the practical relevance of the proposed tests with a novel case study. The data we analyze is based on the Debrecen Photoheliographic Data (DPD) sunspot catalogue (Baranyi et al., 2016; Győri et al., 2016). It contains observations of sunspots locations since 1974 and is a continuation of the Greenwich Photoheliographic Results (GPR) catalogue, which spanned 1872–1976.

Sunspots are darker, cooler regions on the sun's photosphere that correspond to solar magnetic field concentrations. They are temporary phenomena that experience continuous change, lasting for hours to days, and with their shapes and areas varying notably along their lifespans. Prototypical sunspots come in pairs with opposite magnetic polarity, forming the so-called Bipolar Magnetic Regions (BMR), and they are usually clustered in groups that evolve with time. Sunspots are widely used to study and measure solar activity, whose effects, among others, may affect Earth's long-term climate (see, e.g., Haigh, 2007).

As it can be seen in the left panel of Figure 6, sunspots originate following a nearly rotationally symmetric pattern. An explanation for this phenomenon is given by the Babcock (1961) model for solar dynamics. It describes how the force lines of an *initial* rotationally symmetric dipolar field are twisted by the sun's differential rotation (solar plasma rotates slower near the poles than at the equator) to produce a spiral wrapping of the magnetic field, with an amplification of the field strength that depends on the *latitude*. The magnetic buoyancy of locally intense concentrations of the field pushes inner magnetic flux tubes up to the solar surface, forming BMR and producing sunspots as the result of the intersection of BMR with the solar surface. The (magnetic) field intensity required for producing BMR is reached at progressively lower latitudes as the twisting of the initial field advances, a phenomenon known as the *Spörer's law*. After about 11 years, the magnetic field behaves as a dipolar field of reversed polarity. This period constitutes a *solar cycle*. The process repeats itself, attaining the initial conditions after a 22-year cycle. Further details on sunspots and their origin can be consulted in Babcock (1961) and Solanki et al. (2006).

Even though the main driving force generating sunspots is of a rotational symmetric nature (intense magnetic field concentrations at equal latitudes due to the sun's differential rotation), Babcock (1961, pages 574 and 581) points out that sunspots tend to emerge in “preferred zones of occurrence” associated to longitudes where there has been prior activity. Hence, this phenomenon may trigger non-rotational symmetric patterns, of unclear significance, in the emergence of sunspots. We offer a quantification of this significance via the proposed tests. To that aim, we analyze the rotational symmetry of the appeared sunspots during the 23rd solar cycle (August 1996 – December 2008), currently the last fully-observed cycle with curated measurements. The corresponding data $\mathbf{X}_1, \dots, \mathbf{X}_n$, shown in the left panel of Figure 6, consists of $n = 5,373$ central positions of groups of sunspots, understood as the first-ever observations of each group. The DPD catalogue delimits the central position of a group of sunspots through an area-weighted average of the sunspots within the group. Note that, within this setting, both the temporal (observations belong to a single cycle that aggregates the different latitude-appearance regimes) and spatial (clusters of related sunspots are treated as a single observation) dependency of the data is mitigated, therefore better accommodating the independent and identically distributed framework considered in the paper.

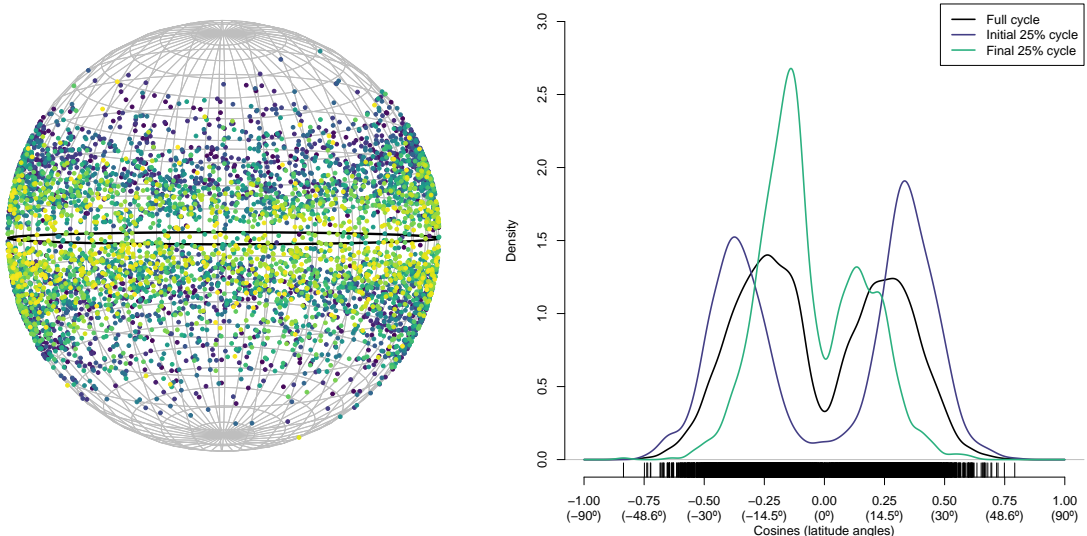


Figure 6: Left: emerging locations of sunspot groups during the 23rd solar cycle. The locations are colored with a blue-yellow gradient according to the relative position of the sunspot appearance date within the solar cycle in order to visualize the Spörer's law. Right: the kernel density estimator of the cosines $v_{\theta_0}(\mathbf{x}_i)$, $i = 1, \dots, n$, for the full cycle and for the data in the initial and final 25% cycle duration. Recall how the hemisphere asymmetry of the initial and final regimes balances out in the full cycle density.

Visual inspection reveals that rotational symmetry about the north pole $\theta_0 = (0, 0, 1)^T$ (or equivalently, about the south pole $-\theta_0$) may be suspected. The tests $\phi_{\theta_0}^{\text{sc}}$ (s-sc), $\phi_{\theta_0}^{\text{loc}}$ (s-loc), and $\phi_{\theta_0}^{\text{hyb}}$ (s-hyb) for rotational symmetry about θ_0 yield p -values equal to 0.1656, 0.4571, and 0.2711, respectively. Therefore, rotational symmetry about θ_0 is not rejected at any usual significance level and a rotationally symmetric model is suitable for the data at hand. As explained in Section 2, this greatly simplifies inference. In particular, to estimate the density $f = f_{\theta_0, g}$ of the sunspot groups on \mathcal{S}^2 , one only needs to estimate the common, *univariate*, density \hat{g}_p of the cosines $v_{\theta_0}(\mathbf{X}_i) = \mathbf{X}_i^T \theta_0$, $i = 1, \dots, n$; see (4)–(5). The left panel in Figure 6 provides a plot of the kernel density estimator (kde) \hat{g}_p based on Gaussian kernel and the direct plug-in bandwidth selector (Sheather and Jones, 1991). Note that, since the sample stays away from the endpoints of $[-1, 1]$, it is not required considering a kde that would specifically address issues associated with boundary effects. Then, from (4)–(5) and since $p = 3$, the final estimator for the density is then $\hat{f}(\mathbf{x}) = \omega_{p-1}^{-1} \hat{g}_p(\mathbf{x}^T \theta_0)$.

Given the large sample size and the fact that only a univariate density was estimated nonparametrically, one may be confident that \hat{f} is a good estimate of f . The kde \hat{g}_p can be applied for further quantitative description of the data (see Chacón and Duong (2018) for a survey of applications). In particular, it provides an estimate of the shortest set of latitudes containing at least 90% of the probability of an emergence of a sunspot group; in the present example, this shortest set, namely $(-29.48^\circ, -2.51^\circ) \cup (2.56^\circ, 28.10^\circ)$, contains the latitudes for which \hat{g}_p exceeds 0.4812. Analysis of \hat{g}_p also reveals two modes at latitudes -13.69° and 16.49° .

Remarkably, however, when performed on the 22nd cycle data, the tests $\phi_{\theta_0}^{\text{sc}}$, $\phi_{\theta_0}^{\text{loc}}$, and $\phi_{\theta_0}^{\text{hyb}}$ for rotational symmetry about θ_0 provide p -values 0.1077, 0.0125, and 0.0103, respectively. Consequently, the location and hybrid tests flag a departure from rotational symmetry about θ_0 , which evidences a significant non-rotational symmetric emergence pattern during that cycle and points to the need of a more complex modeling. The analysis for both cycles were performed for the unspecified- θ case through the tests $\phi_{\dagger}^{\text{sc}}$, $\phi_{\text{vMF}}^{\text{loc}}$, and $\phi_{\text{vMF}}^{\text{loc}}$, reaching the exactly the same conclusions.

7 Perspective for future research

As explained in Section 2.1, the random vector \mathbf{X} with values on \mathcal{S}^{p-1} is rotationally symmetric about θ if and only if, using the notation introduced in (1), (i) the random vector $\mathbf{u}_\theta(\mathbf{X})$ is uniformly distributed over \mathcal{S}^{p-2} and (ii) $\mathbf{u}_\theta(\mathbf{X})$ is independent of $v_\theta(\mathbf{X})$. The tests proposed in this paper are designed to detect deviations from rotational symmetry by testing that (i) holds. As a consequence, they will be blind to alternatives of rotational symmetry for which (i) holds but (ii) does not. This could be fixed by testing that the covariance between $\mathbf{u}_\theta(\mathbf{X})$ and $v_\theta(\mathbf{X})$ is zero, which can be based on a statistic like

$$\Delta_{\theta}^{\text{cov}(n)} := \frac{1}{\sqrt{n}} \sum_{i=1}^n v_{\theta}(\mathbf{X}_i) \mathbf{u}_{\theta}(\mathbf{X}_i).$$

Since $\Delta_{\theta}^{\text{cov}(n)}$ is asymptotically normal with mean zero and covariance matrix $(p-1)^{-1} \mathbf{E}_{\theta,g}[v_{\theta}^2(\mathbf{X}_1)] \mathbf{I}_{p-1}$ under $\mathbf{P}_{\theta,g}^{(n)}$, the resulting test would, at asymptotic level α , reject the null hypothesis of rotational symmetry about θ whenever

$$\frac{p-1}{\sum_{i=1}^n v_{\theta}^2(\mathbf{X}_i)} \sum_{i,j=1}^n v_{\theta}(\mathbf{X}_i) v_{\theta}(\mathbf{X}_j) \mathbf{u}_{\theta}^T(\mathbf{X}_i) \mathbf{u}_{\theta}(\mathbf{X}_j) > \chi_{p-1,1-\alpha}^2.$$

Such a test of course would detect violations of (ii) only and it is natural to design a test that would be able to detect deviations from both (i) and (ii) by considering test statistics that are quadratic forms in $((\Delta_{\theta}^{\text{cov}(n)})^T, (\Delta_{\theta;2}^{\mathcal{T}\mathcal{E}(n)})^T)^T$ or in $((\Delta_{\theta}^{\text{cov}(n)})^T, (\Delta_{\theta;2}^{\mathcal{T}\mathcal{M}(n)})^T)^T$, depending on whether tangent elliptical or tangent vMF alternatives are considered. In the spirit of the hybrid test from Section 4, detecting both types of alternatives can be achieved by considering a quadratic form in $((\Delta_{\theta}^{\text{cov}(n)})^T, (\Delta_{\theta;2}^{\mathcal{T}\mathcal{E}(n)})^T, (\Delta_{\theta;2}^{\mathcal{T}\mathcal{M}(n)})^T)^T$. The quadratic form to be used in each case naturally follows from the asymptotic covariance matrix in the (null) joint asymptotic normal distribution of these random vectors.

Another perspective for future research is the following. In Section 2.2, we proposed new distributions on the unit sphere \mathcal{S}^{p-1} , namely tangent vMF distributions, by imposing that $\mathbf{u}_\theta(\mathbf{X}) = \mathbf{u}_{\theta_{1;p-2}}(\mathbf{X})$ follows its own vMF distribution over \mathcal{S}^{p-2} with location $\mu = \theta_2 \in \mathcal{S}^{p-2}$. In turn, one could specify that $\mathbf{u}_{\theta_{2;p-3}}(\mathbf{X})$ follows a vMF distribution over \mathcal{S}^{p-3} with location θ_3 . Iterating this construction will provide “nested” tangent vMF distributions that are associated with mutually orthogonal directions θ_i , $i = 1, \dots, p$ (strictly speaking, $\theta_i \in \mathcal{S}^{p-i}$ but they can all be considered embedded in the original unit sphere \mathcal{S}^{p-1}). Such distributions provide flexible models on the sphere that are likely to be relevant in various applications of directional statistics.

Acknowledgments

Eduardo García-Portugués acknowledges support from project PGC2018-097284-B-I00, IJCI-2017-32005, and MTM2016-76969-P from the Spanish Ministry of Science, Innovation and Universities, and the European Regional Development Fund. Davy Paindaveine's research is supported by the IAP research network grant nr. P7/06 of the Belgian government (Belgian Science Policy), the Crédit de Recherche J.0113.16 of the FNRS (Fonds National pour la Recherche Scientifique), Communauté Française de Belgique, and a grant from the National Bank of Belgium. Thomas Verdebout's research is supported by the National Bank of Belgium.

References

- Babcock, H. W. (1961). The topology of the sun's magnetic field and the 22-year cycle. *Astrophys. J.*, 133(2):572–587.
- Baranyi, T., Győri, L., and Ludmány, A. (2016). On-line tools for solar data compiled at the Debrecen observatory and their extensions with the Greenwich sunspot data. *Sol. Phys.*, 291(9):3081–3102.
- Boente, G., Rodríguez, D., and González-Manteiga, W. (2014). Goodness-of-fit test for directional data. *Scand. J. Stat.*, 41(1):259–275.
- Boulerice, B. and Ducharme, G. R. (1997). Smooth tests of goodness-of-fit for directional and axial data. *J. Multivariate Anal.*, 60(1):154–175.
- Bunge, H. J. (2015). *Texture Analysis in Materials Science: Mathematical Methods*. Elsevier, Wolfratshausen.
- Chacón, J. E. and Duong, T. (2018). *Multivariate Kernel Smoothing and its Applications*. Chapman and Hall/CRC.
- Chang, T. and Rivest, L.-P. (2001). M-estimation for location and regression parameters in group models: A case study using Stiefel manifolds. *Ann. Statist.*, 29(3):784–814.
- Figueiredo, A. M. S. (2012). Goodness-of-fit for a concentrated von Mises–Fisher distribution. *Comput. Statist.*, 27(1):69–82.
- Fisher, R. A. (1925). *Statistical Methods for Research Workers*. Oliver and Boyd, Edinburgh.
- Giné, E. (1975). Invariant tests for uniformity on compact Riemannian manifolds based on Sobolev norms. *Ann. Statist.*, 3(6):1243–1266.
- Guan, H. and Smith, W. A. (2017). Structure-from-motion in spherical video using the von Mises–Fisher distribution. *IEEE Trans. Image Process.*, 26(2):711–723.
- Győri, L., Baranyi, T., and Ludmány, A. (2016). Comparative analysis of Debrecen sunspot catalogues. *Mon. Not. R. Astron. Soc.*, 465(2):1259–1273.
- Haigh, J. D. (2007). The Sun and the Earth's Climate. *Living Rev. Sol. Phys.*, 4(1):2.
- Hallin, M. and Paindaveine, D. (2006a). Parametric and semiparametric inference for shape: the role of the scale functional. *Statist. Decisions*, 24(3):327–350.
- Hallin, M. and Paindaveine, D. (2006b). Semiparametrically efficient rank-based inference for shape I. Optimal rank-based tests for sphericity. *Ann. Statist.*, 34(6):2707–2756.

- Ilmonen, P. and Paindaveine, D. (2011). Semiparametrically efficient inference based on signed ranks in symmetric independent component models. *Ann. Statist.*, 39(5):2448–2476.
- Jupp, P. E. and Spurr, B. D. (1983). Sobolev tests for symmetry of directional data. *Ann. Statist.*, 11(4):1225–1231.
- Kent, J. T. (1982). The Fisher–Bingham distribution on the sphere. *J. Roy. Stat. Soc. Ser. B*, 44(1):71–80.
- Ko, D. and Chang, T. (1993). Robust M-estimators on spheres. *J. Multivariate Anal.*, 45(1):104–136.
- Kume, A. and Wood, A. T. (2005). Saddlepoint approximations for the Bingham and Fisher–Bingham normalising constants. *Biometrika*, 92(2):465–476.
- Larsen, P. V., Blæsild, P., and Sørensen, M. K. (2002). Improved likelihood ratio tests on the von Mises–Fisher distribution. *Biometrika*, 89(4):947–951.
- Lashkari, D., Vul, E., Kanwisher, N., and Golland, P. (2010). Discovering structure in the space of fMRI selectivity profiles. *Neuroimage*, 50(3):1085–1098.
- Ley, C., Sabbah, C., and Verdebout, T. (2014). A new concept of quantiles for directional data and the angular Mahalanobis depth. *Electron. J. Stat.*, 8(1):795–816.
- Ley, C., Swan, Y., Thiam, B., and Verdebout, T. (2013). Optimal R-estimation of a spherical location. *Statist. Sinica*, 23(1):305–333.
- Ley, C. and Verdebout, T. (2014). Simple optimal tests for circular reflective symmetry about a specified median direction. *Statist. Sinica*, 24:1319–1340.
- Ley, C. and Verdebout, T. (2017a). *Modern Directional Statistics*. Chapman and Hall/CRC.
- Ley, C. and Verdebout, T. (2017b). Skew-rotationally-symmetric distributions on the unit sphere and related efficient inferential procedures. *J. Multivariate Anal.*, 159:67–81.
- Lo, A. Y. and Cabrera, J. (1987). Bayes procedures for rotationally symmetric models on the sphere. *Ann. Statist.*, 15(3):1257–1268.
- Mardia, K. V. and Jupp, P. E. (2000). *Directional Statistics*. Wiley Series in Probability and Statistics. John Wiley & Sons, Chichester, second edition.
- Meintanis, S. and Verdebout, T. (2019). Le Cam maximin tests for symmetry of circular data based on the characteristic function. *Stat. Sinica*, to appear.
- Paindaveine, D. and Verdebout, T. (2015). Optimal rank-based tests for the location parameter of a rotationally symmetric distribution on the hypersphere. In M. Hallin, D. Mason, D. Pfeifer, and J. Steinebach, editors, *Mathematical Statistics and Limit Theorems: Festschrift in Honor of Paul Deheuvels*, pages 249–270. Springer.
- Paindaveine, D. and Verdebout, T. (2016). On high-dimensional sign tests. *Bernoulli*, 22(3):1745–1769.
- Paindaveine, D. and Verdebout, T. (2017). Inference on the mode of weak directional signals: a Le Cam perspective on hypothesis testing near singularities. *Ann. Statist.*, 45(2):800–832.
- Paindaveine, D. and Verdebout, T. (2019). Detecting the direction of a signal on high-dimensional spheres: non-null and Le Cam optimality results. Submitted.
- Pewsey, A. (2002). Testing circular symmetry. *Canad. J. Statist.*, 30(4):591–600.

- Rayleigh, L. (1919). On the problem of random vibrations and random flights in one, two and three dimensions. *Phil. Mag.*, 37(220):321–346.
- Rivest, L.-P. (1989). Spherical regression for concentrated Fisher–von Mises distributions. *Ann. Statist.*, 17(1):307–317.
- Schach, S. (1969). Nonparametric symmetry tests for circular distributions. *Biometrika*, 56(3):571–577.
- Sheather, S. J. and Jones, M. C. (1991). A reliable data-based bandwidth selection method for kernel density estimation. *J. Roy. Statist. Soc. Ser. B*, 53(3):683–690.
- Solanki, S. K., Inhester, B., and Schüssler, M. (2006). The solar magnetic field. *Rep. Prog. Phys.*, 69(3):563–668.
- Tsai, M.-T. and Sen, P. K. (2007). Locally best rotation-invariant rank tests for modal location. *J. Multivariate Anal.*, 98(6):1160–1179.
- Tyler, D. E. (1987). Statistical analysis for the angular central Gaussian distribution on the sphere. *Biometrika*, 74(3):579–589.
- Xiao, Y., and Johnson, M. D. (2015). Spherical statistics for characterizing the spatial distribution of deep brain stimulation effects on neuronal activity. *J. Neurosci. Methods*, 255:52–65.
- Watson, G. S. (1983). *Statistics on Spheres*. Wiley, New York.

Supplement to “On optimal tests for rotational symmetry against new classes of hyperspherical distributions”

Eduardo García-Portugués^{1,2,4}, Davy Paindaveine^{3,4}, and Thomas Verdebout^{3,4}

Abstract

In Section A of this supplement, we detail the delicate construction of Le Cam optimal location tests in the unspecified- $\boldsymbol{\theta}$ problem, hence in particular explain how the test $\phi_{\text{vMF}}^{\text{loc}}$ from Section 3.2 is obtained. In Section B, we then provide the proofs of the main results, with the required lemmas given in Section C. Finally, Section D presents additional simulations.

Keywords: Directional data; Local asymptotic normality; Locally asymptotically maximin tests; Rotational symmetry.

A Construction of optimal unspecified- $\boldsymbol{\theta}$ location tests

As discussed in Section 3, while the replacement of $\boldsymbol{\theta}$ with a suitable estimator $\hat{\boldsymbol{\theta}}$ does not affect the asymptotic behavior of the scatter test statistic $Q_{\boldsymbol{\theta}}^{\text{sc}}$ under the null or contiguous alternatives, this replacement has a non-negligible asymptotic impact for the location test statistic $Q_{\boldsymbol{\theta}}^{\text{loc}}$. Here, we examine this impact and construct (optimal) unspecified- $\boldsymbol{\theta}$ location tests. We first focus on the parametric case where the angular function g is specified (Section A.1), then we will turn to the more realistic semiparametric situation where g remains unspecified (Section A.2).

A.1 The parametric case

When the Fisher information matrix is not block-diagonal, it is well-known that inference on $\boldsymbol{\delta}$ (we consider the model and parametrization from Section 2.4) under unspecified $\boldsymbol{\theta}$ is to be based on the *efficient central sequence*

$$\begin{aligned} \Delta_{\boldsymbol{\theta},g;2*}^{\mathcal{T}\mathcal{M}(n)} &:= \Delta_{\boldsymbol{\theta};2}^{\mathcal{T}\mathcal{M}(n)} - \boldsymbol{\Gamma}_{\boldsymbol{\theta},g;21}^{\mathcal{T}\mathcal{M}} \boldsymbol{\Gamma}_{\boldsymbol{\theta},g;11}^{-} \Delta_{\boldsymbol{\theta},g;1}^{(n)} \\ &= \frac{1}{\sqrt{n}} \sum_{i=1}^n \left(1 - \frac{\mathcal{I}_p(g)}{\mathcal{J}_p(g)} \varphi_g(V_{i,\boldsymbol{\theta}})(1 - V_{i,\boldsymbol{\theta}}^2)^{1/2} \right) \mathbf{U}_{i,\boldsymbol{\theta}} \end{aligned} \quad (12)$$

(throughout, \mathbf{A}^{-} stands for the Moore–Penrose inverse of \mathbf{A}). Under $\mathbf{P}_{\boldsymbol{\theta},g}^{(n)}$,

$$\Delta_{\boldsymbol{\theta},g;2*}^{\mathcal{T}\mathcal{M}(n)} \xrightarrow{\mathcal{D}} \mathcal{N}(\mathbf{0}, \boldsymbol{\Gamma}_{g,22*}^{\mathcal{T}\mathcal{M}}), \text{ with } \boldsymbol{\Gamma}_{g,22*}^{\mathcal{T}\mathcal{M}} := \frac{1}{p-1} \left(1 - \frac{\mathcal{I}_p^2(g)}{\mathcal{J}_p(g)} \right) \mathbf{I}_{p-1},$$

and the corresponding test, $\phi_{\boldsymbol{\theta},g*}^{\text{loc}}$ say, consists in rejecting the null hypothesis of rotational symmetry ($\mathcal{H}_0 : \boldsymbol{\delta} = \mathbf{0}$, with unspecified $\boldsymbol{\theta}$) at asymptotic level α whenever

$$Q_{\boldsymbol{\theta},g*}^{\text{loc}} := (\Delta_{\boldsymbol{\theta},g;2*}^{\mathcal{T}\mathcal{M}(n)})^T (\boldsymbol{\Gamma}_{g,22*}^{\mathcal{T}\mathcal{M}})^{-1} \Delta_{\boldsymbol{\theta},g;2*}^{\mathcal{T}\mathcal{M}(n)} > \chi_{p-1,1-\alpha}^2.$$

¹Department of Statistics, Carlos III University of Madrid (Spain).

²UC3M-BS Institute of Financial Big Data, Carlos III University of Madrid (Spain).

³Département de Mathématique, Université Libre de Bruxelles (Belgium).

⁴ECARES, Université Libre de Bruxelles (Belgium).

⁵Corresponding author. e-mail: edgarcia@est-econ.uc3m.es.

This test has asymptotic level α under $P_{\theta,g}^{(n)}$ and is locally asymptotically maximin, under angular function $g \in \mathcal{G}_a$, in the unspecified- θ problem. A direct application of Le Cam's third lemma yields that, under the same sequence of alternatives as the one considered in Corollary 3,

$$\Delta_{\theta,g;2*}^{\mathcal{T}\mathcal{M}(n)} \xrightarrow{\mathcal{D}} \mathcal{N}(\mathbf{m}_g, \boldsymbol{\Gamma}_{g,22*}^{\mathcal{T}\mathcal{M}}),$$

with

$$\mathbf{m}_g := \lim_{n \rightarrow \infty} \mathbb{E}_{\theta,g} [\Delta_{\theta,g;2*}^{\mathcal{T}\mathcal{M}(n)} (\Delta_{\theta,2}^{\mathcal{T}\mathcal{M}(n)})^T] \mathbf{d}_n = \frac{1}{p-1} \left(1 - \frac{\mathcal{I}_p^2(g)}{\mathcal{J}_p(g)} \right) k \boldsymbol{\mu},$$

so that $Q_{\theta,g*}^{\text{loc}} \xrightarrow{\mathcal{D}} \chi_{p-1}^2(\lambda)$ with non-centrality parameter $\lambda = \mathbf{m}_g^T (\boldsymbol{\Gamma}_{g,22*}^{\mathcal{T}\mathcal{M}})^{-1} \mathbf{m}_g = k^2 (1 - \mathcal{I}_p^2(g) / \mathcal{J}_p(g)) / (p-1)$. Note that this non-centrality parameter is smaller than or equal to the one in Corollary 3. The comments below Theorem 4 imply that the non-centrality parameter is larger than or equal to zero, with equality if and only if g is of the form $g(t) = C \exp(\kappa \arcsin(t))$. In other words, it is only for angular densities of the previous form that the g -optimal unspecified- θ test has asymptotic power α .

Now, even if we are after the construction of a parametric (g -fixed) test, the test $\phi_{\theta,g*}^{\text{loc}}$ is unfortunately infeasible because θ is unknown. We have the following result.

Proposition 2. *Let $\hat{\theta}$ satisfy $A_{\mathcal{G}'}$. Then, for any $\theta \in \mathcal{S}^{p-1}$ and any $g \in \mathcal{G}_a \cap \mathcal{G}'$,*

$$Q_{\hat{\theta},g*}^{\text{loc}} = Q_{\theta,g*}^{\text{loc}} + o_P(1), \quad (13)$$

as $n \rightarrow \infty$ under $P_{\theta,g}^{(n)}$.

It directly follows from Proposition 2 that the g -parametric test ϕ_{g*}^{loc} that rejects the null hypothesis at asymptotic level α whenever $Q_{\theta,g*}^{\text{loc}} > \chi_{p-1,1-\alpha}^2$ has the exact same asymptotic properties as the infeasible test $\phi_{\theta,g*}^{\text{loc}}$ above. In particular, like $\phi_{\theta,g*}^{\text{loc}}$, the test ϕ_{g*}^{loc} is locally asymptotically maximin at asymptotic level α when testing $\bigcup_{\theta \in \mathcal{S}^{p-1}} \{P_{\theta,g}^{(n)}\}$ against $\bigcup_{\theta \in \mathcal{S}^{p-1}} \bigcup_{\mu \in \mathcal{S}^{p-2}} \bigcup_{\kappa > 0} \{P_{\theta,g,\mu,\kappa}^{\mathcal{T}\mathcal{M}(n)}\}$. From contiguity, (13) also holds under the sequences of local tangent elliptical alternatives considered in Corollary 1, which implies that ϕ_{g*}^{loc} has asymptotic power α under such alternatives.

A.2 The semiparametric case

The test ϕ_{g*}^{loc} constructed above is a purely parametric test: it requires the knowledge of the underlying angular function g . In practice, of course, g may hardly be assumed to be known and it is therefore desirable to define a location test that would be valid (in the sense that it meets asymptotically the nominal level constraint) under a broad range of angular functions g . Two options are possible here. The first one aims at uniform optimality in g by reconstructing, at any g , the test statistic $Q_{\theta,g*}^{\text{loc}}$ above. The form of the g -efficient central sequence in (12) makes it clear that this requires estimating nonparametrically the optimal score function φ_g , which typically requires large sample sizes and which makes it hard to control the replacement of θ with $\hat{\theta}$. We therefore favor the second approach, that consists in robustifying the parametric test ϕ_{g*}^{loc} in such a way that it remains *valid* away from the target angular function at which power optimality is to be achieved (of course, in general, the resulting test will not be *optimal* away from the selected target density).

To be more specific, assume that we target optimality at the fixed angular function f . Our goal is to define a test statistic that: (i) is asymptotically equivalent to $Q_{\theta,f*}^{\text{loc}}$ whenever f is the true angular function (which will ensure asymptotic optimality of the resulting test at angular function f); (ii) remains χ_{p-1}^2 under the null with angular function $g \neq f$ (which will guarantee validity away from angular function f). With these objectives in mind, consider the alternative efficient central sequence

$$\Delta_{\theta,f;g;2*}^{\mathcal{T}\mathcal{M}(n)} := \Delta_{\theta,2}^{\mathcal{T}\mathcal{M}(n)} - \boldsymbol{\Gamma}_{\theta,g;21}^{\mathcal{T}\mathcal{M}} \boldsymbol{\Gamma}_{\theta,f;11}^{-1} \Delta_{\theta,1}^{(n)}$$

$$= \frac{1}{\sqrt{n}} \sum_{i=1}^n \left(1 - \frac{\mathcal{I}_p(g)}{\mathcal{J}_p(f;g)} \varphi_f(V_{i,\theta})(1 - V_{i,\theta}^2)^{1/2} \right) \mathbf{U}_{i,\theta}, \quad (14)$$

where $\Gamma_{\theta,f;g;11} := (\mathcal{J}_p(f;g)/(p-1))(\mathbf{I}_p - \theta\theta^T)$ involves the ‘‘cross-information’’ quantity

$$\mathcal{J}_p(f;g) := \int_{-1}^1 \varphi_f(t)\varphi_g(t)(1-t^2)\tilde{g}_p(t) dt.$$

First note that, for $g = f$, this alternative efficient central sequence $\Delta_{\theta,f;g;2*}^{\mathcal{T}\mathcal{M}(n)}$ coincides with the f -version of the efficient central sequence in (12), so that a test based on (14) will meet the objective (i) above. As for the objective (ii), we have the following result.

Proposition 3. *Let $\hat{\theta}$ satisfy $A_{\mathcal{G}'}$. Then, for any $\theta \in \mathcal{S}^{p-1}$ and any $g \in \mathcal{G}_a \cap \mathcal{G}'$,*

$$\Delta_{\hat{\theta},f;g;2*}^{\mathcal{T}\mathcal{M}(n)} = \Delta_{\theta,f;g;2*}^{\mathcal{T}\mathcal{M}(n)} + o_P(1), \quad (15)$$

as $n \rightarrow \infty$ under $P_{\theta,g}^{(n)}$.

This confirms that the alternative efficient central sequence above is defined so that the replacement of θ with $\hat{\theta}$ has no asymptotic impact also under $g \neq f$. Since, under $P_{\theta,g}^{(n)}$,

$$\Delta_{\theta,f;g;2*}^{\mathcal{T}\mathcal{M}(n)} \xrightarrow{\mathcal{D}} \mathcal{N}(\mathbf{0}, \Gamma_{f;g;22*}^{\mathcal{T}\mathcal{M}}),$$

with

$$\Gamma_{f;g;22*}^{\mathcal{T}\mathcal{M}} := \frac{1}{p-1} \left(1 - \frac{2\mathcal{I}_p(g)\mathcal{H}_p(f;g)}{\mathcal{J}_p(f;g)} + \frac{\mathcal{I}_p^2(g)\mathcal{K}_p(f;g)}{\mathcal{J}_p^2(f;g)} \right) \mathbf{I}_{p-1},$$

where we let

$$\mathcal{H}_p(f;g) := \int_{-1}^1 \varphi_f(t)(1-t^2)^{1/2}\tilde{g}_p(t) dt \quad \text{and} \quad \mathcal{K}_p(f;g) := \int_{-1}^1 \varphi_f^2(t)(1-t^2)\tilde{g}_p(t) dt,$$

the resulting test rejects the null hypothesis at asymptotic level α whenever

$$Q_{\theta,f;g*}^{\text{loc}} := (\Delta_{\theta,f;g;2*}^{\mathcal{T}\mathcal{M}(n)})^T (\Gamma_{f;g;22*}^{\mathcal{T}\mathcal{M}})^{-1} \Delta_{\theta,f;g;2*}^{\mathcal{T}\mathcal{M}(n)} > \chi_{p-1,1-\alpha}^2. \quad (16)$$

Le Cam’s third lemma allows showing that, under the sequence of alternatives considered in Corollary 3, $\Delta_{\theta,f;g;2*}^{\mathcal{T}\mathcal{M}(n)}$ is asymptotically normal with covariance $\Gamma_{f;g;22*}^{\mathcal{T}\mathcal{M}}$ and mean

$$\mathbf{m}_{f;g} := \lim_{n \rightarrow \infty} \mathbf{E}_{\theta,g} [\Delta_{\theta,f;g;2*}^{\mathcal{T}\mathcal{M}(n)} (\Delta_{\theta,f;g;2*}^{\mathcal{T}\mathcal{M}(n)})^T] k_n \boldsymbol{\mu} = \frac{1}{p-1} \left(1 - \frac{\mathcal{I}_p(f)\mathcal{H}_p(f;g)}{\mathcal{J}_p(f;g)} \right) k \boldsymbol{\mu},$$

so that $Q_{\theta,f;g*}^{\text{loc}}$ (hence also, $Q_{\theta,f;g*}^{\text{loc}}$) is asymptotically $\chi_{p-1}^2(\lambda)$ with non-centrality parameter λ given by

$$\begin{aligned} & \mathbf{m}_{f;g}^T (\Gamma_{f;g;22*}^{\mathcal{T}\mathcal{M}})^{-1} \mathbf{m}_{f;g} \\ &= \frac{k^2}{p-1} \left(1 - \frac{\mathcal{I}_p(g)\mathcal{H}_p(f;g)}{\mathcal{J}_p(f;g)} \right)^2 \Big/ \left(1 - \frac{2\mathcal{I}_p(g)\mathcal{H}_p(f;g)}{\mathcal{J}_p(f;g)} + \frac{\mathcal{I}_p^2(g)\mathcal{K}_p(f;g)}{\mathcal{J}_p^2(f;g)} \right). \end{aligned} \quad (17)$$

Now, since the test statistic (16) still depends on the unknown underlying angular function g , turning this pseudo-test into a genuine test requires estimating consistently the quantities $\mathcal{I}_p(g)$, $\mathcal{J}_p(f;g)$, $\mathcal{H}_p(f;g)$, and $\mathcal{K}_p(f;g)$. To that aim, we express them as

$$\mathcal{I}_p(g) = (p-2) \mathbf{E}_{\theta,g} \left[\frac{V_{1,\theta}}{(1-V_{1,\theta}^2)^{1/2}} \right],$$

$$\begin{aligned}\mathcal{J}_p(f; g) &= (p-1) \mathbb{E}_{\boldsymbol{\theta}, g} [\varphi_f(V_{1, \boldsymbol{\theta}}) V_{1, \boldsymbol{\theta}}] - \mathbb{E}_{\boldsymbol{\theta}, g} [\varphi'_f(V_{1, \boldsymbol{\theta}}) (1 - V_{1, \boldsymbol{\theta}}^2)], \\ \mathcal{H}_p(f; g) &:= \mathbb{E}_{\boldsymbol{\theta}, g} [\varphi_f(V_{1, \boldsymbol{\theta}}) (1 - V_{1, \boldsymbol{\theta}}^2)^{1/2}], \quad \mathcal{K}_p(f; g) := \mathbb{E}_{\boldsymbol{\theta}, g} [\varphi_f^2(V_{1, \boldsymbol{\theta}}) (1 - V_{1, \boldsymbol{\theta}}^2)]\end{aligned}$$

(the first two identities are obtained from integration by parts, assuming that φ_f is differentiable). Natural estimators of these quantities are

$$\begin{aligned}\hat{\mathcal{I}}_p(g) &:= \frac{p-2}{n} \sum_{i=1}^n \frac{V_{i, \hat{\boldsymbol{\theta}}}}{(1 - V_{i, \hat{\boldsymbol{\theta}}}^2)^{1/2}}, \\ \hat{\mathcal{J}}_p(f; g) &:= \frac{p-1}{n} \sum_{i=1}^n \varphi_f(V_{i, \hat{\boldsymbol{\theta}}}) V_{i, \hat{\boldsymbol{\theta}}} - \frac{1}{n} \sum_{i=1}^n \varphi'_f(V_{i, \hat{\boldsymbol{\theta}}}) (1 - V_{i, \hat{\boldsymbol{\theta}}}^2), \\ \hat{\mathcal{H}}_p(f; g) &:= \frac{1}{n} \sum_{i=1}^n \varphi_f(V_{i, \hat{\boldsymbol{\theta}}}) (1 - V_{i, \hat{\boldsymbol{\theta}}}^2)^{1/2}, \quad \hat{\mathcal{K}}_p(f; g) := \frac{1}{n} \sum_{i=1}^n \varphi_f^2(V_{i, \hat{\boldsymbol{\theta}}}) (1 - V_{i, \hat{\boldsymbol{\theta}}}^2),\end{aligned}$$

at any g for which $\mathcal{I}_p(g)$, $\mathcal{J}_p(f; g)$, $\mathcal{H}_p(f; g)$, and $\mathcal{K}_p(f; g)$ are finite. Consistency follows by successively applying the weak law of large numbers, under $\mathbb{P}_{\boldsymbol{\theta} + n^{-1/2} \mathbf{t}_n, g}^{(n)}$, with $\boldsymbol{\theta} + n^{-1/2} \mathbf{t}_n \in \mathcal{S}^{p-1}$, to random variables of the form $n^{-1} \sum_{i=1}^n H_f(V_{i, \boldsymbol{\theta} + n^{-1/2} \mathbf{t}_n})$ (with H_f a suitable function), the general version of the Le Cam's third lemma (see, e.g., Theorem 6.6 in van der Vaart, 1998), and then Lemma 4.4 from Kreiss (1987).

We consider now the important particular case $f_\eta(r) = \exp(\eta r)$, which will provide the test $\phi_{\text{vMF}}^{\text{loc}}$ described in Section 3.2. Since $f_\eta \in \mathcal{G}_a$ is the vMF angular function with concentration parameter η (we avoid using the standard notation κ , as this notation was used to denote the skewness intensity in the tangent vMF model), we have $\varphi_{f_\eta}(r) = \eta$. Letting

$$D_{p,g} := \frac{(p-2) \mathbb{E}_{\boldsymbol{\theta}, g} [V_{1, \boldsymbol{\theta}} (1 - V_{1, \boldsymbol{\theta}}^2)^{-1/2}]}{(p-1) \mathbb{E}_{\boldsymbol{\theta}, g} [V_{1, \boldsymbol{\theta}}]},$$

we have

$$\Delta_{\boldsymbol{\theta}, \text{vMF}, g; 2*}^{\mathcal{T}\mathcal{M}(n)} := \Delta_{\boldsymbol{\theta}, f_\eta; g; 2*}^{\mathcal{T}\mathcal{M}(n)} = \frac{1}{\sqrt{n}} \sum_{i=1}^n \left(1 - D_{p,g} (1 - V_{i, \boldsymbol{\theta}}^2)^{1/2} \right) \mathbf{U}_{i, \boldsymbol{\theta}}$$

and

$$\boldsymbol{\Gamma}_{\text{vMF}, g; 22*}^{\mathcal{T}\mathcal{M}(n)} := \boldsymbol{\Gamma}_{f_\eta; g; 22*}^{\mathcal{T}\mathcal{M}} = \frac{1}{p-1} \left(1 - 2D_{p,g} \mathbb{E}_{\boldsymbol{\theta}, g} [(1 - V_{1, \boldsymbol{\theta}}^2)^{1/2}] + D_{p,g}^2 (1 - \mathbb{E}_{\boldsymbol{\theta}, g} [V_{1, \boldsymbol{\theta}}^2]) \right) \mathbf{I}_{p-1},$$

where the notation is justified by the fact that, quite nicely, the f_η -efficient central sequence and corresponding Fisher information matrix do not depend on η . In the present case, the quantities to be estimated consistently are therefore

$$\mathbb{E}_{\boldsymbol{\theta}, g} [V_{1, \boldsymbol{\theta}} (1 - V_{1, \boldsymbol{\theta}}^2)^{-1/2}], \quad \mathbb{E}_{\boldsymbol{\theta}, g} [(1 - V_{1, \boldsymbol{\theta}}^2)^{1/2}], \quad \mathbb{E}_{\boldsymbol{\theta}, g} [V_{1, \boldsymbol{\theta}}], \quad \text{and} \quad \mathbb{E}_{\boldsymbol{\theta}, g} [V_{1, \boldsymbol{\theta}}^2], \quad (18)$$

and the corresponding estimators are

$$\frac{1}{n} \sum_{i=1}^n V_{i, \hat{\boldsymbol{\theta}}} (1 - V_{i, \hat{\boldsymbol{\theta}}}^2)^{-1/2}, \quad \frac{1}{n} \sum_{i=1}^n (1 - V_{i, \hat{\boldsymbol{\theta}}}^2)^{1/2}, \quad \frac{1}{n} \sum_{i=1}^n V_{i, \hat{\boldsymbol{\theta}}}, \quad \text{and} \quad \frac{1}{n} \sum_{i=1}^n V_{i, \hat{\boldsymbol{\theta}}}^2, \quad (19)$$

respectively. The same argument as above proves consistency of these estimators at any g in the collection \mathcal{G}_b that was introduced in Section 3.2 (note that the last three expectations in (18) are trivially finite for any g). The resulting test rejects the null of rotational symmetry about an unspecified $\boldsymbol{\theta}$ whenever

$$Q_{\text{vMF}}^{\text{loc}} := (\hat{\Delta}_{\hat{\boldsymbol{\theta}}, \text{vMF}; g; 2*}^{\mathcal{T}\mathcal{M}(n)})^T (\hat{\boldsymbol{\Gamma}}_{\text{vMF}; g; 22*}^{\mathcal{T}\mathcal{M}(n)})^{-1} \hat{\Delta}_{\hat{\boldsymbol{\theta}}, \text{vMF}; g; 2*}^{\mathcal{T}\mathcal{M}(n)} > \chi_{p-1, 1-\alpha}^2,$$

where $\widehat{\Delta}_{\boldsymbol{\theta}, \text{vMF}; g; 2*}^{\mathcal{T}\mathcal{M}(n)}$ and $\widehat{\Gamma}_{\boldsymbol{\theta}, \text{vMF}; g; 22*}^{\mathcal{T}\mathcal{M}(n)}$ result from $\Delta_{\boldsymbol{\theta}, \text{vMF}; g; 2*}^{\mathcal{T}\mathcal{M}(n)}$ and $\Gamma_{\text{vMF}; g; 22*}^{\mathcal{T}\mathcal{M}(n)}$, respectively, by replacing $\boldsymbol{\theta}$ with $\widehat{\boldsymbol{\theta}}$ and the quantities in (18) with their consistent estimators in (19). Clearly, this test is the test $\phi_{\text{vMF}}^{\text{loc}}$ from Section 3.2. While this test was built to be locally asymptotically maximin at asymptotic level α when testing

$$\bigcup_{\boldsymbol{\theta} \in \mathcal{S}^{p-1}} \bigcup_{g \in \mathcal{G}_a \cap \mathcal{G}_b \cap \mathcal{G}'} \{P_{\boldsymbol{\theta}, g}^{(n)}\} \quad \text{against} \quad \bigcup_{\boldsymbol{\theta} \in \mathcal{S}^{p-1}} \bigcup_{\boldsymbol{\mu} \in \mathcal{S}^{p-2}} \bigcup_{\kappa > 0} \{P_{\boldsymbol{\theta}, f_{\eta}, \boldsymbol{\mu}, \kappa}^{\mathcal{T}\mathcal{M}(n)}\},$$

it is also optimal for the problem of testing

$$\bigcup_{\boldsymbol{\theta} \in \mathcal{S}^{p-1}} \bigcup_{g \in \mathcal{G}_a \cap \mathcal{G}_b \cap \mathcal{G}'} \{P_{\boldsymbol{\theta}, g}^{(n)}\} \quad \text{against} \quad \bigcup_{\boldsymbol{\theta} \in \mathcal{S}^{p-1}} \bigcup_{\eta > 0} \bigcup_{\boldsymbol{\mu} \in \mathcal{S}^{p-2}} \bigcup_{\kappa > 0} \{P_{\boldsymbol{\theta}, f_{\eta}, \boldsymbol{\mu}, \kappa}^{\mathcal{T}\mathcal{M}(n)}\}$$

since $Q_{\text{vMF}}^{\text{loc}}$ does not depend on η .

B Proofs of the main results

The lemmas given in Appendix C are used to prove the main results.

Proof of Theorem 1. Consider first the case $\mathbf{X} \sim \mathcal{TE}_p(\boldsymbol{\theta}_0, g, \boldsymbol{\Lambda})$, with $\boldsymbol{\theta}_0 := (1, 0, \dots, 0)^T \in \mathbb{R}^p$. Clearly, $\mathbf{X} = (V, (1 - V^2)^{1/2} \mathbf{U}^T)^T$, with $V := v_{\boldsymbol{\theta}_0}(\mathbf{X}) = X_1$ and $\mathbf{U} := \mathbf{u}_{\boldsymbol{\theta}_0}(\mathbf{X}) = (X_2, \dots, X_p)^T / \sqrt{1 - X_1^2}$, where we used the notation introduced in (1). By definition, \mathbf{U} takes its values in \mathcal{S}^{p-2} , with density $\mathbf{u} \mapsto c_{p-1, \boldsymbol{\Lambda}}^{\mathcal{A}}(\mathbf{u}^T \boldsymbol{\Lambda}^{-1} \mathbf{u})^{-(p-1)/2}$ with respect to σ_{p-2} . Therefore, conditional on $V = v$, $(1 - V^2)^{1/2} \mathbf{U}$ takes its values on the hypersphere $\mathcal{S}^{p-2}(r_v) \subset \mathbb{R}^{p-1}$ with radius $r_v := (1 - v^2)^{1/2}$. Its density with respect to the surface area measure $\sigma_{p-2, r}$ on $\mathcal{S}^{p-2}(r_v)$ is (recall that V and \mathbf{U} are mutually independent)

$$\mathbf{w} \mapsto c_{p-1, \boldsymbol{\Lambda}}^{\mathcal{A}} \left(\frac{\mathbf{w}^T \boldsymbol{\Lambda}^{-1} \mathbf{w}}{r_v^2} \right)^{-(p-1)/2} r_v^{-(p-2)},$$

where $r^{-(p-2)}$ is the Jacobian of the radial projection of $\mathcal{S}^{p-2}(r)$ onto \mathcal{S}^{p-2} . Since $d\sigma_{p-2, r} = r^{p-2} d\sigma_{p-2}$, the density of \mathbf{X} with respect to the product measure $\mu \times \sigma_{p-2}$ (where μ stands for the Lebesgue measure on $[-1, 1]$) is

$$\begin{aligned} \mathbf{x} &\mapsto c_{p-1, \boldsymbol{\Lambda}}^{\mathcal{A}} (\mathbf{u}_{\boldsymbol{\theta}_0}^T(\mathbf{x}) \boldsymbol{\Lambda}^{-1} \mathbf{u}_{\boldsymbol{\theta}_0}(\mathbf{x}))^{-(p-1)/2} \frac{dP_{\boldsymbol{\theta}_0, g, \boldsymbol{\Lambda}}^V}{d\mu}(v_{\boldsymbol{\theta}_0}(\mathbf{x})) \\ &= c_{p-1, \boldsymbol{\Lambda}}^{\mathcal{A}} (\mathbf{u}_{\boldsymbol{\theta}_0}^T(\mathbf{x}) \boldsymbol{\Lambda}^{-1} \mathbf{u}_{\boldsymbol{\theta}_0}(\mathbf{x}))^{-(p-1)/2} \omega_{p-1} c_{p, g} (1 - v_{\boldsymbol{\theta}_0}^2(\mathbf{x}))^{(p-3)/2} g(v_{\boldsymbol{\theta}_0}(\mathbf{x})). \end{aligned}$$

The result for $\boldsymbol{\theta} = \boldsymbol{\theta}_0$ then follows from the fact that (see, e.g., page 44 of Watson, 1983)

$$\frac{d(\mu \times \sigma_{p-2})}{d\sigma_{p-1}}(\mathbf{x}) = (1 - v_{\boldsymbol{\theta}_0}^2(\mathbf{x}))^{(p-3)/2}.$$

To obtain the result for an arbitrary value of $\boldsymbol{\theta}$, let $\mathbf{X} \sim \mathcal{TE}_p(\boldsymbol{\theta}, g, \boldsymbol{\Lambda})$ and pick a $p \times p$ orthogonal matrix \mathbf{O} such that $\mathbf{O}\boldsymbol{\theta} = \boldsymbol{\theta}_0$. Since $\mathbf{O}\boldsymbol{\Gamma}_{\boldsymbol{\theta}} = \boldsymbol{\Gamma}_{\boldsymbol{\theta}_0}$, we have that $\mathbf{O}\mathbf{X} \sim \mathcal{TE}_p(\boldsymbol{\theta}_0, g, \boldsymbol{\Lambda})$. Therefore, the result for $\boldsymbol{\theta} = \boldsymbol{\theta}_0$ implies that the density of \mathbf{X} with respect to σ_{p-1} is

$$\begin{aligned} \mathbf{x} &\mapsto |\det \mathbf{O}| \omega_{p-1} c_{p-1, \boldsymbol{\Lambda}}^{\mathcal{A}} c_{p, g} g(v_{\boldsymbol{\theta}_0}(\mathbf{O}\mathbf{x})) (\mathbf{u}_{\boldsymbol{\theta}_0}^T(\mathbf{O}\mathbf{x}) \boldsymbol{\Lambda}^{-1} \mathbf{u}_{\boldsymbol{\theta}_0}(\mathbf{O}\mathbf{x}))^{-(p-1)/2} \\ &= \omega_{p-1} c_{p-1, \boldsymbol{\Lambda}}^{\mathcal{A}} c_{p, g} g(v_{\boldsymbol{\theta}}(\mathbf{x})) (\mathbf{u}_{\boldsymbol{\theta}}^T(\mathbf{x}) \boldsymbol{\Lambda}^{-1} \mathbf{u}_{\boldsymbol{\theta}}(\mathbf{x}))^{-(p-1)/2}, \end{aligned}$$

as was to be proved. \square

Proof of Theorem 3. Lemma 3 readily entails that

$$\log \frac{dP_{\boldsymbol{\theta}_n, g, \boldsymbol{\Lambda}_n}^{\mathcal{T}\mathcal{E}(n)}}{dP_{\boldsymbol{\theta}, g}^{(n)}} = \log \frac{dP_{\boldsymbol{\theta}_n, g, \boldsymbol{\Lambda}_n}^{\mathcal{T}\mathcal{E}(n)}}{dP_{\boldsymbol{\theta}_n, g}^{(n)}} + \log \frac{dP_{\boldsymbol{\theta}_n, g}^{(n)}}{dP_{\boldsymbol{\theta}, g}^{(n)}} = \log \frac{dP_{\boldsymbol{\theta}_n, g, \boldsymbol{\Lambda}_n}^{\mathcal{T}\mathcal{E}(n)}}{dP_{\boldsymbol{\theta}, g}^{(n)}} + \mathbf{t}_n^T \boldsymbol{\Delta}_{\boldsymbol{\theta}, g; 1}^{(n)} - \frac{1}{2} \mathbf{t}_n^T \boldsymbol{\Gamma}_{\boldsymbol{\theta}, g; 11} \mathbf{t}_n + o_P(1)$$

as $n \rightarrow \infty$ under $P_{\boldsymbol{\theta}, g}^{(n)}$. Therefore, we only need to show that

$$L_n := \log \frac{dP_{\boldsymbol{\theta}_n, g, \boldsymbol{\Lambda}_n}^{\mathcal{T}\mathcal{E}(n)}}{dP_{\boldsymbol{\theta}_n, g}^{(n)}} = (\text{vech} \mathbf{L}_n)^T \boldsymbol{\Delta}_{\boldsymbol{\theta}, 2}^{\mathcal{T}\mathcal{E}(n)} - \frac{1}{2} (\text{vech} \mathbf{L}_n)^T \boldsymbol{\Gamma}_{\boldsymbol{\theta}, 22}^{\mathcal{T}\mathcal{E}} (\text{vech} \mathbf{L}_n) + o_P(1)$$

as $n \rightarrow \infty$ under $P_{\boldsymbol{\theta}, g}^{(n)}$. First note that Theorem 1 gives

$$L_n = -\frac{n}{2} \log (\det \boldsymbol{\Lambda}_n) - \frac{p-1}{2} \sum_{i=1}^n \log (\mathbf{U}_{i, \boldsymbol{\theta}_n}^T \boldsymbol{\Lambda}_n^{-1} \mathbf{U}_{i, \boldsymbol{\theta}_n}) =: L_{n,1} + L_{n,2}, \quad (20)$$

say. Since $\log(\det(\mathbf{I}_{p-1} + \mathbf{A})) = \text{tr}[\mathbf{A}] - \frac{1}{2} \text{tr}[\mathbf{A}^2] + o(\|\mathbf{A}\|^2)$ as $\|\mathbf{A}\| \rightarrow 0$, we have that

$$L_{n,1} = -\frac{n}{2} \log (\det(\mathbf{I}_{p-1} + n^{-1/2} \mathbf{L}_n)) = \frac{1}{4} \text{tr}[\mathbf{L}_n^2] + o(1) \quad (21)$$

as $n \rightarrow \infty$ (recall that $\text{tr}[\mathbf{L}_n] = 0$). Now, write

$$\begin{aligned} L_{n,2} &= -\frac{p-1}{2} \sum_{i=1}^n \log (1 + \mathbf{U}_{i, \boldsymbol{\theta}_n}^T (\boldsymbol{\Lambda}_n^{-1} - \mathbf{I}_{p-1}) \mathbf{U}_{i, \boldsymbol{\theta}_n}) \\ &= -\frac{p-1}{2} \sum_{i=1}^n \log (1 + \text{tr}[\mathbf{U}_{i, \boldsymbol{\theta}_n} \mathbf{U}_{i, \boldsymbol{\theta}_n}^T (\boldsymbol{\Lambda}_n^{-1} - \mathbf{I}_{p-1})]) \\ &=: -\frac{p-1}{2} \sum_{i=1}^n \log (1 + T_{i,n}). \end{aligned}$$

Using (9)–(10) in pages 218–219 from Magnus and Neudecker (2007), we obtain that $T_{i,n} = -n^{-1/2} \mathbf{U}_{i, \boldsymbol{\theta}_n}^T \mathbf{L}_n \mathbf{U}_{i, \boldsymbol{\theta}_n} + n^{-1} \mathbf{U}_{i, \boldsymbol{\theta}_n}^T \mathbf{L}_n^2 \mathbf{U}_{i, \boldsymbol{\theta}_n} + R_{i,n}$, where (due to the uniform boundedness of the $\mathbf{U}_{i, \boldsymbol{\theta}_n}$'s) $\max_{i=1, \dots, n} R_{i,n} = O_P(n^{-3/2})$ as $n \rightarrow \infty$ under $P_{\boldsymbol{\theta}, g}^{(n)}$. Using the fact that $\log(1+x) = x - \frac{1}{2}x^2 + o(x^2)$ as $x \rightarrow 0$, it follows that

$$\begin{aligned} L_{n,2} &= -\frac{p-1}{2} \sum_{i=1}^n \log \left(1 - \frac{1}{\sqrt{n}} \mathbf{U}_{i, \boldsymbol{\theta}_n}^T \mathbf{L}_n \mathbf{U}_{i, \boldsymbol{\theta}_n} + \frac{1}{n} \mathbf{U}_{i, \boldsymbol{\theta}_n}^T \mathbf{L}_n^2 \mathbf{U}_{i, \boldsymbol{\theta}_n} + R_{i,n} \right) \\ &= -\frac{p-1}{2} \sum_{i=1}^n \left\{ -\frac{1}{\sqrt{n}} \mathbf{U}_{i, \boldsymbol{\theta}_n}^T \mathbf{L}_n \mathbf{U}_{i, \boldsymbol{\theta}_n} + \frac{1}{n} \mathbf{U}_{i, \boldsymbol{\theta}_n}^T \mathbf{L}_n^2 \mathbf{U}_{i, \boldsymbol{\theta}_n} - \frac{1}{2n} (\mathbf{U}_{i, \boldsymbol{\theta}_n}^T \mathbf{L}_n \mathbf{U}_{i, \boldsymbol{\theta}_n})^2 \right\} + o_P(1) \end{aligned}$$

as $n \rightarrow \infty$ under $P_{\boldsymbol{\theta}, g}^{(n)}$. Using Lemma 2, the law of large numbers for triangular arrays then yields

$$\begin{aligned} L_{n,2} &= \left(\frac{p-1}{2\sqrt{n}} \sum_{i=1}^n \mathbf{U}_{i, \boldsymbol{\theta}_n}^T \mathbf{L}_n \mathbf{U}_{i, \boldsymbol{\theta}_n} \right) - \frac{p-1}{2} \mathbb{E} \left[\mathbf{U}_{1, \boldsymbol{\theta}_n}^T \mathbf{L}_n^2 \mathbf{U}_{1, \boldsymbol{\theta}_n} - \frac{1}{2} (\mathbf{U}_{1, \boldsymbol{\theta}_n}^T \mathbf{L}_n \mathbf{U}_{1, \boldsymbol{\theta}_n})^2 \right] + o_P(1) \\ &= \frac{p-1}{2\sqrt{n}} (\text{vec} \mathbf{L}_n)^T \sum_{i=1}^n \text{vec} (\mathbf{U}_{i, \boldsymbol{\theta}_n} \mathbf{U}_{i, \boldsymbol{\theta}_n}^T) \\ &\quad - \frac{p-1}{2} (\text{vec} \mathbf{L}_n)^T \left[\frac{1}{p-1} \mathbf{I}_{(p-1)^2} - \frac{1}{2(p^2-1)} (\mathbf{I}_{(p-1)^2} + \mathbf{K}_{p-1} + \mathbf{J}_{p-1}) \right] (\text{vec} \mathbf{L}_n) + o_P(1) \end{aligned}$$

as $n \rightarrow \infty$ under $P_{\theta,g}^{(n)}$. Applying Part (iii $_{\mathcal{T}\mathcal{E}}$) of Lemma 4, and using the identities $\mathbf{K}_{p-1}(\text{vec } \mathbf{A}) = \text{vec}(\mathbf{A}^T)$ and $(\text{vec } \mathbf{A})^T(\text{vec } \mathbf{B}) = \text{tr}[\mathbf{A}^T \mathbf{B}]$ (this second identity provides $(\text{vec } \mathbf{I}_{p-1})^T(\text{vec } \mathbf{L}_n) = \text{tr}[\mathbf{L}_n] = 0$, hence $\mathbf{J}_{p-1}(\text{vec } \mathbf{L}_n) = \mathbf{0}$), we obtain

$$L_{n,2} = \frac{p-1}{2\sqrt{n}} (\text{vec } \mathbf{L}_n)^T \sum_{i=1}^n \text{vec} \left(\mathbf{U}_{i,\theta} \mathbf{U}_{i,\theta}^T - \frac{1}{p-1} \mathbf{I}_{p-1} \right) - \frac{p}{2(p+1)} \text{tr}[\mathbf{L}_n^2] + o_P(1) \quad (22)$$

as $n \rightarrow \infty$ under $P_{\theta,g}^{(n)}$. Plugging (21)–(22) in (20) then provides

$$L_n = \frac{p-1}{2\sqrt{n}} (\text{vec } \mathbf{L}_n)^T \sum_{i=1}^n \text{vec} \left(\mathbf{U}_{i,\theta} \mathbf{U}_{i,\theta}^T - \frac{1}{p-1} \mathbf{I}_{p-1} \right) - \frac{p-1}{4(p+1)} \text{tr}[\mathbf{L}_n^2] + o_P(1),$$

as $n \rightarrow \infty$ under $P_{\theta,g}^{(n)}$, which, by using the definition of \mathbf{M}_p and the matrix identities above, yields (8).

Finally, the CLT ensures that, under $P_{\theta,g}^{(n)}$, $\Delta_{\theta;2}^{\mathcal{T}\mathcal{E}(n)} \xrightarrow{\mathcal{D}} \mathcal{N}(\mathbf{0}, \Gamma_{\theta;22}^{\mathcal{T}\mathcal{E}})$ with

$$\mathbf{M}_p \left(\frac{p-1}{4(p+1)} (\mathbf{I}_{(p-1)^2} + \mathbf{K}_{p-1} + \mathbf{J}_{p-1}) - \frac{1}{4} \mathbf{J}_{p-1} \right) \mathbf{M}_p^T = \frac{p-1}{4(p+1)} \mathbf{M}_p (\mathbf{I}_{(p-1)^2} + \mathbf{K}_{p-1}) \mathbf{M}_p^T = \Gamma_{\theta;22}^{\mathcal{T}\mathcal{E}},$$

where we used the fact that $\mathbf{M}_p(\text{vec } \mathbf{I}_{p-1}) = \mathbf{0}$ (see (v) in Lemma 4.2 of Paindaveine (2008)). \square

Proof of Theorem 4. First note that

$$\log \frac{dP_{\theta_n,g,\delta_n}^{\mathcal{T}\mathcal{M}(n)}}{dP_{\theta,g}^{(n)}} = \log \frac{dP_{\theta_n,g,\delta_n}^{\mathcal{T}\mathcal{M}(n)}}{dP_{\theta_n,g}^{(n)}} + \log \frac{dP_{\theta_n,g}^{(n)}}{dP_{\theta,g}^{(n)}} = \log \frac{dP_{\theta_n,g,\delta_n}^{\mathcal{T}\mathcal{M}(n)}}{dP_{\theta_n,g}^{(n)}} + \mathbf{t}_n^T \Delta_{\theta,g;1}^{(n)} - \frac{1}{2} \mathbf{t}_n^T \Gamma_{\theta,g;11} \mathbf{t}_n + o_P(1).$$

In the parametrization adopted in Theorem 4, recall that δ_n corresponds to a skewness direction $\mu_n := \delta_n / \|\delta_n\| = \mathbf{d}_n / \|\mathbf{d}_n\|$ and a skewness intensity $\kappa_n := \|\delta_n\| = n^{-1/2} \|\mathbf{d}_n\|$. From Theorem 2, we then readily obtain

$$G_n := \log \frac{dP_{\theta_n,g,\delta_n}^{\mathcal{T}\mathcal{M}(n)}}{dP_{\theta_n,g}^{(n)}} = n \left(\log(c_{p-1,n^{-1/2}\|\mathbf{d}^{(n)}\|}) - \log(c_{p-1,0}) \right) + (\mathbf{d}^{(n)})^T \frac{1}{\sqrt{n}} \sum_{i=1}^n \mathbf{U}_{i,\theta_n}.$$

Lemma A.1 in Cutting et al. (2017) implies that

$$n \left(\log(c_{p-1,n^{-1/2}\|\mathbf{d}^{(n)}\|}) - \log(c_{p-1,0}) \right) = -\frac{1}{2(p-1)} \|\mathbf{d}^{(n)}\|^2 + o(1)$$

as $n \rightarrow \infty$, which, by using (iii $_{\mathcal{T}\mathcal{M}}$) in Lemma 4, yields

$$\begin{aligned} G_n &= (\mathbf{d}^{(n)})^T \frac{1}{\sqrt{n}} \sum_{i=1}^n \mathbf{U}_{i,\theta_n} - \frac{1}{2(p-1)} \|\mathbf{d}^{(n)}\|^2 + o_P(1) \\ &= (\mathbf{d}^{(n)})^T \left[\frac{1}{\sqrt{n}} \sum_{i=1}^n \mathbf{U}_{i,\theta} - \frac{\mathcal{I}_p(g)}{p-1} \Gamma_{\theta}^T \mathbf{t}_n \right] - \frac{1}{2(p-1)} \|\mathbf{d}^{(n)}\|^2 + o_P(1) \end{aligned}$$

as $n \rightarrow \infty$ under $P_{\theta,g}^{(n)}$. Therefore,

$$\begin{aligned} \log \frac{dP_{\theta_n,g,\delta_n}^{\mathcal{T}\mathcal{M}(n)}}{dP_{\theta,g}^{(n)}} &= \mathbf{t}_n^T \Delta_{1,\theta}^{(n)} + (\mathbf{d}^{(n)})^T \frac{1}{\sqrt{n}} \sum_{i=1}^n \mathbf{U}_{i,\theta} \\ &\quad - \frac{1}{2} \left(\mathbf{t}_n^T \Gamma_{\theta,g;11} \mathbf{t}_n + \frac{2\mathcal{I}_p(g)}{p-1} (\mathbf{d}^{(n)})^T \Gamma_{\theta}^T \mathbf{t}_n + \frac{1}{p-1} \|\mathbf{d}^{(n)}\|^2 \right) + o_P(1), \end{aligned}$$

as $n \rightarrow \infty$ under $P_{\theta,g}^{(n)}$, which establishes the result. \square

Proof of Proposition 2. Proposition 3.1 of Ley et al. (2013) directly implies that if $\hat{\boldsymbol{\theta}}$ satisfies $A_{\mathcal{G}'}$, then

$$\Delta_{\hat{\boldsymbol{\theta}},g;1}^{(n)} = \Delta_{\boldsymbol{\theta},g;1}^{(n)} - \boldsymbol{\Gamma}_{\boldsymbol{\theta},g;11} \sqrt{n}(\hat{\boldsymbol{\theta}} - \boldsymbol{\theta}) + o_P(1) \quad (23)$$

as $n \rightarrow \infty$ under $P_{\boldsymbol{\theta},g}^{(n)}$. Using this and (10), we obtain that, again as $n \rightarrow \infty$ under $P_{\boldsymbol{\theta},g}^{(n)}$,

$$\begin{aligned} \Delta_{\hat{\boldsymbol{\theta}},g;2*}^{\mathcal{T}\mathcal{M}(n)} &= \Delta_{\hat{\boldsymbol{\theta}},2}^{\mathcal{T}\mathcal{M}(n)} - \boldsymbol{\Gamma}_{\hat{\boldsymbol{\theta}},g;21}^{\mathcal{T}\mathcal{M}} \boldsymbol{\Gamma}_{\hat{\boldsymbol{\theta}},g;11}^- \Delta_{\hat{\boldsymbol{\theta}},g;1}^{(n)} \\ &= (\Delta_{\boldsymbol{\theta},2}^{\mathcal{T}\mathcal{M}(n)} - \boldsymbol{\Gamma}_{\boldsymbol{\theta},g;21}^{\mathcal{T}\mathcal{M}} \sqrt{n}(\hat{\boldsymbol{\theta}} - \boldsymbol{\theta})) - \boldsymbol{\Gamma}_{\boldsymbol{\theta},g;21}^{\mathcal{T}\mathcal{M}} \boldsymbol{\Gamma}_{\hat{\boldsymbol{\theta}},g;11}^- (\Delta_{\boldsymbol{\theta},g;1}^{(n)} - \boldsymbol{\Gamma}_{\boldsymbol{\theta},g;11} \sqrt{n}(\hat{\boldsymbol{\theta}} - \boldsymbol{\theta})) + o_P(1) \\ &= \Delta_{\boldsymbol{\theta},g;2*}^{\mathcal{T}\mathcal{M}(n)} - \boldsymbol{\Gamma}_{\boldsymbol{\theta},g;21}^{\mathcal{T}\mathcal{M}} \sqrt{n}(\hat{\boldsymbol{\theta}} - \boldsymbol{\theta}) + \boldsymbol{\Gamma}_{\boldsymbol{\theta},g;21}^{\mathcal{T}\mathcal{M}} \boldsymbol{\Gamma}_{\hat{\boldsymbol{\theta}},g;11}^- \boldsymbol{\Gamma}_{\boldsymbol{\theta},g;11} \sqrt{n}(\hat{\boldsymbol{\theta}} - \boldsymbol{\theta}) + o_P(1) \\ &= \Delta_{\boldsymbol{\theta},g;2*}^{\mathcal{T}\mathcal{M}(n)} - \boldsymbol{\Gamma}_{\boldsymbol{\theta},g;21}^{\mathcal{T}\mathcal{M}} \sqrt{n}(\hat{\boldsymbol{\theta}} - \boldsymbol{\theta}) + \boldsymbol{\Gamma}_{\boldsymbol{\theta},g;21}^{\mathcal{T}\mathcal{M}} \boldsymbol{\Gamma}_{\hat{\boldsymbol{\theta}},g;11}^- \boldsymbol{\Gamma}_{\boldsymbol{\theta},g;11} \sqrt{n}(\hat{\boldsymbol{\theta}} - \boldsymbol{\theta}) + o_P(1) \\ &= \Delta_{\boldsymbol{\theta},g;2*}^{\mathcal{T}\mathcal{M}(n)} + o_P(1), \end{aligned}$$

where the last equality follows from the fact that $(\mathbf{I}_p - \boldsymbol{\theta}\boldsymbol{\theta}^T)\sqrt{n}(\hat{\boldsymbol{\theta}} - \boldsymbol{\theta}) = \sqrt{n}(\hat{\boldsymbol{\theta}} - \boldsymbol{\theta}) + o_P(1)$ as $n \rightarrow \infty$ under $P_{\boldsymbol{\theta},g}^{(n)}$. The result follows. \square

Proof of Proposition 3. Proposition 3.1 of Ley et al. (2013) actually shows that the asymptotic linearity property in (23) generalizes into

$$\Delta_{\hat{\boldsymbol{\theta}},f;1}^{(n)} = \Delta_{\boldsymbol{\theta},f;1}^{(n)} - \boldsymbol{\Gamma}_{\boldsymbol{\theta},f;g;11} \sqrt{n}(\hat{\boldsymbol{\theta}} - \boldsymbol{\theta}) + o_P(1)$$

as $n \rightarrow \infty$ under $P_{\boldsymbol{\theta},g}^{(n)}$, which, jointly with (10), provides

$$\begin{aligned} \Delta_{\boldsymbol{\theta},f;g;2*}^{\mathcal{T}\mathcal{M}(n)} &= \Delta_{\boldsymbol{\theta},2}^{\mathcal{T}\mathcal{M}(n)} - \boldsymbol{\Gamma}_{\boldsymbol{\theta},g;21}^{\mathcal{T}\mathcal{M}} \boldsymbol{\Gamma}_{\boldsymbol{\theta},f;g;11}^- \Delta_{\boldsymbol{\theta},f;1}^{(n)} \\ &= (\Delta_{\boldsymbol{\theta},2}^{\mathcal{T}\mathcal{M}(n)} - \boldsymbol{\Gamma}_{\boldsymbol{\theta},g;21}^{\mathcal{T}\mathcal{M}} \sqrt{n}(\hat{\boldsymbol{\theta}} - \boldsymbol{\theta})) - \boldsymbol{\Gamma}_{\boldsymbol{\theta},g;21}^{\mathcal{T}\mathcal{M}} \boldsymbol{\Gamma}_{\boldsymbol{\theta},f;g;11}^- (\Delta_{\boldsymbol{\theta},f;1}^{(n)} - \boldsymbol{\Gamma}_{\boldsymbol{\theta},f;g;11} \sqrt{n}(\hat{\boldsymbol{\theta}} - \boldsymbol{\theta})) + o_P(1) \\ &= \Delta_{\boldsymbol{\theta},f;g;2*}^{\mathcal{T}\mathcal{M}(n)} - \boldsymbol{\Gamma}_{\boldsymbol{\theta},g;21}^{\mathcal{T}\mathcal{M}} \sqrt{n}(\hat{\boldsymbol{\theta}} - \boldsymbol{\theta}) + \boldsymbol{\Gamma}_{\boldsymbol{\theta},g;21}^{\mathcal{T}\mathcal{M}} \boldsymbol{\Gamma}_{\boldsymbol{\theta},f;g;11}^- \boldsymbol{\Gamma}_{\boldsymbol{\theta},f;g;11} \sqrt{n}(\hat{\boldsymbol{\theta}} - \boldsymbol{\theta}) + o_P(1) \\ &= \Delta_{\boldsymbol{\theta},f;g;2*}^{\mathcal{T}\mathcal{M}(n)} + o_P(1) \end{aligned}$$

as $n \rightarrow \infty$ under $P_{\boldsymbol{\theta},g}^{(n)}$, which is the desired result. \square

C Required lemmas

Lemma 1. For any $\boldsymbol{\theta} \in \mathcal{S}^{p-1}$ and $g \in \mathcal{G}$, under $P_{\boldsymbol{\theta},g}^{(n)}$:

- (i) $E[\mathbf{U}_{1,\boldsymbol{\theta}}] = \mathbf{0}$,
- (ii) $E[\mathbf{U}_{1,\boldsymbol{\theta}} \mathbf{U}_{1,\boldsymbol{\theta}}^T] = \frac{1}{p-1} \mathbf{I}_{p-1}$,
- (iii) $E[\text{vec}(\mathbf{U}_{1,\boldsymbol{\theta}} \mathbf{U}_{1,\boldsymbol{\theta}}^T) \text{vec}(\mathbf{U}_{1,\boldsymbol{\theta}} \mathbf{U}_{1,\boldsymbol{\theta}}^T)^T] = \frac{1}{p^2-1} (\mathbf{I}_{(p-1)^2} + \mathbf{K}_{p-1} + \mathbf{J}_{p-1})$.

Proof of Lemma 1. The result is a direct consequence of Lemma A.2 in Paindaveine and Verdebout (2016). \square

Lemma 2. For any $\boldsymbol{\theta} \in \mathcal{S}^{p-1}$, $g \in \mathcal{G}$, and any bounded sequence (\mathbf{t}_n) in \mathbb{R}^p such that $\boldsymbol{\theta}_n = \boldsymbol{\theta} + n^{-1/2} \mathbf{t}_n \in \mathcal{S}^{p-1}$ for any n , we have that, as $n \rightarrow \infty$ under $P_{\boldsymbol{\theta},g}^{(n)}$:

- (i) $E[\mathbf{U}_{1,\boldsymbol{\theta}_n}] = o(1)$,

$$(ii) \quad \mathbb{E}[\mathbf{U}_{1,\theta_n} \mathbf{U}_{1,\theta_n}^T] = \frac{1}{p-1} \mathbf{I}_{p-1} + o(1),$$

$$(iii) \quad \mathbb{E}[\text{vec}(\mathbf{U}_{1,\theta_n} \mathbf{U}_{1,\theta_n}^T) \text{vec}(\mathbf{U}_{1,\theta_n} \mathbf{U}_{1,\theta_n}^T)^T] = \frac{1}{p^2-1} (\mathbf{I}_{(p-1)^2} + \mathbf{K}_{p-1} + \mathbf{J}_{p-1}) + o(1).$$

Proof of Lemma 2. All expectations in this proof are under $\mathbb{P}_{\theta,g}^{(n)}$ and all convergences are as $n \rightarrow \infty$. For (i) first note that, letting $\mathbf{Z}_{1,\theta} := \mathbf{\Gamma}_{\theta}^T \mathbf{X}_1$ and $d_{1,\theta} := \|\mathbf{Z}_{1,\theta}\|$, we have

$$\begin{aligned} \|\mathbf{U}_{1,\theta_n} - \mathbf{U}_{1,\theta}\| &\leq \left\| \frac{\mathbf{Z}_{1,\theta_n}}{d_{1,\theta_n}} - \frac{\mathbf{Z}_{1,\theta_n}}{d_{1,\theta}} \right\| + \left\| \frac{\mathbf{Z}_{1,\theta_n}}{d_{1,\theta}} - \frac{\mathbf{Z}_{1,\theta}}{d_{1,\theta}} \right\| \\ &\leq \left| \frac{1}{d_{1,\theta_n}} - \frac{1}{d_{1,\theta}} \right| \|\mathbf{Z}_{1,\theta_n}\| + \frac{1}{d_{1,\theta}} \|\mathbf{Z}_{1,\theta_n} - \mathbf{Z}_{1,\theta}\| \\ &\leq \frac{|d_{1,\theta_n} - d_{1,\theta}|}{d_{1,\theta}} + \frac{1}{d_{1,\theta}} \|\mathbf{Z}_{1,\theta_n} - \mathbf{Z}_{1,\theta}\| \\ &\leq \frac{2\|\mathbf{Z}_{1,\theta_n} - \mathbf{Z}_{1,\theta}\|}{d_{1,\theta}}, \end{aligned}$$

which implies that $\|\mathbf{U}_{1,\theta_n} - \mathbf{U}_{1,\theta}\| = o_P(1)$. Uniform integrability follows because $\|\mathbf{U}_{1,\theta_n} - \mathbf{U}_{1,\theta}\| \leq 2$ almost surely, hence

$$\mathbb{E}[\|\mathbf{U}_{1,\theta_n} - \mathbf{U}_{1,\theta}\|^2] = o(1). \quad (24)$$

Since $\|\mathbb{E}[\mathbf{U}_{1,\theta_n}]\|^2 = \|\mathbb{E}[\mathbf{U}_{1,\theta_n} - \mathbf{U}_{1,\theta}]\|^2 \leq (\mathbb{E}[\|\mathbf{U}_{1,\theta_n} - \mathbf{U}_{1,\theta}\|])^2 \leq \mathbb{E}[\|\mathbf{U}_{1,\theta_n} - \mathbf{U}_{1,\theta}\|^2]$, the result then follows from (i) in Lemma 1. For proving (ii), we have that, since (ii) in Lemma 1 entails that

$$\left\| \text{vec} \left(\mathbb{E}[\mathbf{U}_{1,\theta_n} \mathbf{U}_{1,\theta_n}^T] - \frac{1}{p-1} \mathbf{I}_{p-1} \right) \right\|^2 = \left\| \mathbb{E}[\text{vec}(\mathbf{U}_{1,\theta_n} \mathbf{U}_{1,\theta_n}^T) - \text{vec}(\mathbf{U}_{1,\theta} \mathbf{U}_{1,\theta}^T)] \right\|^2,$$

it is enough to show that

$$\mathbb{E}[\|\text{vec}(\mathbf{U}_{1,\theta_n} \mathbf{U}_{1,\theta_n}^T) - \text{vec}(\mathbf{U}_{1,\theta} \mathbf{U}_{1,\theta}^T)\|^2] = o(1). \quad (25)$$

This follows from (24), the fact that $\|\text{vec}(\mathbf{U}_{1,\theta_n} \mathbf{U}_{1,\theta_n}^T) - \text{vec}(\mathbf{U}_{1,\theta} \mathbf{U}_{1,\theta}^T)\|^2 = \text{tr}[(\mathbf{U}_{1,\theta_n} \mathbf{U}_{1,\theta_n}^T - \mathbf{U}_{1,\theta} \mathbf{U}_{1,\theta}^T)^2] = 2(1 - (\mathbf{U}_{1,\theta_n}^T \mathbf{U}_{1,\theta})^2) = \|\mathbf{U}_{1,\theta_n} - \mathbf{U}_{1,\theta}\|^2$, and the arguments in the proof of (i). For (iii), we proceed as above and use that (iii) in Lemma 1 entails that it is sufficient to show that

$$w_n := \mathbb{E}[\|\text{vec}(\mathbf{U}_{1,\theta_n} \mathbf{U}_{1,\theta_n}^T) \text{vec}(\mathbf{U}_{1,\theta_n} \mathbf{U}_{1,\theta_n}^T)^T - \text{vec}(\mathbf{U}_{1,\theta} \mathbf{U}_{1,\theta}^T) \text{vec}(\mathbf{U}_{1,\theta} \mathbf{U}_{1,\theta}^T)^T\|^2] = o(1).$$

Since $w_n \leq 2(w_{1n} + w_{2n})$, with

$$\begin{aligned} w_{1n} &:= \mathbb{E}[\|\text{vec}(\mathbf{U}_{1,\theta_n} \mathbf{U}_{1,\theta_n}^T) - \text{vec}(\mathbf{U}_{1,\theta} \mathbf{U}_{1,\theta}^T)\| \|\text{vec}(\mathbf{U}_{1,\theta_n} \mathbf{U}_{1,\theta_n}^T)^T\|^2], \\ w_{2n} &:= \mathbb{E}[\|\text{vec}(\mathbf{U}_{1,\theta} \mathbf{U}_{1,\theta}^T) (\text{vec}(\mathbf{U}_{1,\theta_n} \mathbf{U}_{1,\theta_n}^T) - \text{vec}(\mathbf{U}_{1,\theta} \mathbf{U}_{1,\theta}^T)^T)\|^2], \end{aligned}$$

and since \mathbf{U}_{1,θ_n} and $\mathbf{U}_{1,\theta}$ are bounded almost surely, the result follows from (25). \square

Lemma 3. Fix $\theta \in \mathcal{S}^{p-1}$, $g \in \mathcal{G}_a$, and let (\mathbf{t}_n) be a bounded sequence in \mathbb{R}^p such that $\theta_n := \theta + n^{-1/2} \mathbf{t}_n \in \mathcal{S}^{p-1}$ for any n . Then,

$$\log \frac{d\mathbb{P}_{\theta_n,g}^{(n)}}{d\mathbb{P}_{\theta,g}^{(n)}} = \mathbf{t}_n^T \Delta_{\theta,g;1}^{(n)} - \frac{1}{2} \mathbf{t}_n^T \mathbf{\Gamma}_{\theta,g;11} \mathbf{t}_n + o_P(1),$$

as $n \rightarrow \infty$ under $\mathbb{P}_{\theta,g}^{(n)}$, where $\Delta_{\theta,g;1}^{(n)}$ and $\mathbf{\Gamma}_{\theta,g;11}$ are as in Theorems 3 and 4.

Proof of Lemma 3. This follows from Proposition 2.2 in Ley et al. (2013). \square

Lemma 4. For any $\boldsymbol{\theta} \in \mathcal{S}^{p-1}$, $g \in \mathcal{G}_a$, and any bounded sequence (\mathbf{t}_n) in \mathbb{R}^p such that $\boldsymbol{\theta}_n := \boldsymbol{\theta} + n^{-1/2}\mathbf{t}_n \in \mathcal{S}^{p-1}$ for any n , we have that, as $n \rightarrow \infty$ under $P_{\boldsymbol{\theta},g}^{(n)}$:

$$(i_{\mathcal{T}\mathcal{M}}) \quad \frac{1}{\sqrt{n}} \sum_{i=1}^n \left(\mathbf{U}_{i,\boldsymbol{\theta}_n} - \mathbf{U}_{i,\boldsymbol{\theta}} - \mathbb{E}[\mathbf{U}_{i,\boldsymbol{\theta}_n}] \right) = o_P(1),$$

$$(ii_{\mathcal{T}\mathcal{M}}) \quad \frac{1}{\sqrt{n}} \sum_{i=1}^n \mathbb{E}[\mathbf{U}_{i,\boldsymbol{\theta}_n}] = -\frac{\mathcal{I}_p(g)}{p-1} \boldsymbol{\Gamma}_{\boldsymbol{\theta}}^T \mathbf{t}_n + o(1),$$

$$(iii_{\mathcal{T}\mathcal{M}}) \quad \frac{1}{\sqrt{n}} \sum_{i=1}^n (\mathbf{U}_{i,\boldsymbol{\theta}_n} - \mathbf{U}_{i,\boldsymbol{\theta}}) = -\frac{\mathcal{I}_p(g)}{p-1} \boldsymbol{\Gamma}_{\boldsymbol{\theta}}^T \mathbf{t}_n + o_P(1),$$

$$(i_{\mathcal{T}\mathcal{E}}) \quad \frac{1}{\sqrt{n}} \sum_{i=1}^n \left(\mathbf{U}_{i,\boldsymbol{\theta}_n} \mathbf{U}_{i,\boldsymbol{\theta}_n}^T - \mathbf{U}_{i,\boldsymbol{\theta}} \mathbf{U}_{i,\boldsymbol{\theta}}^T - \mathbb{E}[\mathbf{U}_{i,\boldsymbol{\theta}_n} \mathbf{U}_{i,\boldsymbol{\theta}_n}^T] + \frac{1}{p-1} \mathbf{I}_{p-1} \right) = o_P(1),$$

$$(ii_{\mathcal{T}\mathcal{E}}) \quad \frac{1}{\sqrt{n}} \sum_{i=1}^n \left(\mathbb{E}[\mathbf{U}_{i,\boldsymbol{\theta}_n} \mathbf{U}_{i,\boldsymbol{\theta}_n}^T] - \frac{1}{p-1} \mathbf{I}_{p-1} \right) = o(1),$$

$$(iii_{\mathcal{T}\mathcal{E}}) \quad \frac{1}{\sqrt{n}} \sum_{i=1}^n (\mathbf{U}_{i,\boldsymbol{\theta}_n} \mathbf{U}_{i,\boldsymbol{\theta}_n}^T - \mathbf{U}_{i,\boldsymbol{\theta}} \mathbf{U}_{i,\boldsymbol{\theta}}^T) = o_P(1).$$

Proof of Lemma 4. Throughout this proof, expectations are under $P_{\boldsymbol{\theta},g}^{(n)}$, convergences are as $n \rightarrow \infty$, and superscript \mathcal{T} stands for “ $\mathcal{T}\mathcal{M}$ (respectively, $\mathcal{T}\mathcal{E}$)”. For $(i_{\mathcal{T}\mathcal{M}})$ – $(i_{\mathcal{T}\mathcal{E}})$, let $\mathbf{N}_{i,n}^{\mathcal{T}\mathcal{M}} := \mathbf{U}_{i,\boldsymbol{\theta}_n} - \mathbf{U}_{i,\boldsymbol{\theta}}$ and $\mathbf{N}_{i,n}^{\mathcal{T}\mathcal{E}} := \text{vec}(\mathbf{U}_{i,\boldsymbol{\theta}_n} \mathbf{U}_{i,\boldsymbol{\theta}_n}^T) - \text{vec}(\mathbf{U}_{i,\boldsymbol{\theta}} \mathbf{U}_{i,\boldsymbol{\theta}}^T)$. We have to show that

$$\mathbf{T}_n^{\mathcal{T}} = n^{-1/2} \sum_{i=1}^n (\mathbf{N}_{i,n}^{\mathcal{T}} - \mathbb{E}[\mathbf{N}_{i,n}^{\mathcal{T}}]) = o_P(1).$$

Since $\mathbb{E}[\|\mathbf{T}_n^{\mathcal{T}}\|^2] = n^{-1} \sum_{i,j=1}^n \mathbb{E}[(\mathbf{N}_{i,n}^{\mathcal{T}} - \mathbb{E}[\mathbf{N}_{i,n}^{\mathcal{T}}])^T (\mathbf{N}_{j,n}^{\mathcal{T}} - \mathbb{E}[\mathbf{N}_{j,n}^{\mathcal{T}}])] = \mathbb{E}[\|\mathbf{N}_{1,n}^{\mathcal{T}} - \mathbb{E}[\mathbf{N}_{1,n}^{\mathcal{T}}]\|^2] \leq \mathbb{E}[\|\mathbf{N}_{1,n}^{\mathcal{T}}\|^2]$, the result follows from (24) for $\mathcal{T}\mathcal{M}$, and from (25) for $\mathcal{T}\mathcal{E}$. For $(ii_{\mathcal{T}\mathcal{M}})$ – $(ii_{\mathcal{T}\mathcal{E}})$, we consider

$$\mathbf{S}_{\boldsymbol{\theta}}^{\mathcal{T}\mathcal{M}(n)} := \frac{1}{\sqrt{n}} \sum_{i=1}^n \mathbf{U}_{i,\boldsymbol{\theta}} \quad \text{and} \quad \mathbf{S}_{\boldsymbol{\theta}}^{\mathcal{T}\mathcal{E}(n)} := \frac{1}{\sqrt{n}} \sum_{i=1}^n \text{vec} \left(\mathbf{U}_{i,\boldsymbol{\theta}} \mathbf{U}_{i,\boldsymbol{\theta}}^T - \frac{1}{p-1} \mathbf{I}_{p-1} \right).$$

By using Lemma 1, the CLT for triangular arrays implies that, under $P_{\boldsymbol{\theta}_n,g}^{(n)}$,

$$\begin{pmatrix} \mathbf{S}_{\boldsymbol{\theta}}^{\mathcal{T}(n)} \\ \Delta_{\boldsymbol{\theta}_n,g;1}^{(n)} \end{pmatrix} \xrightarrow{\mathcal{D}} \mathcal{N} \left(\mathbf{0}, \begin{pmatrix} \boldsymbol{\Sigma}^{\mathcal{T}} & (\mathbf{C}_{\boldsymbol{\theta}}^{\mathcal{T}})^T \\ \mathbf{C}_{\boldsymbol{\theta}}^{\mathcal{T}} & \boldsymbol{\Gamma}_{\boldsymbol{\theta},g;11} \end{pmatrix} \right), \quad (26)$$

where $\mathbf{C}_{\boldsymbol{\theta}}^{\mathcal{T}\mathcal{M}} = \frac{\mathcal{I}_p(g)}{p-1} \boldsymbol{\Gamma}_{\boldsymbol{\theta}}$, $\mathbf{C}_{\boldsymbol{\theta}}^{\mathcal{T}\mathcal{E}} = \mathbf{0}$, $\boldsymbol{\Sigma}^{\mathcal{T}\mathcal{M}} := \frac{1}{p-1} \mathbf{I}_{p-1}$, and

$$\boldsymbol{\Sigma}^{\mathcal{T}\mathcal{E}} := \frac{1}{p^2-1} (\mathbf{I}_{(p-1)^2} + \mathbf{K}_{p-1} + \mathbf{J}_{p-1}) - \frac{1}{(p-1)^2} \mathbf{J}_{p-1}.$$

By using Lemma 3, Le Cam’s first lemma implies that $P_{\boldsymbol{\theta}_n,g}^{(n)}$ and $P_{\boldsymbol{\theta},g}^{(n)}$ are mutually contiguous. Therefore, one can apply Le Cam’s third lemma to the joint asymptotic normality results in (26), which yields that, under $P_{\boldsymbol{\theta},g}^{(n)}$,

$$\frac{1}{\sqrt{n}} \sum_{i=1}^n \mathbf{U}_{i,\boldsymbol{\theta}_n} + \frac{\mathcal{I}_p(g)}{p-1} \boldsymbol{\Gamma}_{\boldsymbol{\theta}}^T \mathbf{t}_n = \mathbf{S}_{\boldsymbol{\theta}_n}^{\mathcal{T}\mathcal{M}(n)} + (\mathbf{C}_{\boldsymbol{\theta}}^{\mathcal{T}\mathcal{M}})^T \mathbf{t}_n \xrightarrow{\mathcal{D}} \mathcal{N}(\mathbf{0}, \boldsymbol{\Sigma}^{\mathcal{T}\mathcal{M}}) \quad (27)$$

and

$$\frac{1}{\sqrt{n}} \sum_{i=1}^n \text{vec} \left(\mathbf{U}_{i,\boldsymbol{\theta}_n} \mathbf{U}_{i,\boldsymbol{\theta}_n}^T - \frac{1}{p-1} \mathbf{I}_{p-1} \right) = \mathbf{S}_{\boldsymbol{\theta}_n}^{\mathcal{T}\mathcal{E}(n)} + (\mathbf{C}_{\boldsymbol{\theta}}^{\mathcal{T}\mathcal{E}})^T \mathbf{t}_n \xrightarrow{\mathcal{D}} \mathcal{N}(\mathbf{0}, \boldsymbol{\Sigma}^{\mathcal{T}\mathcal{E}}). \quad (28)$$

Now, by using Lemma 2, the CLT for triangular arrays shows that, still under $P_{\boldsymbol{\theta},g}^{(n)}$,

$$\frac{1}{\sqrt{n}} \sum_{i=1}^n (\mathbf{U}_{i,\boldsymbol{\theta}_n} - \mathbb{E}[\mathbf{U}_{i,\boldsymbol{\theta}_n}]) \xrightarrow{\mathcal{D}} \mathcal{N}(\mathbf{0}, \boldsymbol{\Sigma}^{\mathcal{T}\mathcal{M}}), \quad (29)$$

and

$$\frac{1}{\sqrt{n}} \sum_{i=1}^n \text{vec} \left(\mathbf{U}_{i,\boldsymbol{\theta}_n} \mathbf{U}_{i,\boldsymbol{\theta}_n}^T - \mathbb{E}[\mathbf{U}_{i,\boldsymbol{\theta}_n} \mathbf{U}_{i,\boldsymbol{\theta}_n}^T] \right) \xrightarrow{\mathcal{D}} \mathcal{N}(\mathbf{0}, \boldsymbol{\Sigma}^{\mathcal{T}\mathcal{E}}), \quad (30)$$

where the expectations are under $P_{\boldsymbol{\theta},g}^{(n)}$. The result $(ii_{\mathcal{T}\mathcal{M}})$ then follows from (27) and (29), whereas $(ii_{\mathcal{T}\mathcal{E}})$ similarly follows from (28) and (30). Finally, $(iii_{\mathcal{T}\mathcal{M}})$ – $(iii_{\mathcal{T}\mathcal{E}})$ are a direct consequence of $(i_{\mathcal{T}\mathcal{M}})$ – $(i_{\mathcal{T}\mathcal{E}})$ and $(ii_{\mathcal{T}\mathcal{M}})$ – $(ii_{\mathcal{T}\mathcal{E}})$. \square

D Additional simulations

D.1 The specified- $\boldsymbol{\theta}$ problem on \mathcal{S}^3

The third simulation exercise essentially replicates the one in Section 5.2 on \mathcal{S}^3 . Since the Kuiper test $\phi_{\boldsymbol{\theta}}^{\text{KU}}$ only applies for data on \mathcal{S}^2 , we replaced it with the Giné test $\phi_{\boldsymbol{\theta}}^{\text{GI}}$, that, as the Kuiper test, is an omnibus test addressing the specified- $\boldsymbol{\theta}$ problem. For sample sizes $n = 100$ and $n = 200$ and for two types of alternatives to rotational symmetry ($r = 1, 2$), we generated $N = 5,000$ mutually independent random samples of the form $\mathbf{X}_{i;\ell}^{(r)}$, $i = 1, \dots, n$, $\ell = 0, \dots, 5$, $r = 1, 2$, with values in \mathcal{S}^3 . The $\mathbf{X}_{i;\ell}^{(1)}$'s follow a $\mathcal{T}\mathcal{E}_4(\boldsymbol{\theta}, g_2, \boldsymbol{\Lambda}_\ell)$ with location $\boldsymbol{\theta} := (1, 0, 0, 0)^T$ and shape $\boldsymbol{\Lambda}_\ell := 3\text{diag}(1 + \ell/2, 1, 1)/(3 + \ell/2)$. The $\mathbf{X}_{i;\ell}^{(2)}$'s follow a $\mathcal{T}\mathcal{M}_4(\boldsymbol{\theta}, g_2, \boldsymbol{\mu}, \kappa_\ell)$ with skewness direction $\boldsymbol{\mu} = (1, 0, 0)^T$ and skewness intensity $\kappa_\ell := \ell/8$. As in the previous simulation exercises, $\ell = 0$ corresponds to the null of rotational symmetry about $\boldsymbol{\theta}$ and $\ell = 1, \dots, 5$ provide increasingly severe alternatives. For each replication, we performed, at asymptotic level 5%, the specified- $\boldsymbol{\theta}$ tests $\phi_{\boldsymbol{\theta}}^{\text{loc}}$, $\phi_{\boldsymbol{\theta}}^{\text{sc}}$, $\phi_{\boldsymbol{\theta}}^{\text{hyb}}$, $\phi_{\boldsymbol{\theta}}^{\text{LV}}$, and the Giné test $\phi_{\boldsymbol{\theta}}^{\text{GI}}$, as well as the unspecified- $\boldsymbol{\theta}$ tests $\phi_{\dagger}^{\text{sc}}$, $\phi_{\text{vMF}}^{\text{loc}}$, and $\phi_{\text{vMF}}^{\text{hyb}}$ (still based on the spherical mean). In addition, we also considered the Fisher-aggregated hybrid tests $\tilde{\phi}_{\boldsymbol{\theta}}^{\text{hyb}}$ and $\tilde{\phi}_{\text{vMF}}^{\text{hyb}}$, as in \mathcal{S}^3 they differ from $\phi_{\boldsymbol{\theta}}^{\text{hyb}}$ and $\phi_{\text{vMF}}^{\text{hyb}}$. As expected due to their construction, the Fisher-aggregated tests dominate their hybrid counterparts under tangent vMF alternatives, while they are dominated by the latter under tangent elliptical alternatives. The rest of the power curves, that are provided in Figure 7, lead to conclusions that are very similar to those reported in the simulation exercise conducted in Section 5.2.

D.2 Mixtures in the specified- $\boldsymbol{\theta}$ case on \mathcal{S}^2

For the last simulation exercise, we consider two types of mixture distributions on \mathcal{S}^2 : mixtures of vMF distributions ($r = 1$) and mixtures of tangent vMF and tangent elliptical distributions ($r = 2$). For sample sizes $n = 100$ and $n = 200$ and for both types of mixtures, we generated $N = 5,000$ mutually independent random samples of the form $\mathbf{X}_{i;\ell}^{(r)}$, $i = 1, \dots, n$, $\ell = 0, \dots, 5$, $r = 1, 2$, with values on \mathcal{S}^2 . The $\mathbf{X}_{i;\ell}^{(1)}$'s are distributed as the mixture $\frac{1}{2}\mathbf{Y} + \frac{1}{2}\mathbf{Z}_\ell$, where \mathbf{Y} and \mathbf{Z}_ℓ are independent vMF random vectors with respective locations $\boldsymbol{\theta} = (1, 0, 0)^T$ and $\boldsymbol{\theta}_\ell = (\cos(\ell/40), \sin(\ell/40), 0)^T$ and common concentration $\kappa = 5$. The $\mathbf{X}_{i;\ell}^{(2)}$'s are distributed as the mixture $\frac{1}{2}\mathbf{Z}_{1,\ell} + \frac{1}{2}\mathbf{Z}_{2,\ell}$, where $\mathbf{Z}_{1,\ell} \sim \mathcal{T}\mathcal{M}_3(\boldsymbol{\theta}, \exp(5u), \boldsymbol{\mu}, \kappa_\ell)$ and $\mathbf{Z}_{2,\ell} \sim \mathcal{T}\mathcal{E}_3(\boldsymbol{\theta}, \exp(5u), \boldsymbol{\Lambda}_\ell)$ are independent, with $\boldsymbol{\theta} = (1, 0, 0)^T$, $\boldsymbol{\mu} = (1, 0)^T$, $\kappa_\ell = \ell/6$, and $\boldsymbol{\Lambda}_\ell = 2\text{diag}(1 + \ell/2, 1)/(2 + \ell/2)$, $\ell = 0, \dots, 5$. For $r = 1, 2$, the value $\ell = 0$ corresponds to the null hypothesis of rotational symmetry about $\boldsymbol{\theta}$, whereas $\ell = 1, \dots, 5$ provide increasingly severe alternatives. For each replication, we performed, at asymptotic level $\alpha = 5\%$,

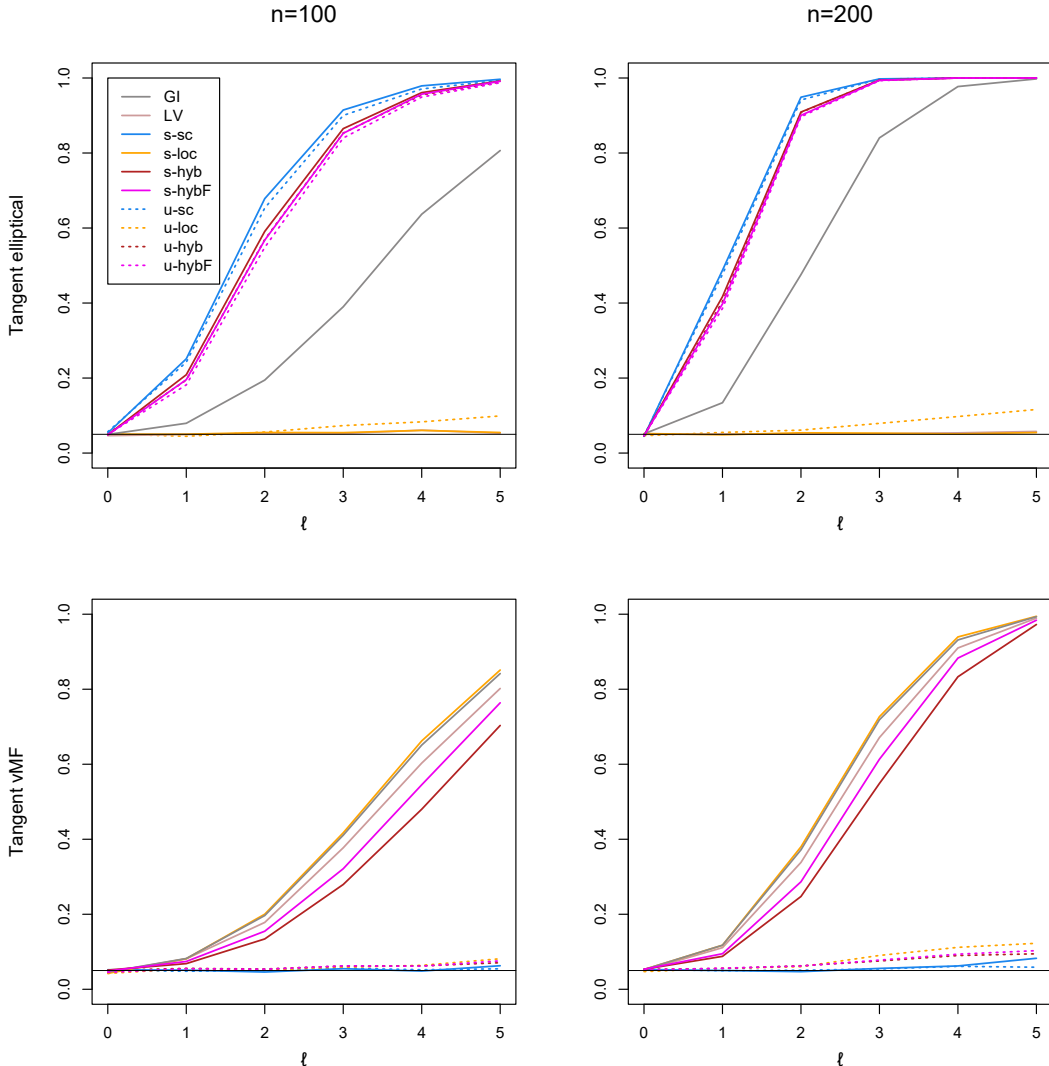


Figure 7: Rejection frequencies, under tangent elliptical alternatives (top row) and tangent vMF alternatives (bottom row), of the specified- $\boldsymbol{\theta}$ tests $\phi_{\boldsymbol{\theta}}^{\text{sc}}$ (s-sc), $\phi_{\boldsymbol{\theta}}^{\text{loc}}$ (s-loc), $\phi_{\boldsymbol{\theta}}^{\text{hyb}}$ (s-hyb), $\tilde{\phi}_{\boldsymbol{\theta}}^{\text{hyb}}$ (s-hybF), $\phi_{\boldsymbol{\theta}}^{\text{LV}}$ (LV), and $\phi_{\boldsymbol{\theta}}^{\text{GI}}$ (GI), as well as the unspecified- $\boldsymbol{\theta}$ tests $\phi_{\dagger}^{\text{sc}}$ (u-sc), $\phi_{\text{vMF}}^{\text{loc}}$ (u-loc), $\phi_{\text{vMF}}^{\text{hyb}}$ (u-hyb), and $\tilde{\phi}_{\text{vMF}}^{\text{hyb}}$ (u-hybF). Sample sizes are $n = 100$ (left column) and $n = 200$ (right column). All tests are performed at asymptotic level 5%; see Section D.1 for details.

the specified- $\boldsymbol{\theta}$ tests $\phi_{\boldsymbol{\theta}}^{\text{loc}}$, $\phi_{\boldsymbol{\theta}}^{\text{sc}}$, $\phi_{\boldsymbol{\theta}}^{\text{hyb}}$, $\phi_{\boldsymbol{\theta}}^{\text{LV}}$, and $\phi_{\boldsymbol{\theta}}^{\text{KU}}$ (based on the true value of $\boldsymbol{\theta}$). For the sake of comparison, we also considered the unspecified- $\boldsymbol{\theta}$ tests $\phi_{\dagger}^{\text{sc}}$, $\phi_{\text{vMF}}^{\text{loc}}$, and $\phi_{\text{vMF}}^{\text{hyb}}$, based on the spherical mean. Figure 8 plots the resulting empirical power curves for sample sizes $n = 100$ and $n = 200$ and for both types of mixtures. Inspection of Figure 8 reveals that the Ley and Verdebout (2017) test performs well against mixtures of vMF distributions, while, as we might have guessed, the (specified- $\boldsymbol{\theta}$) hybrid test dominates the other tests for mixtures of tangent vMF and tangent elliptical distributions. The location and hybrid tests perform well overall.

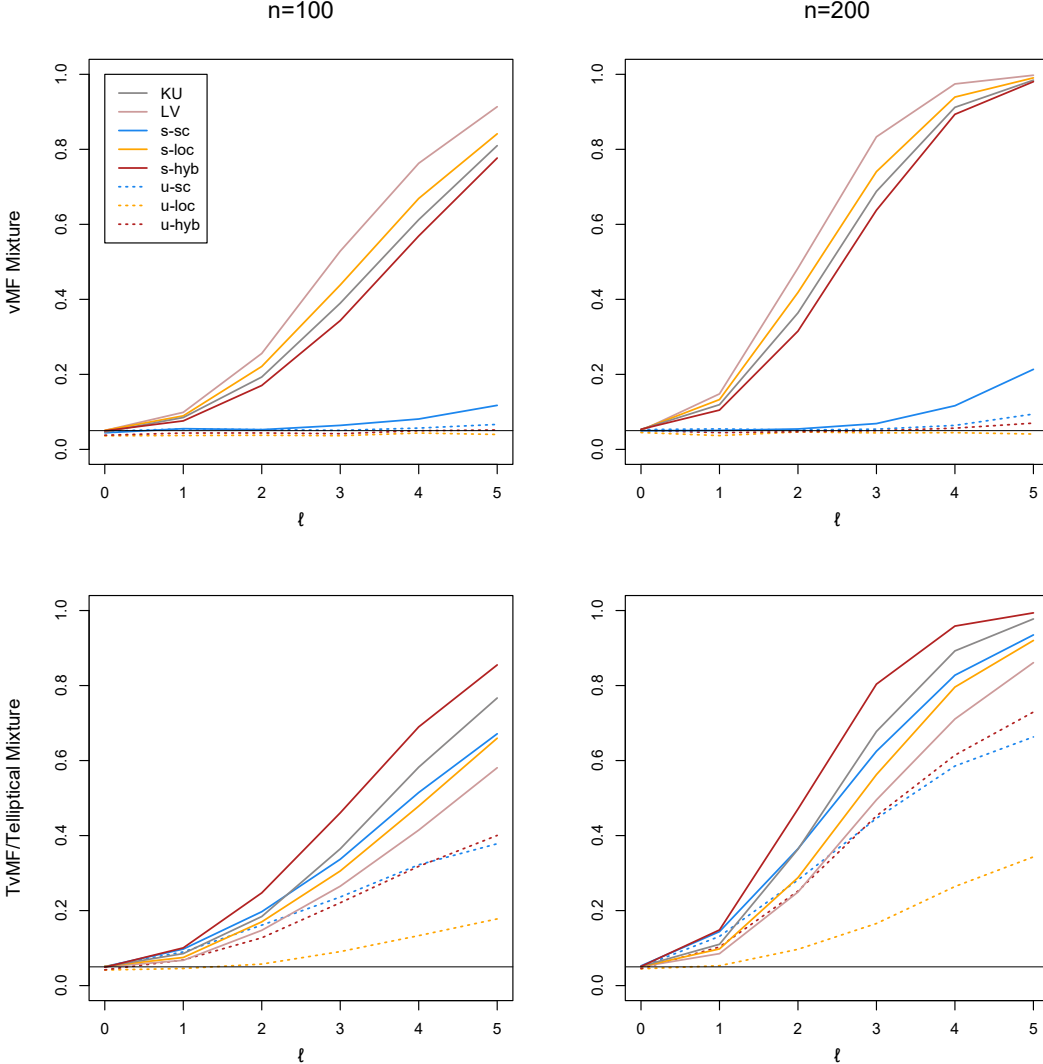


Figure 8: Rejection frequencies, under mixtures of vMF's and mixtures of tangent vMF and tangent elliptical, of the specified- $\boldsymbol{\theta}$ tests $\phi_{\boldsymbol{\theta}}^{\text{sc}}$ (s-sc), $\phi_{\boldsymbol{\theta}}^{\text{loc}}$ (s-loc), $\phi_{\boldsymbol{\theta}}^{\text{hyb}}$ (s-hyb), $\phi_{\boldsymbol{\theta}}^{\text{LV}}$ (LV), and $\phi_{\boldsymbol{\theta}}^{\text{GI}}$ (GI), as well as the unspecified- $\boldsymbol{\theta}$ tests $\phi_{\dagger}^{\text{sc}}$ (u-sc), $\phi_{\text{vMF}}^{\text{loc}}$ (u-loc), and $\phi_{\text{vMF}}^{\text{hyb}}$ (u-hyb). Sample sizes are $n = 100$ (left column) and $n = 200$ (right column). All tests are performed at asymptotic level 5%; see Section D.2 for details.

References

- Cutting, C., Paindaveine, D., and Verdebout, T. (2017). Testing uniformity on high-dimensional spheres against monotone rotationally symmetric alternatives. *Ann. Statist.*, 45(3):1024–1058.
- Kreiss, J. (1987). On adaptive estimation in stationary ARMA processes. *Ann. Statist.*, 15(1):122–133.

- Ley, C., Swan, Y., Thiam, B., and Verdebout, T. (2013). Optimal R-estimation of a spherical location. *Statist. Sinica*, 23(1):305–333.
- Ley, C. and Verdebout, T. (2017). Skew-rotationally-symmetric distributions on the unit sphere and related efficient inferential procedures. *J. Multivariate Anal.*, 159:67–81.
- Magnus, J. R. and Neudecker, H. (2007). *Matrix Differential Calculus with Applications in Statistics and Econometrics*. Wiley Series in Probability and Statistics: Probability and Statistics. John Wiley & Sons, Chichester.
- Mardia, K. V. and Jupp, P. E. (2000). *Directional Statistics*. Wiley Series in Probability and Statistics. John Wiley & Sons, Chichester, second edition.
- Paindaveine, D. (2008). A canonical definition of shape. *Statist. Probab. Lett.*, 78(14):2240–2247.
- Paindaveine, D. and Verdebout, T. (2016). On high-dimensional sign tests. *Bernoulli*, 22(3):1745–1769.
- van der Vaart, A. W. (1998). *Asymptotic Statistics*. Cambridge Univ. Press, Cambridge.
- Watson, G. S. (1983). *Statistics on Spheres*. Wiley, New York.